UNIVERSITY OF SOUTHAMPTON

FACULTY OF ENGINEERING AND THE ENVIROMENT

Institute of Sound and Vibration Research

Modelling multiple excitation mechanisms in the cochlea using a 2D finite difference box model

by

Alice Audrey Halpin

Thesis for the degree of Doctor of Philosophy

February 2017

Declaration of Authorship

I, Alice Audrey Halpin, declare that this thesis titled, 'Modelling multiple excitation mechanisms in the cochlea using a 2D finite difference box model' and the work presented in it are my own. I confirm that:

- This work was done wholly or mainly while in candidature for a research degree at this University.
- Where any part of this thesis has previously been submitted for a degree or any other qualification at this University or any other institution, this has been clearly stated.
- Where I have consulted the published work of others, this is always clearly attributed.
- Where I have quoted from the work of others, the source is always given. With the exception of such quotations, this thesis is entirely my own work.
- I have acknowledged all main sources of help.
- Where the thesis is based on work done by myself jointly with others, I have made clear exactly what was done by others and what I have contributed myself.

Signed: _____

Date: 23/8/18

Acknowledgements

So a PhD is hard, and not just from an academic sense. I have found that the feeling that everything I am doing is wrong and useless never completely going away the root of most of my struggles. My supervisor, Prof. Stephen Elliott, has a seemingly effortless ability to regularly banish these fears. I walked out of every meeting with him feeling positive, however negative I walked in. Without those meetings my PhD would have been a much more painful experience. Thank you Steve. Thank you also for the freedom but continued direction in my research, the opportunities you gave me, and all the support when writing up.

Going into a building full of desk and computers and sitting down at one and doing work every day would be rather boring without the people who occupied the other desks. So thank you to those would sat at the other desks for all the fun. Especially thank you to Jordan and Matt for the many cups of tea and pints of beer, and for being the go-tos for when I needed help with computers and my general not understanding. And lastly, thank you to Ni for all the help and support with my research and spending time answering all my questions.

I do not feel I have always been the best person I can be throughout my PhD. I would like to thank those close to me for supporting and putting up with me. A special thanks to my Dad and Moritz for their time spent proof reading my thesis.

UNIVERSITY OF SOUTHAMPTON

ABSTRACT

FACULTY OF ENGINEERING AND THE ENVIROMENT
Institute of Sound and Vibration Research

Doctor of Philosophy

MODELLING MULTIPLE EXCITATION MECHANISMS IN THE COCHLEA USING A 2D FINITE DIFFERENCE BOX MODEL

by Alice Audrey Halpin

The cochlea is very versatile. It can be excited by a multitude of mechanisms in order to produce a hearing sensation, even when it is severely malformed. The versatility of the cochlea can also be used to our advantage in the creation of novel methods of cochlear excitation when the conventional pathway is obstructed, for instance through bone conduction hearing aids and excitation via the round window. It is thus important to have an in-depth understanding of the various mechanisms that can cause a hearing sensation and how they are affected by the condition and structures of the cochlea.

This thesis investigates the underlying physics associated with various cochlear excitation mechanisms using a 2D finite difference box model. The excitation mechanism examined include; piston-like motion of the stapes, rocking of the stapes, the two inertial components of bone conduction hearing and local excitation of the round window. The model predicts the pressure distribution within the cochlea and allows a direct comparison of the effects of these various excitation mechanisms within the same framework.

The effect of the 'third window' on the cochlear response due to various cochlear excitation mechanisms was investigated by adapting the model to include the cochlear and vestibular aqueducts. It was found that aqueducts do not affect the cochlear response much for volumetric excitation via the oval window, but were demonstrated to have a significant effect for other excitation mechanisms. In particular it was found that the aqueducts had a large effect when an immobile oval window was modelled, as they allowed a volumetric excitation that significantly increased the response at low frequencies.

An air-bone gap has been clinically found in audiograms of patients who have a large vestibular aqueduct, although the reasons for this phenomenon are not fully understood. The effects of a large vestibular aqueduct on the air conduction and bone conduction hearing thresholds have been separately modelled here. It was found that the air-bone gap is predominately caused by the increase of the air conduction hearing threshold due to the internal cochlear pressure forcing fluid through the enlarged aqueduct, reducing the net volumetric excitation.

Contents

List of Figures

List of Tables

Chapter 1

Introduction

1.1 Anatomy of the Ear

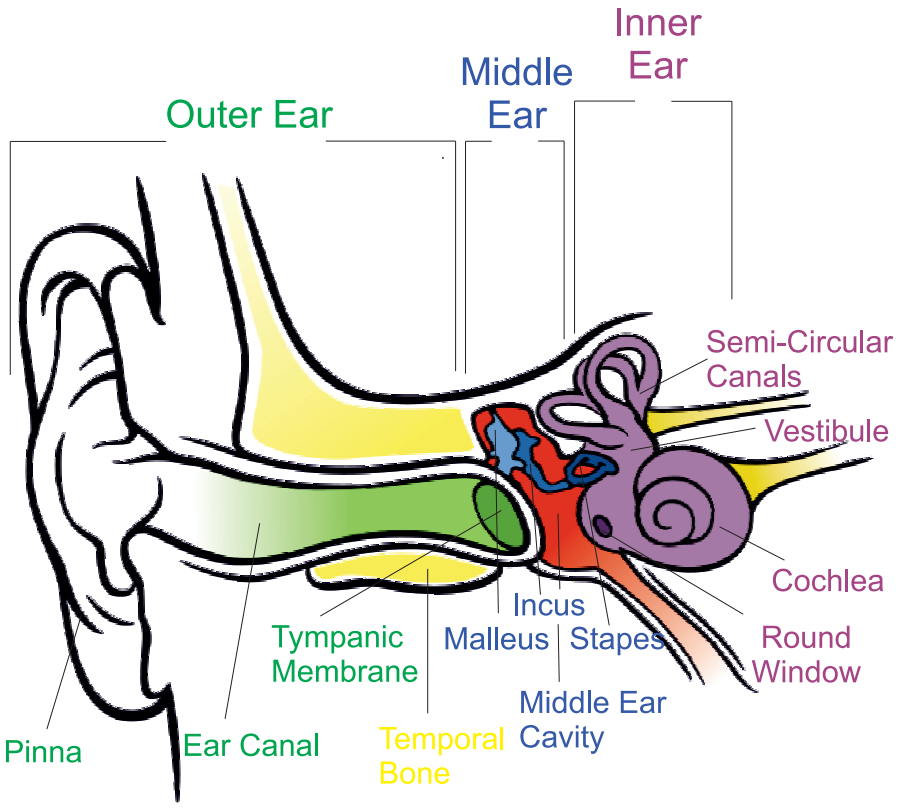

Figure 1.1: Diagram showing main structures of the ear. Picture edited from Brockmannderivativ and Komorniczak (2009).

Hearing is one of the main senses we as humans use to create an understanding of the environment around us. For mammals, it is the ear that collects the acoustical energy from the surroundings and then converts this energy into electrical signals which are then sent to and processed by the brain. When any part of this hearing process is impaired

it can have devastating consequences on a person's quality of life. It is therefore greatly advantageous to be able to treat hearing impairments in order to increase a patients hearing ability and quality of life. A deep understanding of the physical mechanisms of the hearing process of the ear is needed to further develop hearing treatments. This thesis mainly focuses on furthering the knowledge of the physical mechanisms occurring in the cochlea when detecting acoustical energy due to a variety of methods of excitation. Of particular interest was the changes to the cochlear response when the cochlea is malformed.

The ear is made up of three distinct regions: the outer ear, middle ear and inner ear, as shown in Fig. 1.1. The outer ear comprises of the pinna, external auditory canal (or ear canal) and the outer surface of the tympanic membrane. The ear canal is a tube, of about 2.5 cm length, leading from the pinna to the tympanic membrane. It comprises of two parts: the wall of the first third consists of cartilage and soft tissue while the wall of the inner two thirds is made of bone. The middle ear is comprised of the tympanic cavity, that contains the tympanic membrane, auditory ossicles (or middle ear ossicles), which are formed by the mallues, incus and stapes. And lastly the inner ear, consisting of the cochlea, vestibule and semicircular canals, whose outer walls are the bony labyrinth, a series of cavities in the temporal bone. From roughly a third of the way down the ear canal the components of the ear are encased in the temporal bone.

The pinna directs sound waves into the ear canal which then travel along the ear canal to the tympanic membrane, causing it to vibrate. These vibrations are transferred to the cochlea by the middle ear ossicles. The function of the cochlea is to convert the acoustical energy into electrical signals which are sent to the brain via the cochlear nerve and then processed to produce a hearing sensation. This process, where the acoustical energy is transmitted from the pinna to the cochlea, is the most prominent pathway, and is termed air conduction. The cochlea is the essential component of the ear in producing a hearing sensation but there are many other methods of transmitting acoustical energy to the cochlea, some of which will be discussed later in this thesis.

1.2 The Cochlea

The cochlea is a coiled fluid filled structure that is embedded deep inside the skull, in the petrous portion of the temporal bone. It has a complex geometry that is carved out by the bony labyrinth and contains many delicate structures. In humans, the cochlea narrows along its length, has roughly 2.5 turns and would stretch to 35 mm if it was uncoiled. It is a small structure, with a total height of roughly 4 mm and width of 8 mm Braun et al. (2012).

Two membranes separate the cochlea into three fluid chambers, the scala vestibuli, scala media and scala tympani Dallos et al. (1996), as shown in Fig. 1.2. The Reissner's

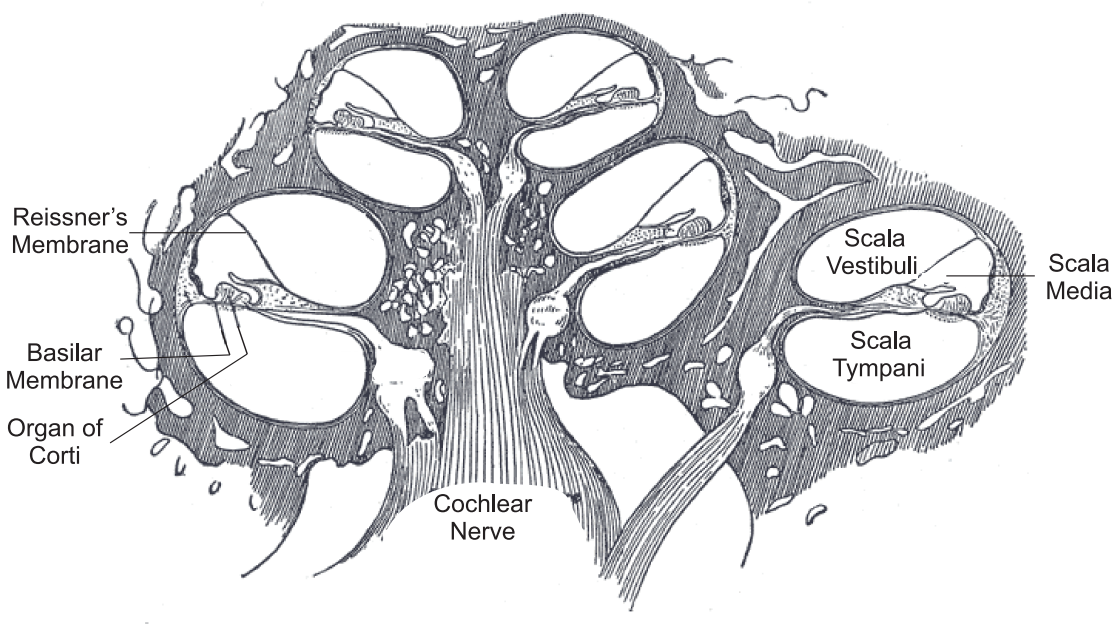

Figure 1.2: Diagram showing a cross section of the cochlea indicating the different fluid chambers and the structures inside. Modified from illustration in Gray (1918).

membrane separates scala vestibuli and scala media and the basilar membrane, BM, separates the scala tympani and scala media. The scala media and scala vestibuli extend into the vestibule, while the scala tympani terminates close to the round window. At the apex of the cochlea, the scala vestibuli and tympani are connected at the helicotrema.

There are two types of fluid in the cochlea, perilymph and endolymph fluid. Both the scala vestibuli and scala tympani contain perilymph fluid while only the scala media contains endolymph fluid. The acoustical behaviour of these two fluids are similar, although they differ chemically as the perilymph is high in sodium concentration and endolymph high in potassium. The endocochlear potential, which is the electrical potential between these two fluids, is in the region of 80 mV (Dallos et al., 1996). The potential difference between these fluids is central to the creation of the electrical nerve signal from BM motion.

The fluid in the cochlea is almost incompressible, however, there are a number of compliant structures on the boundary of the cochlea which allow a motion of the cochlear fluid and hence mechanisms for cochlea excitation. The oval and round windows are the two main structures, which consist of holes in the bony wall of the cochlea covered by membranes. The oval window is located between the scala vestibuli and stapes of the middle ear ossicles, which sits on top of it, allowing for the vibrations of the middle ear ossicles to be transmitted to the cochlea. The round window opens into the tympanic cavity from the scala tympani and therefore can act as a pressure release. There are other smaller outlets into the cochlea, collectively termed the 'third window', which include blood vessels, the cochlear aqueduct and vestibular aqueduct. The cochlear aqueduct is

located in close proximity to the round window and joins the perilymph with the cerebrospinal fluid. The vestibular aqueduct enters the cochlea via the vestibula scala and extends to the surface of the temporal bone. The purpose of these two aqueducts is not entirely clear, but there seem to be significant differences in their dimensions between individuals (Gopen et al., 1997).

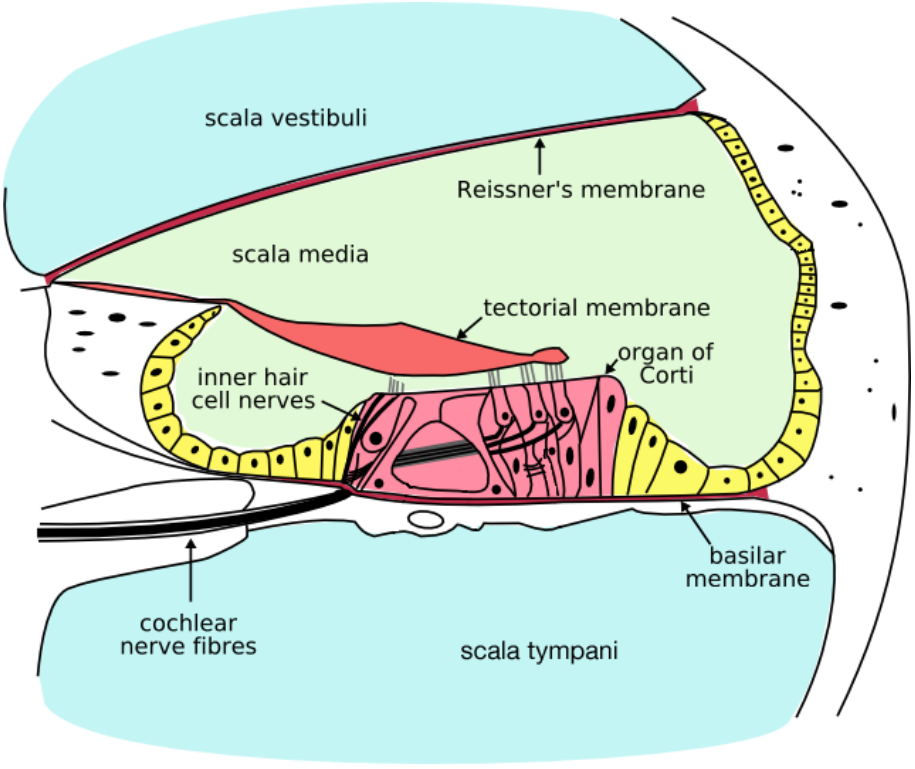

Figure 1.3: Cross section diagram of the cochlea, showing the three fluid chambers and the organ of Corti location on top of the basilar membrane. This image was taken from Oarih (2009) and edited.

The BM is central in the perception and analysis of acoustic energy of the surrounding environment. Acoustic stimulation of the cochlea causes a travelling wave motion along the BM. As shown in Fig. 1.3, the organ of Corti rests on top of the BM, inside of the scala media. It is within the organ of Corti that the mechanical energy due to the acoustical excitation is transformed into electrical signals that are then sent to the central nervous system and processed by the brain. Rows of inner and outer hair cells, one row of inner hair cells and three of outer, which reach up towards the tectorial membrane from the surface of the organ of Corti, as shown in Fig. 1.3.

It is the processes involving the inner hair cells that generate neural signals from the motion of the BM, while the outer hair cells are involved in the process of amplifying the motion of low level sounds. An electrical response caused by relative motion between the BM and tectorial membrane is generated by the inner hair cells through its mechanically sensitive ion channels. This is then transmitted to the nerve fibres and ultimately to the brain. The stereocilia of a hair cell are connected by tip links which transmit mechanical

stress to ion channels of the hair cell causing them to open. A travelling wave along the BM causes a sheering motion between the BM and tectorial membrane which in turn can cause the tip links to be under stress. The opening of the ion channel due to this stress allows for a greater number of cations to pass through the cell ultimately generating an electrical signal.

The geometry of the BM varies along its length: it is narrow and thick at the base of the cochlea and wider and thinner at the apex, resulting in an increasing mechanical admittance along its length. It is this variation in the BM admittance that creates the shape of the motion along the BM, when the cochlea is excited acoustically. The wave motion acts as a frequency analyser; the lower the excitation frequency the further along the BM the travelling wave reaches. The amplitude of the travelling wave increases along the length of the BM to a maximum amplitude which is unique to each frequency and then it sharply drops of. The higher the magnitude of the acoustical energy transferred to the cochlea, the greater the amplitude of the travelling wave along the BM. Hence, the motion of the BM is determined by both the magnitude and frequency of the excitation acoustical energy. In the model of the cochlea used in this thesis, the motion of the BM was assumed to correlate with the magnitude of a hearing sensation, and this motion is therefore used as a comparative measure of the efficiencies of the various hearing mechanisms.

1.3 Mechanisms of Hearing

The most common method of detecting acoustic energy is through the air conduction pathway, which has been described above. However, other mechanisms of detecting sound are possible, including through the naturally occurring bone conduction or artificial excitation through stimulation at the round window. These hearing mechanisms can be utilised to aid patients with particular hearing conditions or in specific environments.

Bone conduction describes the transmission of vibrations through the skull to the cochlea resulting in a hearing sensation. Even though it is termed 'bone conduction', it includes vibration being transmitted through both cartilage and soft tissue, as well as bone. There are multiple pathways by which the vibrations are transmitted to the cochlea, which will be described in detail in Chapter 2, but they all ultimately cause an excitation of the BM. Bone conduction hearing is an everyday phenomena in people with healthy ears. It is known that humans hear their own voice roughly equally through air and bone conduction (Reinfeldt et al., 2010; Pórschmann, 2000). Bone conduction hearing technology is used commercially in bone conduction headphones. They do not block the ear canal so allow for the surrounding environment to be heard as well, which could be useful when out running, for instances. Research has also been carried into using this technology in the military, and was found to be an effective way of providing radio

communication in conjunction with hearing protection in noisy environments (Henry and Letowski, 2007). It has also been exploited clinically to aid patients with conductive hearing loss since at least the early 20th century, with bone anchored hearing aids implanted in the seventies (Mudry and Tjellstrom, 2011). It is clear that the method of hearing by bone conduction has been utilised for centuries, however, the physics behind the mechanisms are not fully understood.

Mixed hearing loss patients have been treated with an implanted transducer at the round window (Colletti et al., 2006). This stimulates the round window, instead of the oval window, as in the healthy cochlea. This idea has been extended in Weddell et al. (2014) by considering a transducer that only partially occludes the round window so that the round window acts as a pressure relief and a mode of excitation at the same time. The net flow through the round window would be zero in this case, and hence the excitation can be termed non-volumetric. This is a similar excitation process that has been examined by, Edom et al. (2013), who investigated the rocking of the stapes at the oval window. This thesis explores the physical process in which these different mechanisms excite the cochlea.

1.4 Reasons for Modelling the Cochlea

The cochlea is fundamental to humans in perceiving their acoustical environment. Understanding the processes involved in the cochlea gives a greater comprehension of how humans hear and it is useful in the development of hearing treatments for those who are impaired. Due to the complex nature of the cochlea, many different techniques and methods must be used together to build an overall understanding of the cochlea. Since the early 20th century experiments have been carried out directly on the cochlea, both in living and deceased human and animals, including, for example, Bekésy and Wever (1960); Tonndorf (1966); Stenfelt and Goode (2005); Nakajima et al. (2009). These type of studies are vital in understanding the cochlea as they produce real life data. However, due to the inaccessible and delicate nature of the cochlea the variability of direct experiments is high and the results are sometimes difficult to interpret. The modelling of the cochlea offers another approach to developing an understanding of the workings of the cochlea, which can be used alongside experimental studies. Information can be gained from a model that would not be possible, or very difficult, in the real cochlea, for instance the detailed pressure distribution in the cochlea fluid. Although techniques have been developed to measure the pressure in the real cochlea, typically only the pressure in a few locations at a time can be measured (Nakajima et al., 2009). A cochlear model can be built so that the pressure distribution can be calculated at every location in the cochlea, for multiple excitation mechanisms. Models allow for greater flexibility in investigating the cochlea as they are not bound by the physical reality of the cochlea. They can be manipulated and altered in order to investigate the effect that

certain parameters of the cochlea have on the cochlear response, which could not be possible or ethical when experimenting on real cochleae. In order to fully understand the mechanisms of the cochlea it is advantageous to use a combination of experimental and modelling techniques, where the experimental results are used to validate the cochlear model results.

The current cochlear models, found within the literature, vary with complexity from simple 1D lumped parameter models, to 2D box model, to complex 3D finite element models, which all have unique benefits. A review of these models are given in Chapter 3. The 2D box model of the cochlea, used here, is the simplest one to allow predictions of the detailed pressure distribution at a position within the cochlea, while still allowing easy visualisation and interpretation of the results.

1.5 Outline of the Thesis

This thesis focuses on building a 2D finite difference model of the cochlea and using it to investigate multiple mechanisms of cochlea excitation. Using the same model, different methods of stimulations can be examined within a single framework and therefore easily compared. The structure of the this thesis is as follows:

Chapter 2 - This chapter examines the different cochlear excitation mechanisms and the hearing conditions investigated in this thesis. The classification of the different BC pathways is outlined and then discussed separately, along with the other hearing mechanisms, with reference to the literature. An introduction to the hearing conditions and treatments modelled in this thesis is given. Both otosclerosis and large vestibular aqueduct syndrome aa well as excitation at the round window, a treatment for conductive hearing loss, are discussed.

Chapter 3 - This chapter focuses on cochlear and middle ear modelling. Firstly, a description of the middle ear model used in this thesis is given and justified. A review of other cochlear models is presented and then the 2D finite difference cochlear box model used in this thesis is outlined. A description of how each hearing mechanism is simulated can be found at the end of this chapter.

Chapter 4 - This chapter presents the results of the 2D finite difference cochlea model. First, a piston-like motion at the stapes is examined, and compared with experimental data. The response due to the rocking motion of the stapes is presented and compared against other models' results. The prediction of the two inertial BC hearing pathways are then given and discussed.

Chapter 5 - This chapter examines the effect of the 'third window' on the cochlear response. The effect on a healthy cochlear is firstly examined, and then a cochlear

diseased with otosclerosis is simulated and the effect under such condition investigated. Predictions are made of both the BC hearing loss due otosclerosis and of that due to a large vestibular aqueduct syndrome. The results of the model are compared with clinical data.

Chapter 6 - The conclusion of the work carried out is summarised in this chapter along with ideas for future work.

1.6 Contributions of this Thesis

The main contributions of this thesis are:

- A 2D finite difference model of the cochlea was created that allows for a number of different cochlear excitations mechanisms to be investigated within a single framework.

- The model suggests that non-volumetric excitation may be significant under certain conditions, especially at high frequencies.

- The effect of the aqueducts in the cochlea on the hearing response to multiple mechanisms has been predicted using a 2D model for the first time.

- It is predicted that the aqueducts have a significant effect on the hearing response when excited by both the fluid inertia and local excitation at the round window, when the oval window is immobile.

- It is predicted that the air-bone gap seen in patients with a large vestibular aqueduct is mainly due to the increase in AC hearing threshold, caused by a flow through the vestibular aqueduct.

Chapter 2

Mechanisms of Exciting the Cochlea and Hearing Conditions

2.1 Introduction

There are multiple mechanisms through which the cochlea can be stimulated in order to produce a hearing sensation. In this chapter various different mechanisms are examined and discussed with reference to the present literature. The mechanisms in this chapter cover both naturally occurring hearing mechanisms, through AC and BC, and artificial excitation of the cochlea at the round window. BC hearing, as previously discussed, is where the vibrations of the skull are transmitted to the cochlea and ultimately cause a hearing sensation. Due to the complex nature of the ear and its location in the temporal bone, there are various mechanisms in which vibrations of the skull bone are transmitted to the cochlea. The overall effect of BC is due to a vectorial combination of these pathways, where the significance of the contribution of each pathway changes with the excitation frequency. In order to gain a better understanding of BC hearing, researchers have classified the mechanisms into different pathways. Stenfelt and Goode (2005), for example, have classified the multiple mechanisms of bone conduction into five pathways, which are:

1. Sound pressure in the ear-canal and the occlusion effect
2. Inertia of the middle ear ossicles
3. Transmission of pressure from the cerebrospinal fluid
4. Compression and expansion of the cochlea walls
5. Inertia of the cochlear fluid

This classification of the different BC pathways has been used in this thesis.

In this chapter, the hearing mechanisms which involve excitation via the middle ear are examined first. This includes both a piston-like motion and a rocking motion of the stapes due to AC, as well as the BC conduction pathways that utilise the middle ear, namely sound pressure in the ear-canal and inertia of the middle ear. A description of BC pathways that excite the cochlear directly is then given and the relevant literature discussed. The literature often includes studies on other mammals, as this can be useful to gain a better understanding of the different hearing mechanisms. Although the structural anatomy of mammals is similar, some caution should be taken with the conclusions drawn from these studies, since the biological dimensions are different to those of the human, which may prevent the results being replicated in the human. Biological experiments can show great variation and so the results are not always very clear. Furthermore, the hearing system is also very intricate and so it is hard to separate the different BC hearing pathways. Thus, in order to understand a hearing mechanisms it must be examined from many different angles using a variety of methods.

As with any biological structure, abnormalities and malformations can occur, either through trauma, disease or genetics. These abnormalities have different effects on the ability of the various cochlear excitation mechanisms to stimulate the cochlea. This can lead to insights into the workings of the cochlea. Two of these malformations are examined in this thesis, otoscelerosis and third window lesion, which are described and discussed later in this chapter. Artificial cochlear excitation mechanisms are used in practise to increase the hearing ability of patients with otoscelereosis. Excitation via the round window is one of these mechanisms and is modelled in this thesis. In this chapter, a short description of the other artificial mechanisms is given, followed by a discussion, with reference to the literature, of excitation via the round window.

2.2 Excitation via the Middle Ear Ossicles

The middle ear ossicles are the three smallest bones in the body and are located between the auditory canal and the cochlea. They hang in the middle ear cavity supported by flexible ligaments, tendons and muscles, but can freely move. The three bones that make up the middle ear ossicles are the malleus, incus and stapes, Fig. 2.1. The malleus is located at the far left of the middle ear cavity, with its handle attached to the tympanic membrane. The incus is the middle ossicle which is attached to the malleus at one extremity and the stapes at the other. The stapes footplate is connected to the border of the oval window, on the cochlea, by the annular stapedial ligament, which is a ring of elastic fibrous tissue. There are two muscles that are attached to the middle ear ossicles, the tensor tympani muscle and the stapedius muscle. Their function is to reduce the motion of the ossicles, in certain conditions, such as for protection when in

the presence of a loud sound. There are also multiple ligaments that support the ossicles by connecting them to the wall of the middle ear cavity. The role of these bones in the hearing process is to transmit their vibrational energy to the cochlea fluids via the oval window which is attached to the stapes. The ossicles can be vibrated by two methods, either via vibration of the tympanic membrane due to acoustic energy in the ear canal or the vibration of the temporal bone.

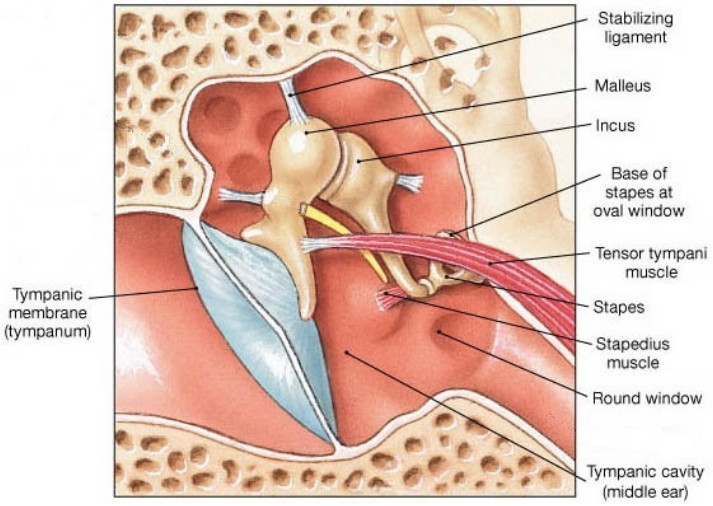

Figure 2.1: Illustration of the middle ear ossicles in the middle ear (Tympanic) cavity, not to scale and not fully complete. It shows the three ossicles, tympanic membrane and a number of ligaments and muscles that support the bones. This illustration was adapted from Droual (2007).

2.2.1 Air Conduction and the Rocking Motion of the Stapes

When modelling excitation due to air-conduction the motion of the stapes is most often assumed to be solely a piston-like motion, for instance in Neely (1981); Elliott et al. (2011); Marquardt and Hensel (2013). However, as early as the 1960s the motion of the stapes was described as having also a rocking component, (Bekésy and Wever, 1960). Recently, laser doppler vibrometer, LDV, techniques have been utilised in experiments on temporal bone samples to measure the motion of the stapes footplate and it was found that both a rocking and piston-like motion of the stapes existed when the middle ear was stimulated with AC (Heiland et al., 1999; Hato N, 2003; Sim et al., 2010). There are three components of the stapes motion, one piston and two rotational. The two rotational components are due to a rocking about the long axis and short axis of the stapes footplate. The three components of the stapes motion are illustrated clearly in Sim et al. (2010), and so are shown here, in Fig. 2.2, for clarity.

The rocking components of the stapes motion are non-volumetric, in that the amount of fluid in the cochlea displaced inwards, due to the inwards motion of the stapes, is equal to the volume of fluid displaced outwards, by the outward motion of the stapes.

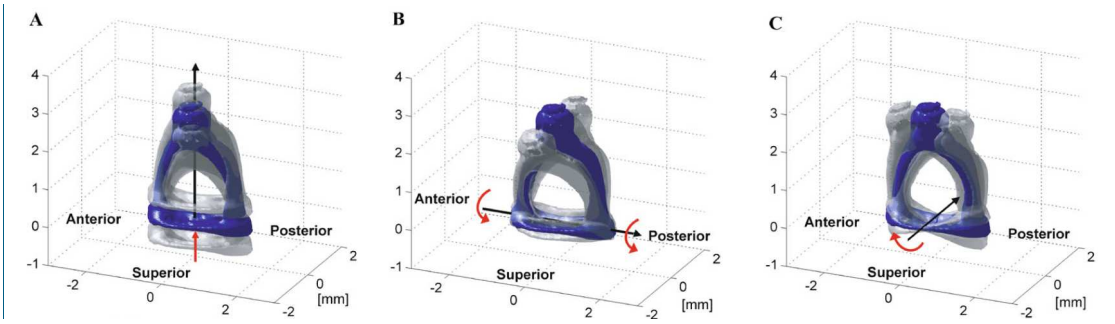

Figure 2.2: Illustrations of the three components of the stapes motion, taken from Sim et al. (2010). **A** is the piston-like motion of the stapes, **B** the rocking motion about the long axis of the stapes footplate and **C** the rocking motion about the short axis of the footplate.

Whereas, the piston-like motion is volumetric, as it causes a net volume of fluid to be displaced at the oval window.

Heiland et al. (1999) carried out a study on 10 temporal bones, where the vibrations of the stapes were measured when a pure-tone sound pressure level was generated at the tympanic membrane, simulating AC hearing. Three reflective targets were placed on the stapes footplate to aid the measurements of its motion using a LDV. Due to the locations of the targets, only the rocking motion about the short axis and the piston-like motion of the stapes could be calculated. It was found that there was very little rocking component below 1 kHz, but by 4 kHz the magnitude of the rocking and piston-like motions were equal.

Hato N (2003) carried out experiments on 10 temporal bones, again simulating AC hearing and using a LDV to measure the stapes footplate motion. However, in this study measurements were taken on five positions on the stapes footplate allowing for both the rocking motions to be calculated. The relative motion between that of the posterior edge of the stapes, due to only the rotational component, and the centre of the stapes footplate was calculated. Similarly, the relative motion between the superior edge and the stapes centre was calculated. These calculations gave a measure of the relative motion between the short axis rocking motion and the piston-like motion of the stapes. It was found that the short axis rocking component was about 20 dB lower than the piston-like stapes motion in the range of $0.1 - 1$ kHz and then rose with frequency to a peak at 6 kHz where the rocking motion was greater than the piston-like motion. The rotational velocity due to the short axis rocking was found to be greater than for the long axis rocking motion below 2 kHz, above this frequency the two rocking motions were similar. The effect of the cochlea fluid on the motion of the stapes was examined by also carrying out experiments on a drained cochlea. It was found that the draining of the cochlea had the greatest effect on the piston-like motion of the stapes, such that

the piston-like motion dominated over both of the rocking components over the whole frequency range.

Sim et al. (2010) also utilised a scanning LDV system to measure the motion of the stapes footplate when stimulated by AC, on six temporal bones. In this study measurements were taken at five locations on the footplate, in such positions that all three components of the stapes motion could be calculated. The relative motion of the rocking motion about the short axis of the stapes with respect to the piston-like motion was also calculated in this study. The rocking motion was found to be about 15 dB lower than the piston motion, up to about 1.5 Hz, and then rose to a peak at about 6 kHz. The magnitude of the rocking about the short axis was found to be greater in this study than found by Heiland et al. (1999) and Hato N (2003) at frequencies below 4 kHz, but above this frequency agreed well. In this study the two rocking motions were found to be similar at lower frequencies, but the rocking about the short axis greater at high frequencies, which is in contradiction to the results found by Hato N (2003).

In all these studies the variability between the measurements on the different temporal bone specimens was large. This is partially due to anatomical differences, for instance, Sim et al. (2010) found a large standard deviation, 8.5%, of the footplate area in temporal bones used in their study. It also could partially be due to the small scale of the stapes bone and that its displacement due to AC hearing is in the nano metre range, making it difficult to measure accurately. Whilst there are differing results between the studies, they all agree that the component of rocking motion about the short stapes axis increases with stimulus frequency and the peak response is around 6 kHz. Also, above 4 kHz in all these studies the piston-like motion is of comparable magnitude to this rocking motion.

These studies have shown conclusively that the motion of the stapes is not purely piston-like but is complex. However, just because there is a rocking component, it does not mean that this motion excites the cochlea, or that if it does that it is significant.

The classical theory is that the cochlear is excited by a net fluid flow through the cochlear windows. It is assumed that window flush with the cochlear bone is at rest position. Any motion of the window from this position is therefore due to a net fluid flow either in or out of the cochlea, depending on the direction of motion. It is the flexibility of the windows that allows for this fluid flow. Excitation via the rocking motion of the stapes is therefore in contradiction to the classical theory as this motion does not cause a net flow through the cochlear windows. There has been much discussion in the literature whether this motion causes a hearing sensation, and if it does, whether is it significant. Experimental evidence of the measured pressure in the cochlear, due to AC excitation, supports the theory that a rocking motion does not contribute to the overall cochlear response (Decraemer et al., 2007; Voss et al., 1996; de La Rochefoucauld et al., 2008). However, the Huber et al. (2008) study suggests that the rocking components may lead to a hearing response which could be significant to the overall response in a healthy

cochlea. It should be noted that all these studies were carried out on animals and not humans and so the assumption is made that the processes in all mammalian cochlea are the same.

The rocking motion of the stapes has been investigated using a mathematical model of the cochlea in Edom et al. (2013). Edom et al. (2013) investigated the rocking motion about the short axis of the footplate and the piston-like motion using a 2D box model of the cochlea, solved using the Navier stokes equation. It was found that the non-volumetric rocking stapes can excite a travelling wave along the BM, however, it is of a much smaller magnitude than that of piston-like motion.

It is possible that even if the rocking motion of the stapes does not significantly contribute to the cochlear response in a healthy cochlea, it does so in a diseased one. Round window atresia effects a very small percentage of the population, however, its affect on the hearing thresholds can potentially lead to a greater understanding of the workings of the cochlea (Linder et al., 2003). Round window atresia is when the round window is not present, either due to not forming properly at birth or a due to bony growth over the round window, similar to otoscerlosis. Patients with this condition present with a reduction of both AC and BC hearing, with a air-bone gap at low frequencies (Linder et al., 2003; Nageris et al., 2012). Even with such a hearing loss, some sound is still detected through AC. Since the round window is immobile, then the classical excitation via a net volume displacement at the cochlear windows is not possible. It has been suggested that the rocking motion of the stapes could be causing the hearing response in these cases, or alternatively that the 'third window' is playing a role, creating a volumetric excitation mechanisms (Edom et al., 2013).

2.2.2 Sound Pressure due to Bone Conduction in the Ear-Canal

One of the BC pathways listed in Section 2.1 is due to the vibrations of the skull stimulating a compression and expansion of the ear canal. These vibrations will produce a sound pressure in the ear canal, which then is transmitted to the cochlea in the conventional way, via the tympanic membrane and middle ear ossicles. In this pathway the cochlea is excited in the same ways as AC, it is just the generation of the source of the pressure wave that differs. The significance of this pathway at low frequencies has been debated in the past and it has been reported that a sound pressure is present in the ear canal when the skull vibrates. However, Stenfelt et al. (2003b) found that the sound pressure in the ear canal is about 10 dB lower when excited by BC than at the air conduction hearing threshold at frequencies below 2 kHz and a greater difference at higher frequencies. This result, along with the evidence that patients with hearing diseases that causes a conductive hearing loss have normal BC thresholds at low frequencies, strongly suggests that this mechanisms of BC hearing is not a significant pathway in the healthy ear (Stenfelt et al., 2003b).

The creation of sound pressure in the ear canal by vibrations of the skull, may be a negligible pathway in normal conditions, however, when the ear is occluded, it has been shown that this mechanisms becomes significant at low frequencies. An example of this effect is the increase in hearing one's own voice when fingers are placed in ones ear. The placement of the occluding device is important, because if it is too far down the ear canal, no occlusion effect is experienced (Stenfelt et al., 2003b).

The significance of this mechanisms lies in its generation of sound pressure by the vibration of the ear canal. Once this has been established the cochlea is excited in the same manner as with AC. In this thesis, this pathway is not investigated because this thesis is mainly concerned with the modelling of the cochlea not the ear canal. Also, it have been shown to be a negligible pathway under most conditions.

2.2.3 Inertia of the Middle Ear Ossicles

Another BC pathways which utilises the middle ear ossicles is the inertia of the middle ear. This pathway is where vibrations of the temporal bone induce a motion of the middle ear ossicles relative to the cochlea. The ossicles are supported by ligaments to the temporal walls of the middle ear cavity, thus when the skull vibrates, the ossicles vibrate due to their own inertia which can cause a relative motion between the stapes and the oval window. In much the same way as AC excites the cochlea, via a motion of the stapes, so too does the middle ear inertia component. The significance of this mechanism to the overall effect of BC hearing has been investigated by many authors, but is still it not fully understood. It is difficult to predict its effect on the overall BC response, by experiment or patient perception data, due to the inability to isolate it from the other BC pathways.

It has been theorized that this component is significant in the region of 2 kHz but not at significantly higher or lower frequencies. There is experimental evidence that suggests that the inertia of the middle ear component is not significant at low frequencies, but could be at frequencies between 1.5 kHz and 3.1 kHz (Stenfelt, 2006). A comparison was made between the motion of the stapes, when temporal bones were stimulated at the AC threshold and at the BC threshold. Corrections to the data and estimates of the relative thresholds on stimulating temporal bones were made in order to calculate a reasonable comparison. The argument of this work is that both AC and the middle ear inertial component of BC stimulate the cochlea ultimately via the stapes, and so the motion of the stapes at threshold, must be similar when excited by BC and AC for the middle ear inertial component to be significant. It was found that this was true between 1.5 kHz and 3.1 kHz. A limitation of these results is that experiments were carried out on temporal bones and only excited by vibrations in one direction and so the full effect of compressional waves were not included. However, results from a cadaver showed similar magnitudes and phase to the temporal bone measurements, suggesting that the results

from the temporal bone experiments are not too dissimilar from reality (Stenfelt et al., 2002). Another limitation is that the stapes motion was calculated with the cochlea still intact and so the vibration will have induced the fluid inertia component of BC as well. This could force the motion of the stapes from inside the cochlea, and so alter the overall response of the stapes. It was found that draining the cochlea, and hence removing the fluid inertia component, increased the stapes response, however, these experiments were carried out when the ossicles chain was disrupted.

Mathematical models have been utilised to develop an understanding of the motion of the middle ear ossicles due to vibrations of the temporal bone. In the 1930s Bárány (1938) deduced an expression for the motion of the ossicles due to vibrations of the skull from the moment of inertia of the ossicles. In this model it was assumed that the motion of the ossicles was only in one direction and the skull only had one mode of motion. Bárány (1938) found that the location of the centre of gravity of the ossicles had an effect on the response of the ossicles due to vibration. This simple model was later used in 2003 by Mason (2003), who used it to predict the effect of the ossicles anatomy in different species of golden moles. Some species of golden moles have enlarged ossicles, and are thought to be sensitive to seismic vibrations, as they have been observed burying their head in sand and orienting themselves towards prey. Mason (2003) used the model to predict the responses of the ossicles, due to vibrations of the different golden mole species, by changing the parameters of the model so that they reflected the anatomical geometry data. This model was utilised to understand the effects of different anatomy in mammals, and provided evidence to a theory that explains certain behaviours of the golden moles.

This simple model have been used to described the function of the middle ear motion by simplifying and lumping aspects of the middle ear together. It has not allowed for detailed analyses of the motion of the ossicles. Modern day modelling techniques, such as finite element modelling, have allowed for detailed investigations of the motion of the ossicles. A parallel advance in experimental techniques has enabled more detailed measurements of the motion of the ossicles for the models to be validated against.

Homma et al. (2009) carried out experiments on temporal bones, and used a LDV to measure the response of the middle ear ossicles to stimulus. The motion of the middle ear was investigated when excited by two methods: shaking the temporal bones in the plane perpendicular to the tympanic membrane, simulating the middle ear inertia component of BC hearing, and applying a pressure at the tympani membrane, simulating AC hearing. It was found that the "dominant mode of motion" and the respective natural frequency of the middle ear ossicles is different in AC than BC. The average of the primary resonance was found to be 1.72 kHz and 1.26 kHz for BC and AC respectively. The BC result agrees with those from Stenfelt et al. (2002) who carried out experiments on temporal bones and measured the stapes motion while the bone was

shaken, as shown in Fig. 2.3. In this study, it was found that the resonance frequency was between 1.5 kHz and 2 kHz.

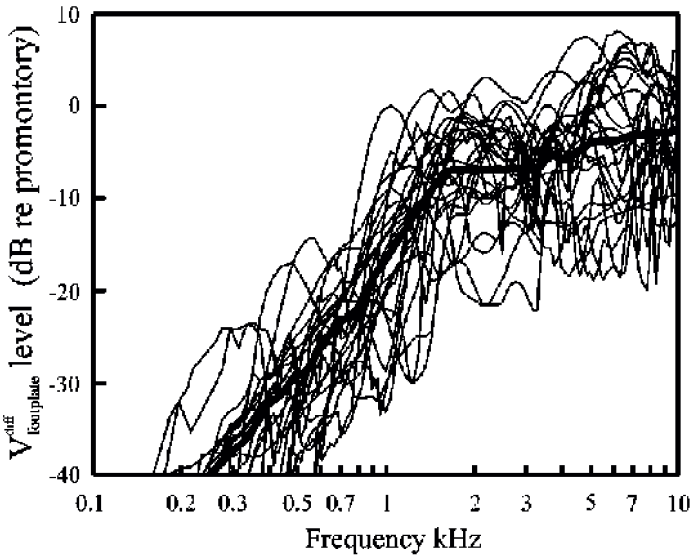

Figure 2.3: Relative motion between footplate and promontory bone, measured on temporal bones connected to a shaker. Thin lines are individual results and thick line average result. Reprinted with permission from Stenfelt et al. (2002). Copyright 2002, Acoustic Society of America.

Homma et al. (2009) built a finite element model of the middle ear ossicles, using knowledge gained from experimental results, along with other parameters. The dominant motion of the ossicles for BC hearing was shown to be a pivoting motion about the incus ligament, Fig.2.4, when shaken approximately perpendicular to the tympanic membrane plane. This is a different dominant mode of motion than that was found by AC stimulus, where the motion is 'hinging' or 'rocking' about an axis from the incus ligament to a point on the mallues handle.

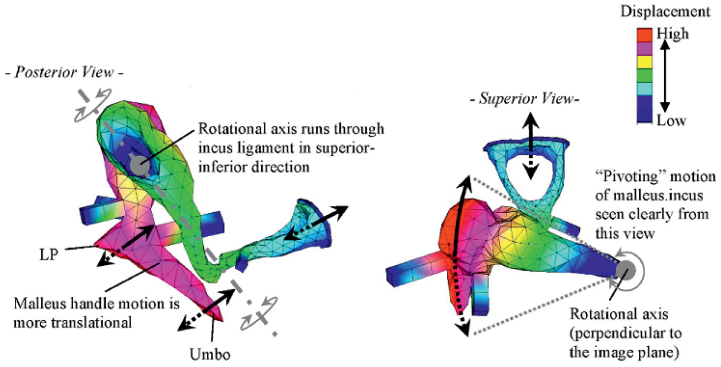

Figure 2.4: Motion of the middle ear ossicles in response to vibration of the temporal bone in the direction perpendicular to the tympanic membrane plane. Reprinted with permission from Homma et al. (2009) copyright 2009 Acoustic Society of America.

2.3 Hearing Pathways that Do Not Involve the Middle Ear Ossicles

The three BC pathways which do not transmit vibration to the cochlea via the middle ear ossicles are introduced and discussed in this section. They include, transmission of pressure from the Cerebrospinal fluid, compression and expansion of the cochlea walls and inertia of the cochlear fluids.

2.3.1 Transmission of Pressure from the Cerebrospinal Fluid

One pathway by which skull vibrations have been suggested to be transmitted to the cochlea is not via the skull bone but through the soft biological material such as the brain, soft tissue and fluid, including the cerebrospinal fluid (CSF). It is thought that fluid channels such as the cochlear aqueduct, vestibular aqueduct and blood vessels are capable of transmitting pressure in the cranium to the cochlea. The cochlear aqueduct directly connects the CSF to the perilymph fluid in the cochlea and has potential to be a main component of this pathway. It has been found that the pressure changes in the CSF are translated to the cochlea fluids in Yoshida and Uemura (1991); Marchbanks and Reid (1990); Traboulsi and Avan (2007) for instance. However, these studies do not examine the acoustical transmission and are not concerned with excitation of the cochlea to generate a hearing response. It is thought that the cochlea aqueduct acts as a low-pass filter, which would suggest that it would not be capable of transmitting acoustical energy in the hearing range (Marchbanks and Reid, 1990; Traboulsi and Avan, 2007).

Freeman et al. (2000) carried out experiments on fat sand rats, where a bone vibrator was applied to various locations and a hearing responses was monitored by recording the auditory nerve brainstem evoked responses (ABR). ABR is the detection electrical signals in the brainstem generated by acoustic stimulation of the cochlea via electrodes placed on the skull. It is a process than can be used to provide information about the auditory function. It is not used to predict hearing threshold when behavioural methods can be used, but it is a common approach to predict hearing function in animals.

In this study, an ABR response was recorded when the vibrator was placed on an intact skull, on the bone of a skull with a craniotomy and directly onto the brain. The results showed that an ABR response could be detected when BC stimulation was applied directly onto rats brain. However, the threshold when the bone vibrator was applied directly on the brain was 20 dB lower than when the bone vibrator was applied to the intact skull. In this study the transducer was applied directly to the brain, however, in normal conditions, the transmission of skull vibrations to the brain is most likely to

be very small. Thus, this pathway may not be significant, as the threshold difference is already 20 dB between stimulations on an intact skull and the brain.

The effect of reducing the intra-cranial fluid volume on the hearing response of rats was also investigated in Freeman et al. (2000). The intra-cranial water content was reduced in rats by injecting them with a drug called mannitol. With this drug administered to the rats, the ABR threshold for AC was lowered by 3.9±3.4 dB which was suggested to be due to the increased cochlear blood flow. However, the BC ABR threshold of an intact skull was elevated on average by 7.5 ± 3.8 dB . It is argued that the reduction in intra-cranial fluid decreases the ability to transmit pressure alterations to the cochlea, and hence, the elevation in the BC threshold is evidence for the transmission of pressure alteration in the cranial fluid to cochlea being a major BC pathway. It is proposed that because of the decrease in AC threshold when the drug is applied, that the actual BC threshold change could be greater than measured. It has been shown that reducing the amount of cranial fluid will reduce the pressure in this fluid, which will be translated to the cochlea (Yoshida and Uemura, 1991). However, there is not a complete understanding of what effect this drug has, given that it is not understood why the AC thresholds changes and so it can not be said for certain that the changes in BC threshold are due to the reduction of the transmission of pressure through intra-cranial fluids. It is possible that whatever mechanisms induced by the drug to lower the AC threshold could also have an effect on other BC pathways.

Sohmer and Freeman (2004) used pairs of rats and guinea pigs, where their cranial fluids were connected via a plastic tube filled with saline solution, to investigate the transmission of CSF pressure to the cochlea. A vibrator was placed on the skull of animal A to stimulate BC while an ABR was recorded in animal B. It was found that the level of stimulation needing to be applied to animal A in order to give a response in animal B was $15 - 30$ dB higher than the ABR threshold of animal B when the vibrator was applied to the cranial cavity (Sohmer and Freeman, 2004). Precautions were taken to make sure that vibrations of the tube or electrical signals were not transmitted from one animal to the other. In was concluded that pressure alterations in the fluid were transmitted between animal via the fluid in the tube, and that this was further evidence that there is a significant non-osseous mechanism of BC hearing.

All of these experiments were carried out on animals, which, since their the ears are similar to humans, give an insight to the possible hearing mechanisms but they cannot give a total understanding. Experiments carried out on humans included studies on neonatal babies, neurosurgical patients and normal hearing females (Sohmer et al., 2000).

The ABR thresholds of neonatal babies were compared with the vibrator was placed on a bony part of the skull and placed on the fontanelle. When the vibrator was placed on the fontanelle it was found that large vibrations of the skull were not induced. Sohmer et al. (2000) found the thresholds to be similar in both sites and in one case lower when

stimulated on the fontanelle. It was concluded that the ABR response was generated through soft tissue and through minimal if any vibration of the skull. BC thresholds of neurosurgical patients where measured using an audiogram when a bone vibrator was positioned on their intact skull and also on their craniotomy. It was found that the thresholds in both positions were comparable. Audiometric thresholds of 10 young females were obtained when stimulated by a bone vibrator at several sites - eye, forehead, mastoid and temporal bone and then compared. The eye is considered to be a natural craniotomy in which it is likely that vibrations are transmitted through the CSF and soft tissue to the cochlea. Sohmer et al. (2000) considered the audiometric thresholds measured when the eye was vibrated to be similar to the thresholds of the other sites on the skull. However, it was stated that the thresholds when the eye was stimulated were significantly higher than when the mastoid was vibrated. In all these experiments, the soft tissue is directly stimulated by a transducer, which would induce much greater soft tissue vibrations than if the skull was directly stimulated. Hence, these results do suggest that hearing can occur through soft tissue, however, it can not be concluded that this pathway is significant in a normal environment from these results.

It is clear from the studies discussed above that this method of hearing and its significances are not full understood. There is some evidence that this pressure can be transmitted to the cochlea, inducing a hearing perception, but it is not clear if this is a significant pathway under normal conditions. Also, the patency of the cochlea is greatly variable between people (Gopen et al., 1997), which suggests that this mechanism of hearing could have a varied effect on different people. This pathway has not been investigated mathematically in this thesis, as there is insufficient experiential evidence to suggest that it is a significant pathway of BC hearing.

2.3.2 Compression and Expansion of Cochlear Walls

The vibrations of the skull can cause an expansion and compression of the cochlea walls. This deforms the space inside the cochlea which causes the fluid to flow between the scalae, generating a wave motion along the BM. Below about 1 kHz the skull vibrates approximately like a rigid body (Hakansson et al., 1994; Stenfelt and Goode, 2005). When the skull vibrates as a rigid body there is no compression and expansion of the cochlear walls. Therefore this mode of BC only has the potential of contributing to BC hearing from skull vibrations mostly above 1 kHz. It would be very challenging to carry out experiments to investigate this mechanism due to the difficulty of measuring the compression and expansion of the cochlear walls accurately. It is however suggested, to be an important BC pathway at high frequencies, when the skull bone exhibits deformations due to vibrations.

Tonndorf (1962) investigated this pathway by experimenting on a physical box cochlea model. The model consists of a rectangular box, about five times the length of a human

cochlea, separated length ways by an elastic membrane that acts as the BM and creates the two scalae. A space is at the end which acts as the helicotrema. There are two elastic structures on the ends of the box which imitate the oval and round window, as shown in the schematic diagram of the model in Fig.2.5. The model was adaptable such that the relative volumes of the scalae and stiffness's of the windows can be altered.

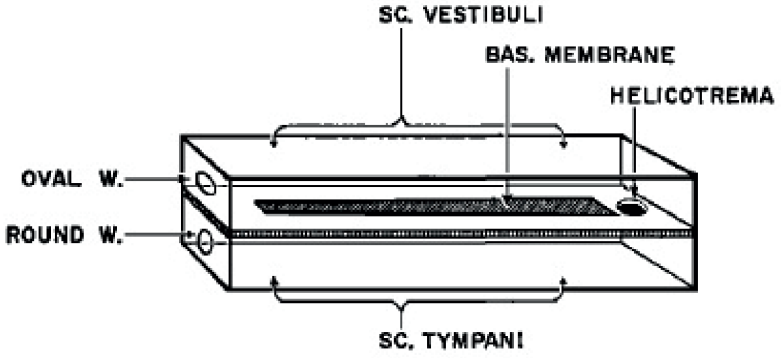

Figure 2.5: Schematic diagram of physical cochlear model used in Tonndorf's experiments. Reprinted with permission from Tonndorf (1962). Copyright 1962, Acoustic Society of America.

It was found that the elastic membrane, representing the BM, was not stimulated into motion by vibrations when the model had scalae of equal volume and identical stiffness of the windows. A response from the membrane did occur when the compliance windows were not equal or the sizes of the scalae were not identical.

A model representing a more anatomically realistic cochlea, where the scalae were of unequal volumes and the oval window was stiffer than the round, was also used. When this model was vibrated but had rigid windows, a travelling wave of small amplitude along the parting membrane was induced. This result suggests that some hearing sensation can be achieved by this BC pathway without any openings in the cochlea. The concept of the displacement of the membrane with unequal scalae and closed windows was illustrated by Tonndorf (1962) using the idea of a sphere partitioned unequally into two chambers, V and T, by a flexible membrane fixed to the periphery, as shown in Fig. 2.6. This is obviously a gross simplification but demonstrates the concept well.

When the sphere is lengthened in the horizontal direction, Fig. 2.6(b), the volume of T' decreases, relative to T, due to the displacement of the membrane from V' into T'. As the sphere is lengthened in the vertical direction, Fig. 2.6(c), the reverse happens. The volume of T" relative to T, is increased due to the displacement of the membrane from T" into V".

A lumped parameter model of the cochlea was used to investigate this BC pathway, along with the fluid inertia pathway in Stenfelt (2014). It was predicted that this pathway was

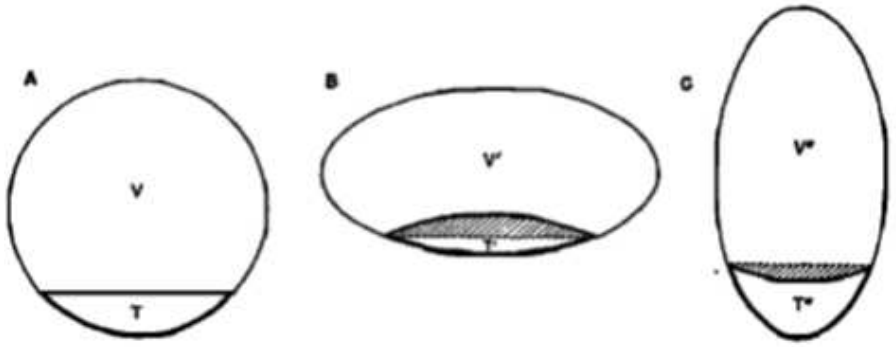

Figure 2.6: Diagram illustrating that the BM will still be displaced when the cochlea is vibrated even if the windows are rigid by the use of a sphere separated two chambers, V and T, by a flexible membrane fixed to the periphery. 3(a) no distortion of space, 3(b) horizontal lengthening 3(c) vertical lengthening. Reprinted with permission from Tonndorf (1962). Copyright 1962, Acoustic Society of America.

less effective at exciting the cochlea over the frequency range of 100 Hz to 10 kHz, though it was comparable at the extremities of this frequency range. The lumped parameter model used was clearly a very simplified representation of the cochlea and so the results must be taken with some caution, however, it does suggest that this component is not as significant as the fluid inertia pathway to the overall response, at most frequencies.

2.3.3 Inertia of Cochlear Fluids

Vibrations of the temporal bone cause a motion of the cochlear fluids by inducing an inertial forces upon them. In a healthy cochlea, fluid is forced out of the complaint oval and round windows and it is this net flow through the cochlear that ultimately generates the BM travelling wave (Kim et al., 2011). Stenfelt et al. (2004) measured the volume of fluid displaced at the oval and round window on temporal bones which were vibrated at 1 mms^{-1}, which is approximately equivalent to $80-100$ dB HL (hearing level) (Stenfelt and Goode, 2005). The volume displacement was less than 1 millionth of the total fluid volume in the cochlea, which gives an indication of the small scale of motion of fluid necessary for cochlear excitation.

The significance of this pathway to the overall BC response has been debated within the literature. If the middle ear inertia component is assumed to only have a significant effect in the 2 kHz region, then the components which directly stimulate the cochlear must be the most significant. This leaves the fluid inertia and compression and expansion components, as there is little evidence as yet that suggest that the fluid pressure transmission significantly contributes to the overall response.

Investigations were carried out on the cochlear window response to the fluid inertia component of BC and compared with that of AC. Stenfelt et al. (2004) investigated the fluid displacement at the oval and round windows by experimenting on temporal bones stimulated by BC. A diagram of his set-up is shown in Fig.2.7

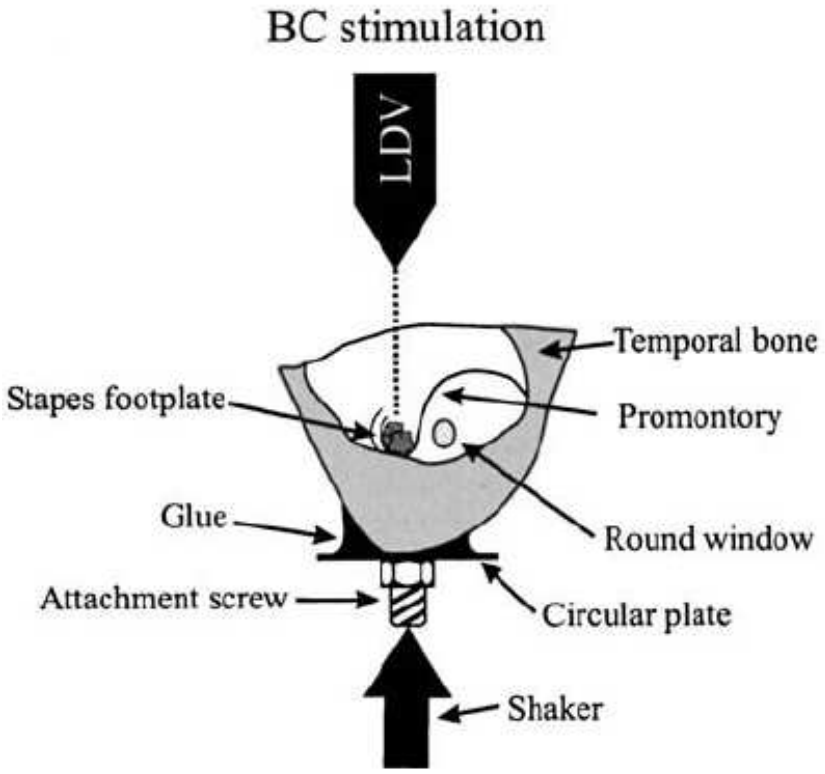

Figure 2.7: Experimental set-up of temporal bones used by Stenfelt et al. (2004). Reprinted with permission from Stenfelt et al. (2004) Copyright 1962, Acoustic Society of America.

A LDV was used to take measurements of the stapes footplate and the round and oval windows. A shaker was attached to the specimen to stimulate BC. The tympanic membrane and the middle ear ossicles, apart from the footplate, were removed from the specimen. Only the bone surrounding the cochlea and semi-circular canals were not removed. Results on temporal bones were compared to measurements on a cadaver head and were found to be comparable. In Fig.2.8, the graphs displaying the volume displacements and phases of the oval and round windows found by Stenfelt et al. (2004), for both BC and AC stimulation, are shown. The AC results are given to illustrate the differences in cochlear window responses due to the different excitation mechanisms.

It would be expected that the fluid displacement at each window would be equal and 180° out of phase from each other. The results of Stenfelt et al. (2004) clearly show that this is not the case for BC, as shown in Fig.2.8. When subjected to AC stimulation, however, the fluid displacement at the windows was seen to be similar and out of phase by 180° as expected. Therefore it can be concluded that the differences to the fluid

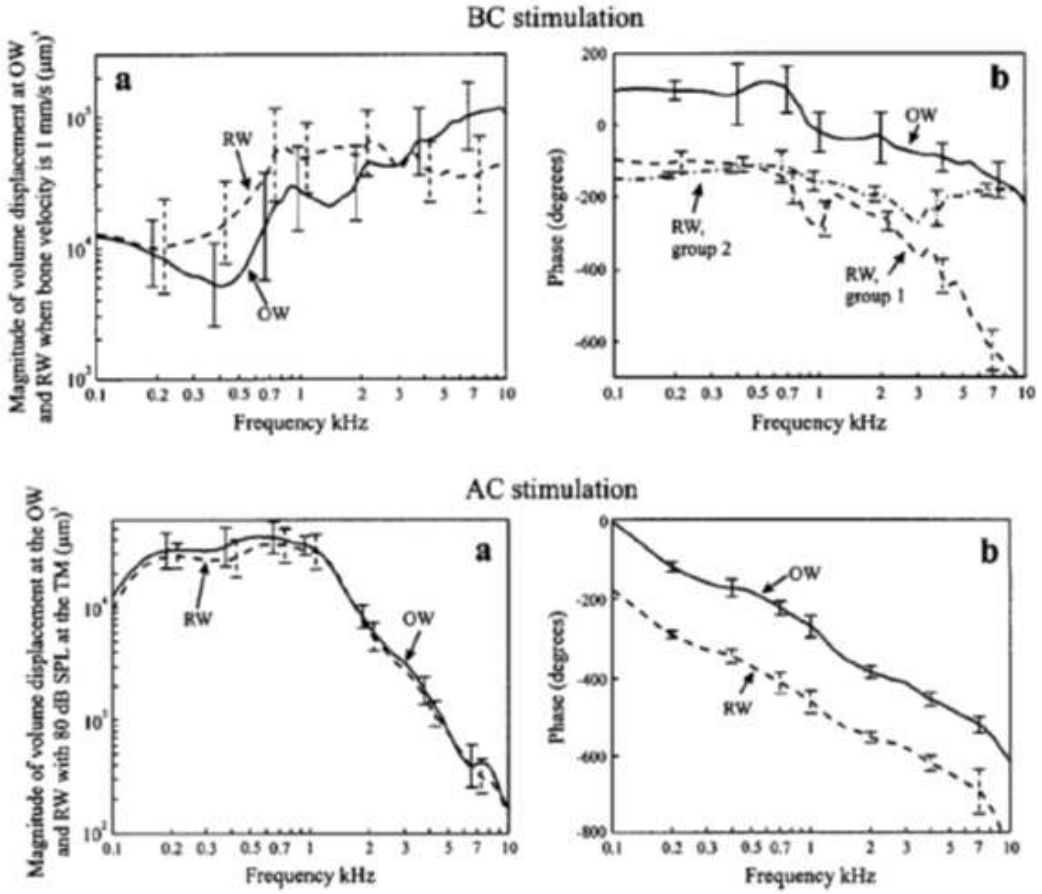

Figure 2.8: Magnitude and phase of the oval and round window volume displacement when the cochlea is simulated to be excited by BC and AC. Reprinted with permission from Stenfelt et al. (2004) Copyright 1962, Acoustic Society of America.

displacement is inherent to BC. Stenfelt et al. (2004) hypothesized that the reason for this discrepancy in displacement and in phase was due to a combination of several factors: the fluid flow through the third window, the bending of the cochlear bone and the compression and expansion of the cochlea walls and cochlea fluid. In particular, this research suggests that the 'third window' may have a significant role to play in the mechanisms of the fluid inertia component of BC, as will be explored later in this thesis.

2.4 Hearing Impairments that Cause Conductive Hearing Loss

Hearing loss is separated into two categories, sensorineural and conductive, although mixed hearing loss can also occur, which is a combination of the two. The different effects that the types of hearing loss have on BC thresholds means that the measurement of the thresholds can be used to help distinguish between the types of hearing losses.

Sensorineural hearing loss is due to the loss of function of the production or processing of electrical signals, and therefore is due to impairments in the inner ear, nerves or brain. This means that the this type of hearing loss effects both BC and AC hearing to the same degree.

Conductive hearing loss is due to the reduced ability to transfer acoustical energy to the cochlea via the outer or middle ear and so an increase in the AC hearing thresholds are seen. The causes are often, but not exclusively, due to malformations of the middle ear. There are varying effects on the BC thresholds which are dependable on the abnormalities which cause the conductive hearing loss. However, conductive hearing loss always produces an increase in the AC thresholds that is greater than that in BC thresholds. There is therefore a difference in BC and AC thresholds which is termed an air-bone gap.

There are multiple ear malformations and diseases that can cause a conductive hearing loss, due to a reduction to the flow of acoustical energy from the outer to inner ear. Their effect on hearing thresholds can lead to a greater understanding of the working of the cochlea. If the ear canal becomes obstructed it will prevent the progression of sound to the tympanic membrane, and hence a conductive hearing loss. Possible causes include, Otitis Externa which is an infection of the auditory canal and a build-up of earwax that causes a blockage. These are temporary problems which can be treated. Patients could experience a reduction in AC hearing, but possibly also a decrease in BC thresholds, due to the occlusion effect.

Otitis Media is an inflammatory infection of the mucous-membrane lining of the middle ear cavity. The infection in the middle ear space causes a reduction in the ability of ossicles motion. Patients with this condition exhibit conductive hearing loss, which, if the disorder becomes chronic, will have a lasting effect.

Otosclerosis is a disease which causes an abnormal bone growth on the ossicles, most often the over stapes which restricts its movement and hence its ability to stimulate the cochlea. This is a degenerate condition and often eventually completely immobilises the stapes. This disease reduces, if not eliminates, the contribution to BC hearing from the components which transmit acoustical energy through the middle ear ossicles. Since it has been shown that the pressure in the ear canal component is insignificant in most cases, only the contribution of the middle ear inertia component is reduced. BC audiograms of patients presenting with otosclerosis are relatively normal, apart from a 'notch' that appears around 2 kHz, named 'Carhart's notch' after Carhart who discovered it (Carhart, 1950, 1971). The removal of the middle ear inertia component of BC is attributed to the elevated BC threshold around 2 kHz, thus it is theorized that this pathway is significant around 2 kHz. There is evidence to suggest that the 'notch' does not always appear at 2 kHz for all patients but at other frequencies (Perez et al.,

2009). This was reasoned to be potentially due to other fixations of the middle ear ossicles, such as incus, but could also be due to variations between patients ossicles.

Clinical audiograms are only measured at a few frequencies, (100 Hz, 500 Hz, 1 kHz, 2 kHz, 4 kHz) and therefore detail analyses of frequencies response of a patient with otosclerosis has not been found in the literature. A complication of this disease is that the process that causes a bony growth at the stapes, may also cause a malformation of the cochlea. This means that a sensorineural hearing loss may also be present at the same time, making it harder to diagnose. It has been argued that the immobilisation of the oval window also restricts fluid flow within the cochlea, which will affect the other pathways of BC hearing. The increase in threshold being solely due to the removal of the middle ear inertia contribute may not but fully valid (Stenfelt et al., 2002).

Some diseases which cause a permanent conductive hearing loss are treated with a stapedectomy or stapedoctomy, where in both cases a prosthesis is used at the stapes to stimulate the cochlea. Either the whole stapes is removed, stapedectomy, or a small hole is made in the fixed stapes and the prosthesis placed in the hole, stapedoctomy.

This treatment is often used for patients with otosclerosis, and the reduction of BC threshold after the stapedectomy or stapedoctomy gives further insight into the significance of the middle ear inertia. An analysis of 2405 cases of treated otosclerosis concluded that the loss of BC thresholds is 10 dB at 250 Hz, 15 dB at 500 Hz, 15 dB at 1 kHz, 20 dB at 2 kHz and 15 dB at 4 kHz (Ginsberg et al., 1978). This is further evidence for Carhart's notch, but the data also suggests there is great variation between patients. More recent work shows similar results for the increase in BC hearing when otoscelrosis was treated, for instance in Quaranta et al. (2005). The decrease in threshold due to surgery suggests that it is attributed to the reintroduction of the middle ear inertia component, but, as previously stated, this could also be due to the effect on other BC pathways.

2.4.1 Non-Volumetric Motion at the Round Window

A relatively new technique to treat certain diseases which cause conductive hearing loss, including otoscerlosis, is through artificial excitation of the round window. This is where a floating mass transducer is placed on the round window, and so vibrations are transmitted to the cochlear via the round window instead of conventionally through the oval window. Patients who have received this procedure have shown to have an increase in hearing thresholds and speech intelligibility (Colletti et al., 2006; Kiefer et al., 2006; Beltrame et al., 2009; Cuda et al., 2009). It has also been shown, that in certain cases this method of treatment may be more beneficial than other more traditional treatments, such as bone anchor hearing aids (Mojallal et al., 2015) or a total ossicular replacement prosthesis (Colletti et al., 2009). The cases that have been discussed in the literature

include patients with multiple hearing problems such that not in all cases, but in some, the oval window is completely immobile. A great variation in results has been found, which is likely to be due to the variation in the functionality of cochlea and middle ear. However, the largest cause of this variation is potentially due to the coupling between the transducer and the round window (Schraven et al., 2011).

The size and shape of the round window varies greatly between different cochlea, whereas the area of the transducers in contact with the round window was typically 1.8 mm^{-2}. It is likely, due to the relative size and shape of the window and transducer that the whole of the window was not covered by the transducer. Weddell et al. (2014) explored the idea of the round window acting simultaneously as a pressure release as well as stimulation location due to the round window being only partially occluded through experiments that were carried out on guinea pigs, as well as theoretical calculations. It was proposed that due to the relatively high impedance of the middle ear ossicles looking out from the cochlea, the section of the round window not occluded by the transducer was able to act as a pressure release. It was found that the stiffening of the oval window did not effect the cochlear response. This led to the conclusion that the mobility of the oval window has little function in the mechanism that excites the guinea pig cochlea, when excited by a partially occluded round window. The driving mechanism in this case was proposed to be a near-field, jet like, component of the pressure distribution that extended from the round window, generating a travelling wave along the BM.

2.4.2 Third Window Lesions

It has been documented in the literature that third window lesions, which are any abnormal opening in the inner ear, excluding the two cochlear windows, can cause an air-bone gap similar to that of those who have conductive hearing loss (Govaerts et al., 1999; Merchant SN, 2008). This has led to misdiagnoses, where a middle ear condition is assumed rather than an inner ear. Two forms of third window lesion are discussed here; large vestibular aqueduct syndrome and semi-circular canal dehiscence.

Large vestibular aqueduct syndrome, as the name suggests, is when the vestibular aqueduct is abnormally large. The link between hearing loss and an enlarged vestibular aqueduct was first discovered in 1978 by Valvassori and Clemis (1978) and coined 'large vestibular aqueduct syndrome'. In this study a large aqueduct was defined as having a diameter larger than 1.5 mm, however, later studies have used different definitions (Gopen et al., 2011). This condition generally occurs alongside other conditions and therefore the influence of an enlarged aqueduct is hard to decipher. It has been reported that patients with a large vestibular aqueduct can present an air-bone gap at low frequencies (Govaerts et al., 1999; Mimura et al., 2005; Merchant et al., 2007a; Merchant SN, 2008; Gopen et al., 2011).

The reason for an air-bone gap is unclear and there are multiple theories (Gopen et al., 2011). An increase in cochlear fluid pressure is often seen alongside this condition, and it is proposed that this has an increasing effect on the AC threshold. It has also been suggested that the reduction in AC thresholds is due to a 'third window' effect, where the decreased admittance of the oval window side of the cochlea shunts the acoustical energy away, causing a reduction in the pressure difference across the BM and hence increases the threshold. The increased admittance is suggested to decrease the BC threshold and hence an air-bone gap is seen (Mimura et al., 2005; Merchant SN, 2008; Merchant et al., 2007a).

Semi-circular canal dehiscence describes an opening in the bone overlying the superior semicircular canal. It has been reported that the auditory symptoms of this condition include an increase in the patients AC thresholds and either an unaffected or decrease in BC thresholds at low frequencies, creating an air-bone gap (Minor et al., 2003; Merchant et al., 2007b; Rosowski et al., 2004). Other symptoms of this condition are vestibular, such as vertigo. However, due to the air-bone gap this condition has been misinterpreted in patients as otosclerosis and so stapedectomies have been carried out that have not been successful (Minor et al., 2003). The creation of an air-bone gap in a patients audiogram is debated in the literature, but there is strong evidence to suggest that it is due to energy been shunted away from the cochlea with a AC stimulus and due to a greater impedance difference across the BM when the stimulus is the compression component of BC (Rosowski et al., 2004; Merchant et al., 2007b).

A theoretical investigation into the effect of a dehiscence by Rosowski et al. (2004), where a simple elemental model of the auditory system was used predicted a decrease in AC threshold and an increase of BC, due to the compressional component, at low frequencies. The magnitude of the corner frequencies seen with a AC stimulus was related to the relative impedances between the cochlea and the dehiscent canal. It was found that the behaviour of the compressional component of BC was sensitive to the symmetry of the resistances of the two fluid chambers; a combination of the impedance of the middle ear and acoustic mass of the semi-circular canal and the relative impedances of the cochlea windows. This was a simple model, but provided evidence that the reason for the air-bone gap is due to the change of impedance of the cochlea, which resulted in different effects on the AC and BC thresholds. It has been suggested that the large vestibular aqueduct syndrome effect on the hearing thresholds is due to a similar reason. A 3D finite element model of the cochlea and middle ear was used to investigate this condition. It was found that the shape and position of the dehiscence had a large effect on the perceived hearing as well as the direction of vibration causing BC (Kim et al., 2013).

2.5 Conclusion

There are multiple pathways by which the cochlea can be excited to produce a hearing sensation besides from the conventional AC. These include BC hearing and the artificial excitation of the round window. Hearing through BC can be separated into five different pathways, which all transmit vibrations of the skull to the cochlea.

The middle ear ossicles are a delicate complicated system, which are fundamental in the transmission of vibration from the ear canal to the cochlea. They are utilised in both AC and two BC pathways, sound pressure in the ear canal and the middle ear inertia. Their motion, when induced by AC, has been shown to be composed of three components, a piston-like motion as well as two rocking motions. The experimental data in the literature is conflicting over the relative magnitudes of these components, but there is general consensus that the rocking components increase with frequency. There is debate within the literature if a rocking motion of the stapes, which is non-volumetric, would produce an excitation of the BM, and if so, if it would be significant. It has been shown by the use of a simple box model of the cochlea that a travelling wave can be induced by a the rocking motion of the stapes, however, in a healthy cochlea its efficiency is much less than a piston-like motion (Edom et al., 2013).

Sound pressure in the ear canal can be induced by vibrations of the skull compressing and expanding the walls of the ear canal. This sound pressure is then transmitted to the cochlea via the middle ear ossicles in the same was as for AC hearing. This component of BC has been shown to be insignificant, unless the ear canal is occluded.

The vibrations of the skull are also transmitted to the middle ear ossicles where they cause a relative displacement between the surrounding temporal bone and the ossicles, ultimately exciting the cochlea via the stapes. It is suggested that this BC pathway is only significant in the mid frequency range around 2 kHz. The predominant motion of ossicles have been shown to differ from that of AC and where resonance due to vibration excitation is about 1.7 kHz.

The three other BC pathways do not utilise the middle ear ossicles in transmitting the vibration of the skull to the cochlea. It has been theorised that there is a transmission of pressure from the cerebrospinal fluid, induced by skull vibrations, to the cochlea which causes a hearing response. It is thought that the vibrations are transmitted through the 'third window', primarily the cochlear aqueduct. Experiments on animals and humans suggest that this is a possible method of hearing. However, the relative significance of this pathway compared with other BC pathways is not clear. Due to the variation in the opening of the cochlear aqueduct between people, it may be that there is great variation between the effectiveness of this pathway. This also suggests that this pathway is generally not a significant one.

A compression and expansion of the cochlear walls are thought to be caused by the vibrations of the skull. Due to the asymmetry of the cochlea this can cause a travelling wave along the BM. The significance of this pathway is unknown but it has a greater potential of having a significant effect at higher frequencies when the vibrations of the skull bone cause deformations. It is predicted to have a lesser contribution to the total BC response than the fluid inertia pathway by the results from a lumped parameter model of the cochlea (Stenfelt, 2014).

The vibrations of the temporal bone of the skull also impart inertia forces on the fluid, which can cause a travelling wave along the BM. The fluid forced out through the cochlear windows due to the vibrations of the cochlea, has been shown to be what ultimately generates the BM travelling wave. The fluid displaced at both windows has been shown to be not equal for this pathway. Thus suggests the 'third window' may have a significant function when excited by this hearing mechanisms. The importance of this pathway on the total response is debated within the literature, but it is thought to be most significant at low frequencies.

Conductive hearing loss is due to the a restriction in the ability of acoustical energy to be transmitted to the cochlea via the conventional AC pathway. This is often caused by a malformation or disease of the ear canal or middles ear ossicles. This type of hearing loss produces an air-bone gap, where the BC threshold is relatively normal but the AC threshold increases. Otosclerosis is a disease which causes conductive hearing loss due to a bony growth over the oval window, restricting the motion of the stapes. In patients with this disease a 'notch' in the BC audiogram around 2 kHz is seen, however, the frequency location of such a notch has been suggested to differ between patients. This disease has been shown to be successfully treated with an implant that artificially excites the round window. The size of the transducer that is used to simulate the round window can often not completely cover the window. It has been therefore suggested that the round window can act as both a pressure release and a source of excitation simultaneously. In this case a near-field pressure component originating from the round window and extending to the BM is thought to drive the BM motion.

Third window lesions also produce an air-bone gap, thus an apparent conductive hearing loss. An enlarged vestibular aqueduct has been shown to produce a large air-bone gap at low frequencies, however, its magnitude varies greatly between patients. There are multiple theories for the cause of the induced air-bone gap, but there is no consensus in the literature of the overriding reason or reasons.

Chapter 3

Description of the 2D Finite Difference Cochlear Model and Middle Ear Model

This chapter describes the mathematical techniques used to model the cochlea and the middle ear. The cochlear model described in this chapter is used to investigate all the different cochlear excitation mechanisms discussed in this thesis. The cochlear model and a simple lumped parameter model of the middle ear are used in conjunction to predict the middle ear inertia response. The motion of the stapes due to vibration of the skull is calculated from the middle ear model and then used as an input into the cochlear model at the oval window. All other mechanisms are simulated solely using the cochlear model.

The cochlea has previously been modelled using a number of different approaches, from full 3D geometrically realistic models to simple lumped parameter models, which will be discussed in section 3.2. The 2D box model described here allows a simple visualisation of the different fluid coupling mechanisms and provides a convenient tool for quantifying the effect of many different excitation mechanisms.

3.1 Lumped Parameter Model of the Middle Ear

The middle ear inertia component of BC is investigated in this thesis by separately predicting the motion of the stapes due to BC stimulus and then using this motion as an input into a cochlea model. Predictions of the detailed motion of the components of the ossicles are not necessary, it is the magnitude of the stapes motion and how it behaves with frequency that is critical. It was therefore decided that a simple lumped parameter model, which enables an expression for the stapes motion per vibration input,

was appropriate for the need of this investigation. The output stapes frequency response of this model was validated against experimental data.

The complicated structure of middle ear ossicles have been simplified here to a lumped parameter model, shown in Fig.3.1. The purpose of this model is to produce a frequency dependent response of the stapes due to the vibration of the temporal bone. As discussed in the previous chapter, the motion of these small bones is very complex, however, a in-depth detailed response is not necessary for the purpose of this model. Only a reasonable realistic prediction of the response is needed that shows a realistic resonant frequency of the ossicles due to vibration of the temporal bone, a realistic magnitude and shape of response.

In reality the tendons and ligaments are intricate structures which provide a stiffness in all directions of motion of the ossicles. Here, the complicated three dimensional structure of the ossicles is simply represented by a mass on a lever, with an arm representing the stapes. The stiffness and resistance of the tendons and ligaments supporting the ossicles are represented by an angular damper, c_h, a linear damper, c_m and a spring, k_m. The box surrounding the system corresponds to the temporal bone which encases the middle ear cavity in which the ossicles are located.

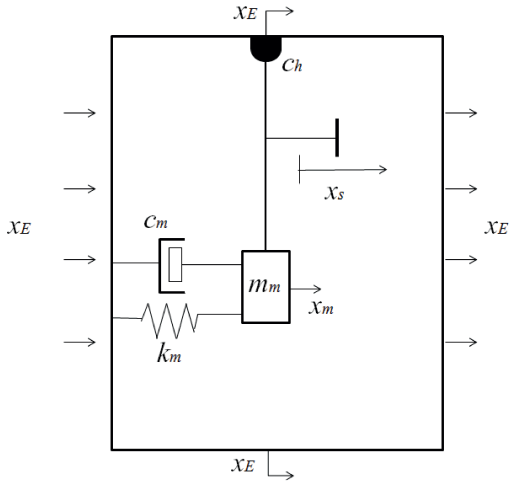

Figure 3.1: Lumped Parameter model of the middle ear.

The collective stiffness acting on the ossicles due to the vibrations of the temporal bone is represented by one spring. The stiffness of this spring could be estimated from values of the Youngs module of the tendons and ligaments used in finite element models, (Homma et al., 2009; Koike et al., 2002), or the net impedance of the middle ear estimated from experimental results (Merchant et al., 1996). However, the values of the Youngs modulus vary, (incudostapedial joint Youngs modulus 4.4×10^5 in Homma et al. (2009) and 6×10^6 in Koike et al. (2002)) and approximations of the size, shape and directional

components of stiffness of each ligament and tendon would have to be made. It is impractical to predict the stiffness in this way, since too many assumptions would have to be made. Also, the experiments carried out to find the impedance of the middle ear use air pressure as a stimulation, not vibrations. It has been shown that the dominant middle ear motion is not the same when being stimulated by air pressure and vibrations (Homma et al., 2009) and so the total stiffness acting on the ossicles for each mechanism would not be the same. Thus, calculating the stiffness from the impedance of the middle ear measured from experiments that stimulate the middle ear using pressure at the tympanic membrane would not give a realistic value. Due to the complexity of the middle ear structure the stiffness acting on it is hard to predict from analysing its structure. However, resonant frequency of the ossicle when simulated by BC and mass to the ossicles have been measured. The values are not absolute, since it is a biological system, but an acceptable range is known. Therefore, the stiffness acting on the ossicles, k_m, was calculated from an assumed resonance frequency, f_n where $\omega_n = 2\pi f_n$, of the system and an estimated mass of the ossicles, m_m.

$$k_m = \omega_n^2 m_m \tag{3.1}$$

It was assumed here that the resonance frequency of the system is 1.7kHz, which is within the range shown by experiments, (Homma et al., 2009; Stenfelt et al., 2002). The total mass of the three ossicles was estimated at 5.5×10^{-6}kg (Wever and Lawrence, 1954). Using Eq.3.1, the middle ear stiffness was calculated to be 6400Nm^{-1}.

Homma et al. (2009) calculated the damping ratio, ζ, of the middle ear as a whole, in response to vibrations to be 0.2, where,

$$\zeta = \frac{c_T}{2m_m w_n}. \tag{3.2}$$

This value is assumed here, giving a Q factor of 2.5. Using Eq.3.2, the damping acting on the whole system, c_T, was thus calculated to be 0.24 Nsm^{-1}, where, c_T is the total damping acting on the system which is equal to, $c_m + c_h/L_m$, and L_m is the distance between the hinge and the mass. The relative displacement of the stapes to the excitation displacement, x_s, caused by vibrations of the skull, x_E, is related to the mass displacement, x_m by a lever ratio, L_r,

$$x_s = \frac{1}{L_r}(x_m - x_E). \tag{3.3}$$

The lever ratio is the ratio of the distance between the hinge and the mass and the distance between the mass to the stapes arm which were defined as 7 mm and 5 mm respectively. This gives a lever ratio, L_r, of 1.4.

The motion of this system, which represents the middle ear ossicles due to the vibrations of the temporal bone, is described by the equation,

$$m_m\ddot{x}_m = -k_m(x_m - x_E) - c_m(\dot{x}_m - \dot{x}_E) - c_h\dot{\theta}, \tag{3.4}$$

where, using the small angle approximation, $(\frac{\dot{x}_m - \dot{x}_E}{L_m}) = \dot{\theta}$. Substituting Eq.3.3 into Eq.3.4, assuming a harmonic time dependence of the form $e^{i\omega t}$ and rearranging, the relative stapes displacement per excitation displacement is expressed as,

$$\frac{x_s}{x_E} = \frac{1}{L_r}\frac{\omega^2 m_m}{k_m - \omega^2 m_m + i\omega c_T}. \tag{3.5}$$

This equation, Eq.3.5, describes the displacement of the stapes per external displacement due to the inertia of the middle ear when the skull is vibrated in a direction in line with the middle ear. Its frequency response is plotted in Fig. 3.2.

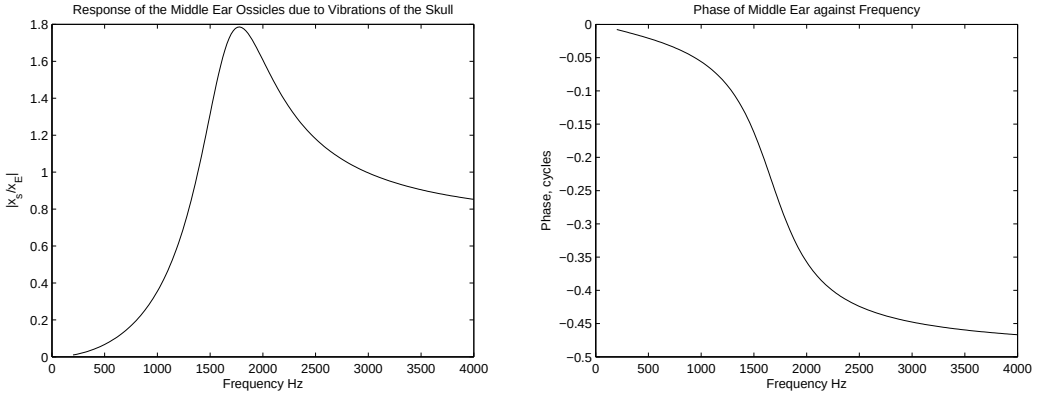

(a) (b)

Figure 3.2: Modulus and phase of the relative stapes displacement per external displacement for the assumed model.

The magnitude of these results were compared with those of Stenfelt et al. (2002) for the magnitude of relative differential footplate velocity, Fig.3.3. When the response is averaged (thick line) the detail of the shape of the response is lost. It is therefore important to compare both the average and individual results from Stenfelt et al. (2002) to results from the lumped parameter model. GetData Graph Digitizer software was used to extract Stenfelt's results. It was hard to distinguish between the individual results so only a few could be plotted and only over a small frequency range. Only those that were of magnitudes higher than the average, and around the resonance frequency were able to be differentiated.

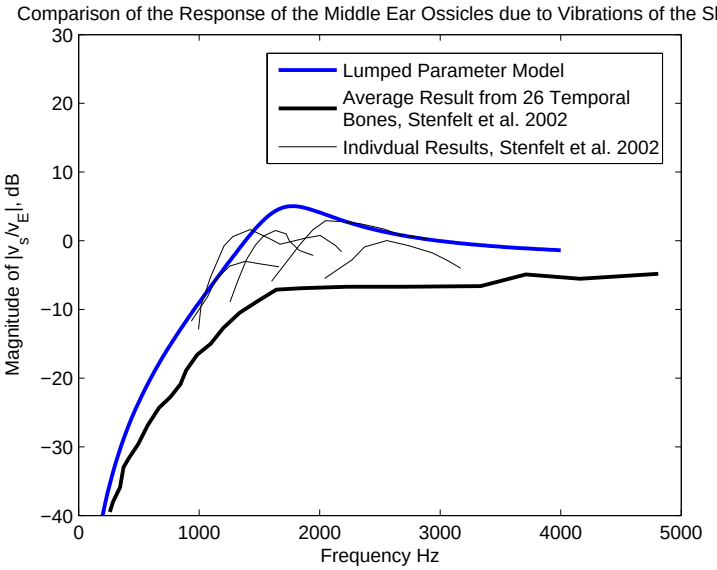

Figure 3.3: Magnitude of the relative velocity of the stapes per excitation of the skull velocity against frequency predicted by lumped parameter model compared with average result and a few individual results for the relative differential footplate velocity taken from Stenfelt et al. (2002).

It can be seen from Fig.3.3 that the lumped parameter results show a similar shape of response to the experimental data, but with a higher magnitude. However, there is a large variation in the response of the biological system and so the results from the lumped parameter model are plausible, since the results of only 26 temporal bones have been measured.

It was assumed in this model that the vibration of the skull is equal to the vibration of the temporal bone. This means that the skull is assumed to vibrate as one, which is only valid at low frequencies, below 1 kHz (Hakansson et al., 1994; Stenfelt and Goode, 2005). Above this frequency there is a change in motion of the skull due to vibrations. It has also been assumed that only one mode of motion of the middle ear is present. In reality there is more than one, but it is the mode that is modelled here, (Homma et al., 2009).

3.2 Review of Mathematical Cochlear Models

Mathematical modelling have been used widely in the literature to gain a better understanding of many of the physical processes behind the cochlea's part in the hearing process. All of the models simplify the cochlea to a greater or a lesser extent, ranging from simple 1D lumped parameter models to complex 3D finite element models. However, all models include, at least, the scala vestibuli, scala tympani, the BM and the oval and round window, since these structures are fundamental to the working of the

cochlea. The modelling techniques used in these studies are dependent on aspect of the cochlea mechanisms that is being investigated.

1D lumped parameter models greatly simplifying the complex cochlea to its fundamentally important components, in order to understand the interactions between them. They benefit from being accessible and easily understood. However, by simplifying to such an extent, certain aspects are neglected, which may have a significant influence to the overall response. 2D models can contain greater detail, particularly of the fluid motion. Being two dimensional means that the fluid flow in both the longitudinal and transverse directions are modelled, as well as the pressure distribution in the fluid. Approaching geometrically realistic 3D finite element models will clearly contain greater details in the model and can be effective in investigations that examine the effect of the geometry on the cochlear response. They are, however, computational demanding and it can be difficult to reproduce the model, given the difference in modelling techniques between the various commerical finite element packages.

Some of the most simple models used to investigate the physical processes occurring in the cochlea are lumped parameter models. For instances, Marquardt and Hensel (2013) used a lumped parameter model of the cochlea, that was analogous to an electrical circuit where the voltage corresponded to the sound pressure and the current to the acoustic volume velocity, to investigate the cochlear response to low frequency sound. These authors also provide a comprehensive review of lumped parameter models that had previously been reported in the literature. The mass of the fluid in the chambers, the impedances of the BM, middle ear, round window and helicotrema were all represented by lumped elements. The values were adjusted to represent different mammalian cochlea of cats, guinea pigs and humans and the results from this model were compared against experimental data. The results represented well the cochlear impedance and intracochlear pressure experimental data and was used to predict experimentally unavailable data. This model showed that a simple lumped parameter model, containing a relatively small numbers of elements, can describe some of the acoustic properties of the cochlea. Due to the simple nature of this model, it is clear which component or components of the cochlea are responsible for certain aspects of the response.

More recently, Stenfelt (2014) used a lumped parameter impedance model to investigate the relative contribution of BC pathways. A box shaped representation of the cochlea was assumed, which included two fluid chambers, the BM and cochlear windows, as well as the vestibular and cochlear aqueducts. A lumped impedance representation of these elements was then used to solve for the fluid volume displaced at the BM due to different BC excitation mechanisms. It was assumed that the volume displaced at the BM is proportional to the hearing response. Although, the simplification of a lumped parameter model will restrict the information that can be gained, such as the details

of fluid flow and the details of the BM response, this type of model can give a good indication to the underlying physical processes.

Box models of the cochlea have previously been used to predict the BM response and the fluid flow in the cochlear due to a range of excitations. It is generally believed that for stimulation at the oval window the effect of the coiled geometry on the macromechanical BM response is negligible and so a straight model is adequate (Steele and Zais, 1985). 1D box models, for example Neely and Kim (1986), assume that the pressure is transversely uniform across each of the fluid chambers and so can only represent the plane wave, or 'far field' component of the fluid pressure distribution (Elliott et al., 2011). Both Neely (1981) and Edom et al. (2013) have used 2D cochlear box models to predict the BM response due to excitation at the oval window. 2D models can reproduce the near field pressure distribution across the fluid chamber, as well as the averaged fluid pressure. Edom et al. (2013) calculated the BM response by solving the Naiver Stoke equation using a finite difference method, due to a piston-like and rocking motion of the stapes. The model included two fluid chambers, the BM and the two cochlear windows and was solved for the BM response and the cochlear fluid velocity. The geometry of this model is unusual, in that it appears to be the first model that has defined the oval window to be parallel to the BM. Other box models assume that the oval window is perpendicular to the BM. In this model, the cochlear fluid was assumed to be incompressible. The inertia of the BM is assumed, in this model, to be dominated by the inertia of the fluid displaced by the motion of the BM and the damping to be dominated by the fluid viscosity. The passive BM is hence only modelled to vary in stiffness, while its physical mass and damping are assumed to be zero. The stiffness variation is calculated so that a reasonable tonotopic map is produced. One benefit of this model over a 1D model is that the distribution of the fluid flow and pressure can be determined.

Neely (1981) used a 2D box model of the cochlea, solved using a finite difference approximation, to predict the BM response due to acoustic excitation and vibration of the cochlear walls. The model used in this thesis, as describe later in this chapter, is based on a modified form of this model. In Neely (1981) a symmetrical cochlea was assumed, with a BM ending in the apex at the Helicotrema, with two cochlear windows located on the end of the cochlea, perpendicular to the BM. Due to the symmetry of the assumed cochlea geometry, only one chamber needed to be considered and this model was solved for the pressure difference between the chambers. The cochlear fluid was assumed to be incompressible and inviscous and so the fluid pressure difference between the two chambers satisfies the Laplace equation. In this model, the variation of the admittance along the BM was represented by a variation of the stiffness, however, the mass and damping of the BM remained constant along the length. In contrast to the Edom et al. (2013) model, the inertia and damping of the BM in Neely (1981) were modelled as physical parameters of the BM. Due to the assumed symmetry and the method of solving the model, the flow through both cochlear windows are equal.

The previous models have all simplified the geometry of the cochlea such that the coiling is not included. The benefit of 3D models is that the coiled geometry of the cochlea can be included, which could potentially have an effect for certain excitation mechanisms. One of the first models to include a more realistic geometry of the cochlea was the Böhnke and Arnold (1999) coiled model. The model was solved using a finite element method for the BM response to acoustic stimulus and was used to calculate the cochlear acoustic input impedance. A passive BM was modelled, where the change in admittance occurred due to an increase in width and decreasing thickness of the modelled BM. The damping was introduced into the model at the BM, where the element defining the BM contained a material damping component. Two coiled fluid chambers were modelled, separated by the BM, where the fluid was coupled to the BM structure. The cochlear fluid was assumed to be inviscous but compressible. Hence, the only damping in the model is the physical damping of the BM. The results of the BM response were found to be comparable with experimental data of pressure and BM displacements as well as the cochlear impedance.

Models with a more realistic geometry, solved using a finite element method, have also been used to investigate the BM response due to unconventional hearing mechanisms, including through prosthetic hearing aids. For example, Zhang and Gan (2011) built a model of the cochlea and used it to investigate the response when excited by implantable hearing devices, including a floating mass transducers located on the ossicles and round window and a cochlear implant. The model consisted of an auditory canal, middle ear vestibule and cochlea, where the geometry of the cochlea was based on a set of histological sections of the human temporal bone. In this model three chambers were modelled and two membranes. The admittance variation of the BM was simulated in a similar way to Böhnke and Arnold (1999), based on the variation in geometry of the BM elements along the length. In this model the cochlear fluid had viscosity, which is in contrast to the Böhnke and Arnold (1999) model. The cochlear model was validated by applying a pure tone at a set distance from the tympanic membrane and then comparing the calculated ratio between the fluid pressure at the base of the scala vestibuli and the sound pressure in the ear canal to published experimental data. Preliminary results of this model predicted that driving the cochlea by a floating mass transducer is more efficient in the reverse direction, ie via the round window, than through the oval window. This could be due to the way in which the transducer was coupled to the ear in both cases. The influence of the cochlear geometry may be significant but this was not investigated in this paper. In Zhang and Gan (2011), the results that are presented illustrate well the types of information that could be gained from a 3D coiled model. Little explaination is given and the model could benefit from further validation against experimental results, such as from driving the cochlea via a floating-mass transducer.

A series of studies have been carried out using finite element cochlear models which investigate BC hearing (Kim et al., 2011, 2013, 2014). A straighten cochlear model was

used in Kim et al. (2011) to investigate the cochlear response to inertial BC and the mechanisms with which it excites the cochlea. This model was further developed into a coiled model, including the semi-circular canals, where the geometry of the coiled model was determine from micro-computed tomography images of the human cadaver temporal bones. Only two fluid chambers were considered, separated by the BM. In this model the Young's modulus of the BM elements vary along its length, giving the admittance variation seen in the real cochlea. This is an alternative approach of modelling the BM to that in Böhnke and Arnold (1999) and Zhang and Gan (2011). The model was validated against experimental results of pressure-gain functions, the cochlear impedance, BM velocity and best-frequency map. The model was used in Kim et al. (2013) to investigate the effect of superior-semi-circular canal dehiscence of sound conduction and in Kim et al. (2014) to investigate the effect of the geometry in the hook region on BC hearing. Both of these investigations have great advantage on using a realistic geometry model. The shape and positioning of the dehiscence was examined, which would not be possible without a realistic geometry. The hook region, which is at the base of the cochlea and is geometrical complex, would be difficult to represent in a 1D or 2D model, and hence a 3D model is important to provide insight into the contribution this region has on the BM response. When excited by the fluid inertia component of BC, the effect of the direction of vibration of the cochlea was investigated. The results indicated that the BM has the greatest response when the direction of the vibration is perpendicular to the BM in the hook region. This suggests that the large cross-sectional area of the scalaes in the hook region is significant to the excitation via the fluid inertia component.

There are benefits and disadvantages with each of these models that must be considered when selecting the appropriate model in investigations. Simple 1D models are easier to build and manipulate. They are more intuitive to interpret and understand. They can provide fundamental information about the workings of the cochlea, however, they are limited by the types of fluid excitation that can be reproduced. 2D box models of the cochlea are able to give a visual insight into other forms of fluid excitation in the cochlea, by illustrating the flow of the fluid and the pressure distribution. The modelling process can be relatively accessible and is easy to interpret. There are limitations imposed by a 2D model, such as the geometry, which may potentially have a significant effect on the response. Coiled 3D finite element models have been used to model the cochlea with a greater attention to detail. These models are beneficial for examining aspects of cochlear mechanisms that depend on the geometry of the cochlea. The disadvantages of this models are that they are less intuitive to understand compared to 1D and 2D models and that there is a significant increase in computational power needed. The 3D models are mostly built using commercial software, which can limit their reproducibility to some extent, as the mathematics behind commercial software may change between programs; for instances the definitions of material interactions may not be explicitly stated. Models built on commerical software should be able to be reproduced on any appropriate software if enough model detail is given. Reproducibility of a model is

important in science because if results can not be reproduced, they cannot be tested and hence their value diminishes.

All types of cochlear models have their merits. An ultimate objective would be for a complete understanding of the cochlear processes where there is consensus between all models of all dimensions. This would involve a 1D model which would explain the underlying physical processes, while the 2D model can build on this knowledge and detail processes unavailable in a 1D model. The 3D model can take into account the geometry of the cochlea and the effect this has on the cochlea response. This thesis is mainly concerned with a 2D model of the cochlea and its use to further the understanding of the physical processes behind different mechanisms of cochlear excitations.

3.3 Outline of 2D Finite Difference Model

In this thesis a 2D finite difference box model of the cochlea is used to investigate the underlying processes behind multiple mechanisms of cochlear excitation. This type of model was chosen due to its ability to be built from the fundamentals and that it is easily manipulated. It does not rely on finite element packages and therefore all parameters are known and how they are implemented able to be controlled. It is important when building a model to decide which structures are necessary to understand the processes you are investigating, as discussed above. The model described here is used to investigate the various fundamental physical processes that lead to a hearing sensation. It was therefore decided that it was only necessary in the first instance to model two fluid chambers, the BM, helicotrema, and the cochlear windows.

It is clear that the BM is an important structure to model as it is the motion of the BM that drives the organ of Corti, ending in an electrical signal being sent to the brain. The conversion of acoustical to electrical energy is not examined in this model and so modelling the details of the organ of Corti is unnecessary. It is assumed in this model that the motion of the BM is directly proportional to the hearing sensation. A passive BM also is assumed, because it is the physical processes of the overall excitation that are being examined, which are not reliant on an active BM. A simple active model BM could be implemented into this model at a later date without too much difficulty, but is out of the scope of this investigation.

The cochlear windows are necessary in the model since they are fundamental in the excitation of the cochlea. For instances, in air conduction the location of stimulus is at the oval window and the round window acts as a pressure release. They are the major compliant structures in the cochlea that allow a net fluid flow through the cochlea.

The cochlea is modelled with only two fluid chambers, as the scala media and vestibuli are assumed to be one chamber. This is justified since although the Reissner membrane

is a barrier to the chemical mixing of the two types of cochlear fluids (endolymph and perilymph) it is believed to be transparent with respect to the mechanics of the fluids. This model is solved for the pressure of the fluid, which is irrelevant to the chemical make up and so the modelling of the Reissner membrane is unnecessary. The fluid in the model is assumed to be compressible to a slight extend, which was partially due to the modelling process, see Appendix A for further details.

Although, this model is based on the Neely (1981) model the differences include: the pressure is solved for, rather than the pressure difference; the chambers are assumed to be asymmetric here; the fluid is assumed to be slightly compressible; the variation of the BM admittance is different as are the size and location of the cochlear windows.

3.3.1 Geometry

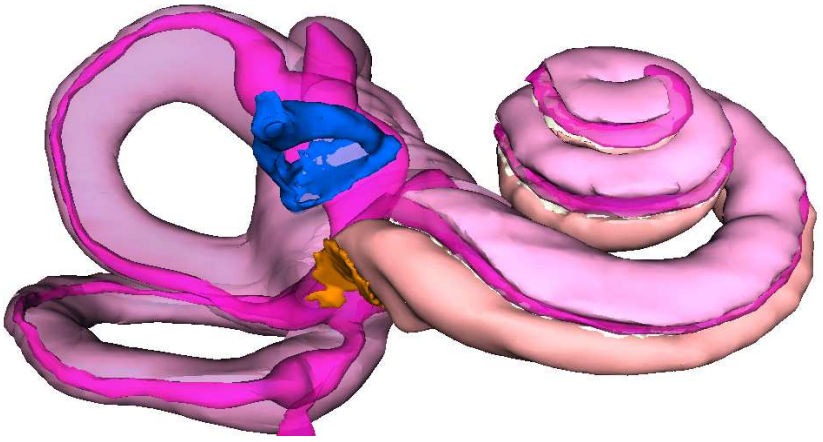

Figure 3.4: Diagram of the cochlea and related structures taken from Liberman et al. (2009). The blue structure is the stapes and the orange patch is the round window. The light pink and peach coloured chambers are the scala vestibuli and tympani respectively, while the fluid in the scala media is the strong pink chamber. The semi-circular canals are located on the left of the diagram, where the colours relates to the fluid type. The BM is the white structure between the chambers.

The complex coiled structure of the cochlea, shown in Fig. 3.4, is simplified and represented by a 2D box model, shown in Fig. 3.5. A passive elastic membrane of varying mechanical admittance, representing the BM, separates the two fluid chambers along the length of the cochlea. At the apex of the cochlea, the chambers are connected by the helicotrema. The parameters used to define the structures in this model are listed in Table 3.1.

The cochlear windows are positioned on the upper and lower cochlear walls, parallel to the BM. This is in contrast to most box models of the cochlea, which assume that the cochlea windows are perpendicular to the BM. In reality, the region of the cochlea in which the windows are located is geometrically complicated, as shown in Fig.3.6. It can

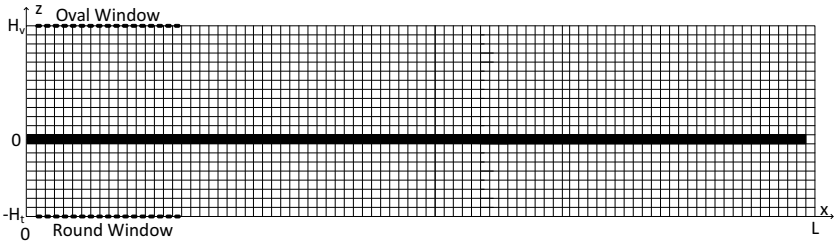

Figure 3.5: The 2D box model and the division of the two fluid chambers into N nodes in the x-direction and M nodes in the z-direction. The thick black structure is the BM and the dotted lines represent the cochlear windows.

be seen in Fig.3.6 that the round window is roughly parallel to the long edge of the BM and so it is positioned on the bottom of the cochlear model, parallel to BM, Fig.3.5, in the present model. The oval window is located on the face of the cochlea, perpendicular to the long edge of the BM, Fig.3.6. Only a 2D model is solved here, and so it is not possible to model the oval window on the face of the chamber. There are two options for the location of the oval window in the model: on the wall perpendicular or parallel to the BM. The area of the cochlear windows is important for some of the forms of excitation considered here and so determined the location of the oval window in this model.

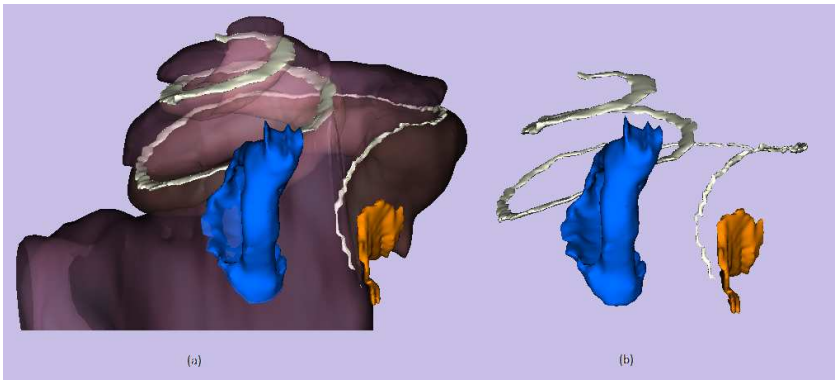

Figure 3.6: Diagram of the cochlea highlighting the relating positions of the BM (shown in white) and stapes (blue) and round window (orange) Liberman et al. (2009).

The area of the human cochlear windows were calculated from the average values of the length and width given in Braun et al. (2012). They were found to be of similar size, equal to roughly 3.2 mm^2. As a first approximation, the windows are assumed to be circular and hence have a diameter of about 2 mm, which is larger than the assumed height of the cochlea model. It can be seen in Fig.3.6 that the cochlear windows are located in the bulbous region between the cochlea and the semi-circular canals, called the hook region, and hence it is possible for windows to be this large. In this model, the cochlea is simplified and uniform cochlear chambers are modelled, without the increase in volume at the hook region. It would not be possible to position a window of this size on the cochlear wall perpendicular to the BM and so the windows are positioned

Table 3.1: List of parameters used in the cochlear model.

Variable	**Parameter**	**Value**
L	Length of cochlea	35 mm
H_v	Height of scala vestibuli	1.5 mm
H_t	Height of scala tympani	1 mm
N	Number of nodes in x-direction	295
M	Number of nodes in z-direction	22
k_{ow}	Stiffness of the oval window	830 Nm^{-1}
c_{ow}	Resistance of the oval window	0.1 $Nm^{-1}s$
m_{ow}	Mass of the oval window	4.5×10^{-6} kg
k_{rw}	Stiffness of the round window	300 Nm^{-1}
A_w	Area of cochlear windows	3.2×10^{-6} m^{-2}
c_o	Speed of sound in cochlear fluid	1500 ms^{-1}
ω_B	Natural frequency at the base of the cochlea	20 kHz
m_o	Physical mass of BM	0.0187 kgm^{-2}
m_{add}	Inferred fluid mass on the BM	0.2713 kgm^{-2}
l	Frequency distribution characteristic length	$7 \times 10^{-3}m$
Q_o	Q factor of passive cochlea	2.5

on opposite cochlear walls parallel to the BM in this model. The implicit width of the window in this 2D model is about 1.8 mm, so the longitudinal extent of the windows were set to be 2.2 mm.

3.4 Modelling the Fluid Coupling and the Basilar Membrane Dynamics

The fluid in the cochlear chambers is assumed to be able to flow in both the x and z directions. The fluid pressure in the cochlea must satisfy the 2D fluid wave equation. The time independent form of this equation is used (Helmholtz equation) and so the fluid pressure distribution is described by,

$$\frac{\partial^2}{\partial x^2}p(x,z) + \frac{\partial^2}{\partial z^2}p(x,z) + \left(\frac{\omega}{c_o}\right)^2 p(x,z) = 0, \tag{3.6}$$

where, the complex pressure is assumed to be proportional to $e^{i\omega t}$, in which ω is the excitation frequency, and c_o the speed of sound in the cochlea fluid. The last term defines the compressibility of cochlear fluid, which here it is assumed to be the same as water, which is very low and so the fluid is close to being incompressible. Similarly, it is possible to approximate the effect of fluid viscosity by including an imaginary component in the speed of sound in Eq. 3.6.

In order to solve for the fluid pressure distribution, the 35 mm length of the model is separated into 294 elements in the x-direction, and the 2.5 mm height into 21 elements

in the z-direction, as illustrated in Fig. 3.6. The number of nodes in the x-direction was increased to 512 but this did not substantially affect the results. It was therefore concluded that 294 elements was sufficient. The size of each element in the x and z direction are Δx and Δz respectively, which are of equal size. A finite difference approximation to Eq.3.6 is used to solve for the pressure distribution in the cochlea, which can be expressed as,

$$\frac{p[n+1,m]-2p[n,m]+p[n-1,m]}{\Delta x^2}+\frac{p[n,m+1]-2p[n,m]+p[n,m-1]}{\Delta z^2}+\left(\frac{\omega}{c_o}\right)^2 p[n,m]\approx 0, \tag{3.7}$$

where the pressure $p(x,z)$ at location $(n\Delta x, m\Delta z)$, is written for convenience, as $p[n,m]$, where n denotes node number in the x-direction and m that in the z-direction. The approximation inherent in Eq.3.7 is good provided Δx and Δz are significantly lower then the wavelength of the resulting BM motion.

3.4.1 Boundary Conditions

The boundary conditions are implemented using Newton's second law, applied to a small element of fluid, whilst assuming harmonic motion,

$$\frac{\partial p(x,z)}{\partial x} = -i\omega\rho u(x,z), \tag{3.8a}$$

$$\frac{\partial p(x,z)}{\partial z} = -i\omega\rho v(x,z), \tag{3.8b}$$

where u and v are the fluid velocities in the x and z direction respectively. The velocity in these equations are the input into the model which define the boundary condition.

3.4.2 Cochlear Walls

The cochlear walls are all assumed to be rigid and so the velocity at each location of the wall must be equal. The cochlear wall perpendicular to the BM are, for every cochlear excitation mechanism investigated here, stationary. Therefore velocities of the perpendicular walls, which are at the locations $(0,-Ht:Hv)$ and $(L,-Ht:Hv)$, are equal to zero. The cochlear walls parallel to the BM are, for most mechanisms investigated, also assumed to be stationary, and hence the velocity equal to zero. However, when modelling the fluid inertia component they have a non-zero velocity, denoted by v_w, which is positive upwards for both upper and lower surfaces. For ease and continuity in the explanation of other boundary conditions of the model, v_w will be used in the

description of other boundary conditions, but it should be remembered that for when the stimulus is at the cochlear windows, which is most cases, this term is equal to zero.

3.4.3 Modelling the Basilar Membrane

In the real cochlea, the BMs' properties vary along its length: it is narrow and stiff at the base and becomes wider and more compliant towards the apex. The admittance of the BM therefore changes with distance from its base. For simplicity the BM is assumed in this model to have constant width. The BM is modelled as a series of locally reacting single degree of freedom systems, as shown in Fig. 3.7, where the admittance variation of the BM is simulated by a gradual change of the physical parameters along the series. When the BM is in its rest state, or non-excited state, the relative motion between it and the cochlear walls is zero. Thus, the base of the BM systems must move with the velocity of the cochlear walls so that when there is no excitation of the BM the relative velocity between the walls and BM is zero.

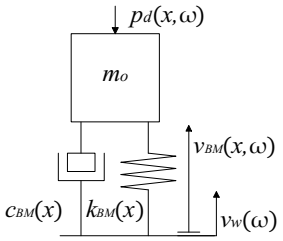

Figure 3.7: Diagram of one locally reacting single degree of freedom system which is part of a series that represents the BM

In Fig. 3.7, $c_{BM}(x)$, $k_{BM}(x)$ and m_o are the resistance, stiffness and physical mass of the BM at location x along the cochlea. $p_d(x,\omega)$ is the pressure difference across the BM and $v_{BM}(x,\omega)$ the BM relative velocity between the BM and the cochlear walls. The physical BM mass per unit area for each element is assumed to be constant. However, the stiffness and resistance vary along the length of the cochlea as,

$$k_{BM}(x) = \omega_B^2 m e^{\frac{-2x}{l}}, \tag{3.9a}$$

$$c_{BM}(x) = \frac{\sqrt{k_{BM} m}}{Q_o}, \tag{3.9b}$$

representing the distribution of natural frequencies along the cochlea and with a damping representative of the passive cochlea. ω_B is the natural frequency at the base of the cochlea and equal to $20kHz$. Q_o is a constant estimated to be equal 2.5 in a passive cochlea (Elliott and Shera, 2012) and l, is the characteristic length, which here it has been set to equal 7×10^{-3} m.

The total mass of each BM element, m, was assumed to be 0.29 kgm^{-2} (Elliott et al., 2011), which is the sum of the physical mass and the added mass of the BM, m_{add}. The

motion of the fluid immediately adjacent to the BM, which effectively adds mass to the BM, is termed added mass. The values of m_o and m_{add} where found by comparing the position of the peak BM response with zero damping, when the model was excited at a range of frequencies to the desired tonotopic map, Fig.3.8. The desired variation of frequency to position is,

$$F_D = \frac{\omega_B e^{-\frac{x}{l}}}{2\pi}. \tag{3.10}$$

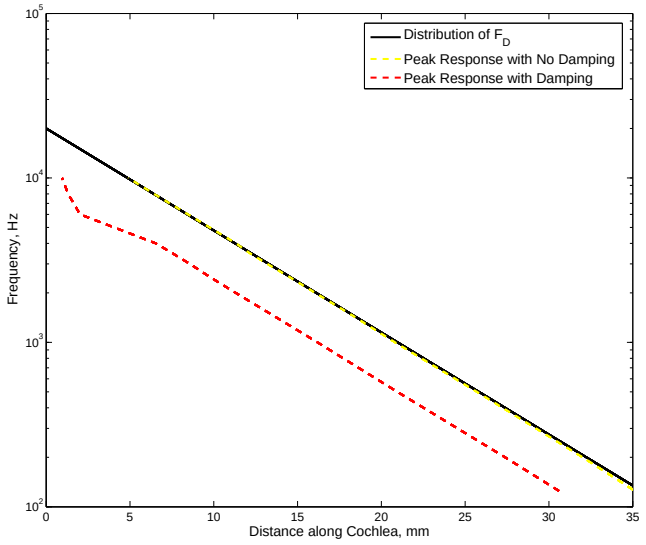

Figure 3.8: Comparison of desired tonotopical map (black line) with tonotopical map of the cochlear model determined from the peak BM response, without damping (yellow dashed line) and with damping (red dashed line).

The values of m_o and m_{add} needed to match the peak positions to the desired tonotopical map were found to be 0.0187 kgm^{-2} and 0.2713 kgm^{-2} respectively. It should be noted that the values of these masses are dependant on the size of elements used in the model. For further discussion on this see Appendix A. Adding damping shifts the position of the peak response towards the base of the cochlea. The difference in frequency at one location on the BM between the peak response with and without damping is about an octave.

It has been assumed that there is no longitudinal coupling between the single degree of freedom systems, meaning each system acts independently. The equation of motion of each of the BM elements using the parameters shown in Fig. 3.7, for a given location x, is,

$$p_d = i\omega m_o v_{BM} + (c_{BM} + \frac{k_{BM}}{i\omega})(v_{BM} - v_w). \tag{3.11}$$

This can be rearranged and written as,

$$v_{BM}(x) = -Y_{BM}(x)p_d(x) + T_{BM}(x)v_w(x), \tag{3.12}$$

where the pressure difference across the BM at location x is defined as,

$$p_d(x) = p[n,1] - p[n,-1], \tag{3.13}$$

and $Y_{BM}(x)$ is the admittance of the BM, at location x, which is equal to,

$$Y_{BM}(x) = \frac{i\omega}{i\omega c_{BM}(x) + k_{BM}(x) - \omega^2 m_o}. \tag{3.14}$$

The relative transmissibility, T_{BM}, from the wall velocity to the relative BM velocity is equal to,

$$T_{BM} = \frac{\omega^2 m_o}{i\omega c_{BM}(x) + k_{BM}(x) - \omega^2 m_o}. \tag{3.15}$$

The variation of the admittance and transmissibility with frequency, at a single location, 29 mm along the BM, is plotted in Fig.3.9.

The admittance at this location peaks around 1.2 kHz and then falls off at higher frequencies. The relative transmissibility increases and than tends to a value of 1 at higher frequencies. This means that at locations far beyond the characteristic place the relative BM velocity is almost the same velocity as the cochlear walls.

The BM is located between the nodes, $[n,0]$ and $[n,1]$. The structural behaviour of the BM is implemented into the model through Eq. 3.8b, where it is assumed that the velocity in the z direction, both below and above the BM, is equal to the relative BM velocity v_{BM}, defined in Eq. 3.12. Hence, the two equations, that defined the BM boundary conditions expressed in a finite difference form are,

$$-p[n,2] + (1 + i\omega\rho dz Y_{BM}(x))p[n,1] - i\omega\rho Y_{BM}(x)p[n,0] = i\omega T_{BM}(x)v_w, \tag{3.16a}$$

$$p[n,-1] - (1 + i\omega\rho dz Y_{BM}(x))p[n,0] + i\omega\rho Y_{BM}(x)p[n,1] = i\omega T_{BM}(x)v_w. \tag{3.16b}$$

The right-hand terms in both equations are equal to zero when the cochlear walls are assumed to be stationary, as discussed in section 3.4.2. Defining the BM velocity and the fluid velocity adjacent to the BM to be equal couples the BM motion into the fluid. The velocity of the BM is an output of the model, and as can be seen by Eqs.3.16, are dependant on the pressure in the cochlear fluid, which is generated by the stimulus to the cochlea.

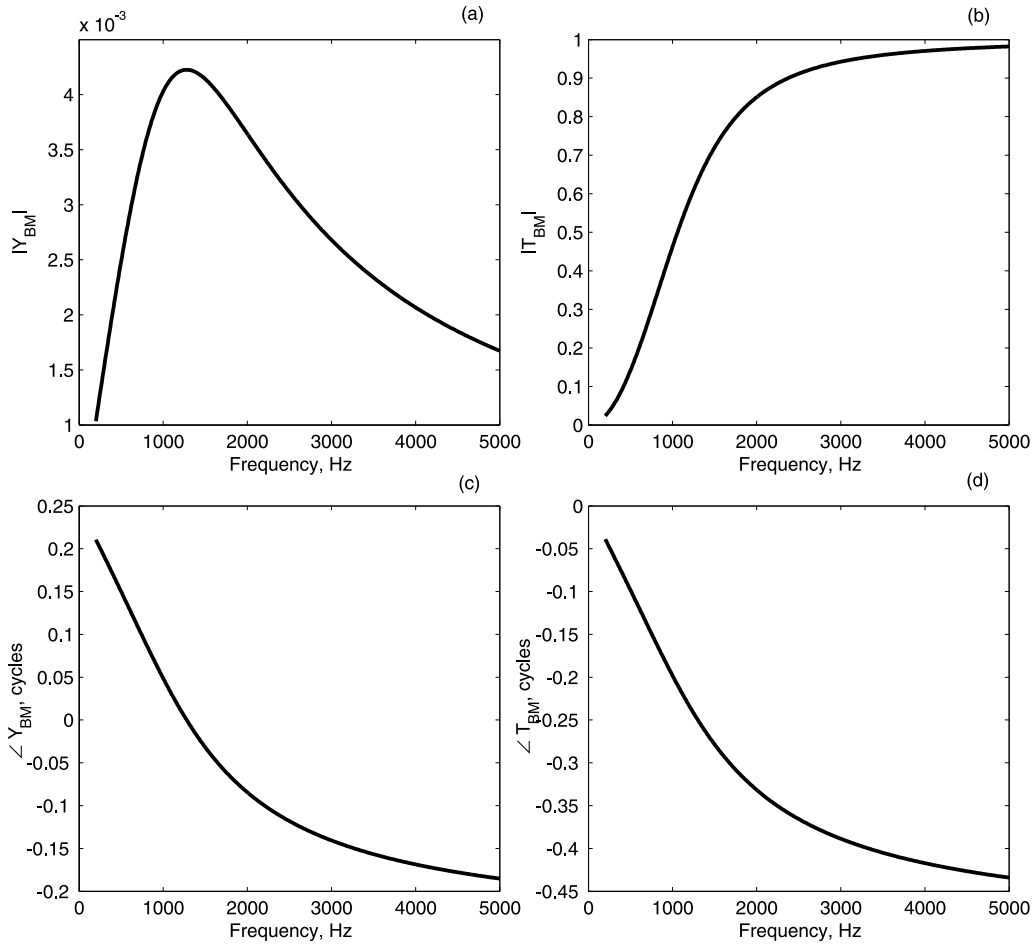

Figure 3.9: Magnitude of the BM admittance (a) and BM transmissibility (b) and their phases (c), (d), calculated at one node (n=244) along the BM, for a range of frequencies.

3.4.4 Modelling the Cochlear Windows

The modelling of the cochlea window is similar to the modelling of the BM, in that the windows are all represented by a series of single degree of freedom system, and their behaviour is described by boundary condition equations. The admittances are those felt by the fluid looking out from the cochlea. Both windows stretch along the x axis from 0.12 to 2.3 mm from the base of the cochlea and are located at the cochlear walls.

A flexible round window is modelled as a series of springs, each with the same stiffness, k_{rw}. They are not coupled together mechanically, however, their motion is dependant on the cochlear fluid pressure at the round window, and so the motion of the individual systems are coupled via the fluid pressure. The velocity of each system is related to the fluid pressure at x positions of the round window, (x, H_t), and the admittance of each system by,

$$v_{rw} = v_w - Y_{rw} p(x, H_t). \tag{3.17}$$

where,

$$Y_{rw} = \frac{i\omega A_w}{k_{rw}}. \tag{3.18}$$

Similarly, the flexible oval window is modelled as a series of single degree of freedom systems, much like the BM, although the parameters do not vary longitudinally. The admittance experienced by the fluid looking out of the cochlea is mostly due to the dynamics of the middle ear, and is defined as,

$$Y_{ow} = \frac{iA_w\omega}{(k_{ow} + i\omega c_{ow} - \omega^2 m_{ow})}. \tag{3.19}$$

The stiffness, resistance and mass describing the admittance at the oval window, due to the middle ear, are represented by, k_{ow} c_{ow} and m_{ow}. The values of these parameters of the oval window are taken from Puria (2003). The round window stiffness is also assumed to be one tenth that of the oval window, as suggested in Gopen et al. (1997). A_w is the area of the window. All the values of the parameters used in the model are listed in table 3.1. The admittance is related to the oval window velocity by,

$$v_{ow} = v_w + Y_{ow} p(x, H_v). \tag{3.20}$$

The v_w term in both Eq. 3.17 and 3.20 means that if the admittance of the window tends to zero, the velocity of the window tends to the same velocity as that of the cochlea wall it is part of.

The boundary conditions of the cochlear windows are defined in two ways, depending on the excitation mechanisms being modelled, but both use Eq. 3.8b. When a window is assumed to be flexible, the velocity is an output of the model, determined by the pressure in the cochlear fluid which is generated by the stimulus to the cochlea. In this case the fluid velocity in the z direction is described, for a flexible window, as the window velocity in Eqs. 3.17 and 3.20. If the cochlea is excited at one of the windows, the velocity in Eq. 3.8b becomes an input to the model and hence is chosen.

3.4.5 Numerical Solution

The 2D time independent wave equation along with the boundary conditions that describe the cochlea structures, discussed in the previous sections, are expressed in finite

difference form and then solved for the pressure distribution in the cochlea, using the matrix equation,

$$\mathbf{Ap} = \mathbf{q}, \quad \text{solved in the form} \quad \mathbf{p} = \mathbf{A^{-1}q}. \tag{3.21}$$

When expanded this equation can be expressed as,

$$\begin{bmatrix} \mathbf{p_1} \\ \mathbf{p_2} \\ \mathbf{p_3} \\ \vdots \\ \vdots \\ \vdots \\ \mathbf{p_{N-2}} \\ \mathbf{p_{N-1}} \\ \mathbf{p_N} \end{bmatrix} = \begin{bmatrix} \mathbf{I_1} & \mathbf{-I_1} & 0 & 0 & 0 & \dots & \dots & \dots & \\ \mathbf{-I_n} & \mathbf{A_{2cw}} & \mathbf{-I_n} & 0 & 0 & \dots & \dots & \dots & \\ 0 & \mathbf{-I_n} & \mathbf{A_{3cw}} & \mathbf{-I_n} & 0 & \dots & \dots & \dots & \\ & & \ddots & \ddots & \ddots & & & & \\ & & & \ddots & \ddots & \ddots & & & \\ & & & & \ddots & \ddots & \ddots & & \\ & \dots & \dots & \dots & 0 & \mathbf{-I_n} & \mathbf{A_{(N\times M)-2}} & \mathbf{-I_n} & 0 \\ & \dots & \dots & \dots & 0 & 0 & \mathbf{-I_n} & \mathbf{A_{(N\times M)-1}} & \mathbf{-I_n} \\ & \dots & \dots & \dots & 0 & 0 & 0 & \mathbf{-I_1} & \mathbf{I_1} \end{bmatrix}^{-1} \begin{bmatrix} \mathbf{q_1} \\ \mathbf{q_2} \\ \mathbf{q_3} \\ \vdots \\ \vdots \\ \vdots \\ \mathbf{q_{N-2}} \\ \mathbf{q_{N-1}} \\ \mathbf{q_N} \end{bmatrix} \tag{3.22}$$

Each element of the matrix represents a location in the cochlea. The equation is designed so that the Helmholtz equation and boundary conditions are described in the matrix $\mathbf{A}$, while the external excitation is defined in the $\mathbf{q}$ vector. The pressure vector, $\mathbf{p}$, is solved for, which describes the pressure distribution in the cochlea. Each pressure vector, $\mathbf{p_k}$, is a vector of pressures where k denotes the x-th position such that,

$$\mathbf{p_n} = \begin{bmatrix} p(n,M_v+1) \\ \vdots \\ \vdots \\ \vdots \\ p(n,1) \\ p(n,0) \\ p(n,-1) \\ \vdots \\ \vdots \\ \vdots \\ p(n,-M_t+1)) \end{bmatrix} \tag{3.23}$$

$\mathbf{A}$ is a large tri-diagonal matrix made up of a $N \times N$ block matrix where each element is a $M \times M$ matrix. The outside diagonals are made up of incomplete identity matrices, of size $M \times M$, which have zeros at locations representing the BM and cochlear walls, allowing for the boundary condition to be implemented.

$$I_n = \begin{bmatrix} 0 & 0 & 0 & \dots & & & & & & \\ 0 & -1 & 0 & \dots & & & & & & \\ & & \ddots & & & & & & & \\ \dots & 0 & 0 & -1 & 0 & 0 & \dots & & & \\ & & \dots & 0 & 0 & 0 & 0 & \dots & & \\ & & \dots & 0 & 0 & 0 & 0 & \dots & & \\ & & & \dots & 0 & 0 & -1 & 0 & 0 & \dots \\ & & & & & & & \ddots & & \\ & & & & & & \dots & \dots & 0 & -1 & 0 \\ & & & & & & \dots & \dots & 0 & 0 & 0 \end{bmatrix} \tag{3.24}$$

In a general model the diagonal elements of this matrix would be equal to $\frac{\Delta z}{\Delta x}^2$, however, since the elements of the model are square, elements of the matrix are equal to one. The middle diagonal of the large $\mathbf{A}$ matrix, $\mathbf{A_k}$ have the form,

$$A_k = \begin{bmatrix} C_{ow} & -1 & 0 & 0 & ... & & \\ -1 & 4-\left(\frac{\omega\Delta z}{c_o}\right)^2 & -1 & 0... & & & \\ 0 & -1 & 4-\left(\frac{\omega\Delta z}{c_o}\right)^2 & -1 & 0... & & \\ & & \ddots & & & & \\ & & & & & & \\ & & \ddots & & & & \\ & & & & & & \\ ... & 0 & -1 & 1+i\rho Y_{BM}(x)\Delta z & -i\rho Y_{BM}(x)\Delta z & 0 & ... \\ ... & 0 & i\rho Y_{BM}(x)\Delta z & -(1+i\rho Y_{BM}(x)\Delta z) & 1 & 0 & ... \\ & & & \ddots & & & \\ ... & ... & 0 & -1 & 4-\left(\frac{\omega\Delta z}{c_o}\right)^2 & -1 & 0 \\ & ... & ... & 0 & -1 & 4-\left(\frac{\omega\Delta z}{c_o}\right)^2 & -1 \\ & ... & ... & 0 & 0 & 1 & C_{rw} \end{bmatrix} \tag{3.25}$$

The first and last rows of these matrix elements define the boundary conditions of the parallel cochlear walls. The cochlear windows interrupt these walls and so for specific matrices the boundary conditions of the windows are defined in these rows. When the flexible cochlear windows are modelled,

$$C_{ow} = -1 + iw\rho Y_{ow}\Delta z \tag{3.26a}$$

$$C_{rw} = -1 + iw\rho Y_{rw}\Delta z. \tag{3.26b}$$

However, when a rigid wall is modelled,

$$C_{ow} = 1 \tag{3.27a}$$

$$C_{rw} = -1. \tag{3.27b}$$

The BM boundary conditions are described by the rows containing the BM admittance. The $A_{(N\times M)-1}$ element contains the helicotrema admittance, instead of the BM. The middle diagonal of the $\mathbf{A_k}$ matrix element defines the fluid compressibility of the model. In general, these central elements are equal to, $2 + 2\frac{\Delta z^2}{\Delta x^2} - \left(\frac{\omega\Delta z}{c_o}\right)^2$, however, again due to the square shape of the model elements, Δx and Δz are equal and hence this term reduces to $4 - \left(\frac{\omega\Delta z}{c_o}\right)^2$.

3.5 Methods of Exciting the Model

Each cochlear excitation mechanisms is simulated by a unique set of boundary conditions. The external excitation is defined in the $\mathbf{q}$ matrix, which is made up of N vectors each of length M, as shown in Eq. 3.22. Each sub-vector, $\mathbf{q_n}$, represents a vertical strip of the cochlear model, such that the first element represents the upper wall and the bottom the lower wall of the cochlear model. In the following sections a description is given of each of the excitation methods simulated in this cochlear model.

3.5.1 Piston Motion at the Stapes

A piston-like motion of the stapes is used to excite the cochlea when simulating AC hearing and the middle ear inertial component of BC hearing. The velocity of the oval window, v_{ow}, is assigned a value which is the same for every location so that the window moves in unison. This is implemented in the model by assigning the elements in the $\mathbf{q}$ vector which represent the window locations a value of, $-i\omega v_{ow}\rho\Delta z$.

3.5.2 Rocking Motion of the Stapes

The rocking motion of the stapes is modelled to be non-volumetric, which means that the net flow through the oval window is zero. The velocity at the ends of the windows are equal in magnitude but opposite in direction. The velocity linearly decreases in magnitude towards the centre on both sides such that the window moves symmetrically about the mid point of the window, as shown in Fig. 3.10.

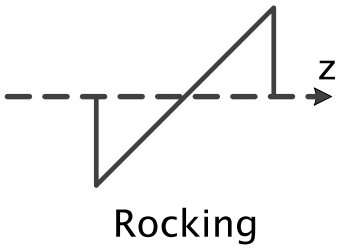

Figure 3.10: Schematic diagram of the velocity profile of the oval window when it is excited by a rocking motion.

This velocity gradient is applied to the model at the oval window locations, via $\mathbf{q}$, in the same way as the piston-like motion, however in this case the velocity of each of the elements are not equal.

3.5.3 Middle Ear Inertia

When modelling the middle ear inertia the motion of the stapes is assumed to be piston-like. The motion of the stapes due to vibration of the temporal bone is predicted by the lumped parameter model of the middle ear, as discussed in Section 3.1. The output of the lumped parameter model is combined with the cochlea box model to simulate this pathway. The ratio of the relative stapes displacement to the excitation frequency, defined in Eq.3.5, is used to determine the velocity of the oval window,

$$v_{ow} = i\omega \frac{x_s}{x_E}. \tag{3.28}$$

3.5.4 Fluid Inertia

The fluid inertia component of BC is where vibrations of the temporal bone impart inertia forces on the cochlear fluid, causing an excitation of the BM, as discussed in Chapter 2. This is modelled by assuming the cochlear walls parallel to the BM vibrate harmonically. In reality the vibrations of the skull vibrate the complex structure of the cochlea in all three dimensions. In this 2D model this is not possible to simulate, however, if the cochlea is vibrated in all planes, there will always be a component in the direction parallel to the BM. Given the limitation of this model, it is this component of vibration that is being modelled here. The velocity of the parallel cochlear walls are defined to be equal, so that $v_w = v_e$, where v_e is the excitation velocity.

3.6 Benefits of the Model

The flexibility of this model means that it can be manipulated to simulate a wide variation of cochlear excitation mechanisms, allowing them to be compared under one framework. The output of the model is a pressure vector which holds the information of the pressure distribution within the cochlea. From this information, data such as the BM response, cochlear window velocity and volume velocity through the BM and windows,can be easily extracted. This model was solved here using MATLAB software, but could also be built and solved in other similar software. The run time of the model is very short, approximately 30s for a single frequency on a personal computer (2.67 GHz processor, 8 cores and 8 GB of RAM). This allows for a large number of analyses to be run in a short time span and without having to meet high computational demands.

3.7 Conclusion

The cochlea has been modelled using a methods ranging from, simple lumped parameter model to complex finite element models. The structures that are fundamental to all models are the: BM, two cochlear windows and at least two fluid chambers.

The cochlear model in this thesis, consisting of two asymmetrical chambers, separated by an electric structure of varying admittance and two windows, was used to investigations multiple hearing mechanisms. The model simplified the complex geometry of the cochlea to a simple rectangular box shape. A finite difference approach was used to solve the 2D time independent wave equation for the fluid pressure distribution in the cochlea. The elastic membranes of the BM and cochlear windows are represented by a series of simple single degree of freedom systems. Boundary conditions are used to define the motion of the these structures within the model, as well as the rigid cochlear walls. The model can be excited in multiple ways which simulate the different cochlear excitation mechanisms. In this chapter, enough information was given so that a reader could reproduced this model in a similar software package. It has been shown that this is a very flexible model, allowing investigations to be carried out within one framework and, due to the short run time, over a relatively short time period.

In order to model the middle ear inertia component of BC hearing the relative motion of the stapes was estimated using a lumped parameter model of the middle ear ossicles. The velocity relative of the stapes was then used as an input into the cochlea model to find the cochlear response to this hearing mechanism. The parameters of the model were calculated from the known resonant frequency and the mass of the ossicles. The output was validated against experimental results on measurements on temporal bones and shown to be similar.

Chapter 4

Results from the 2D Finite Difference Model

4.1 Introduction

In this chapter the cochlear excitation results are presented due to stimulating the cochlea via the stapes and BC, specifically by a piston-like motion of the stapes, the non-volumetric excitation due to of rocking motion of the stapes and the two inertial components of BC. These mechanisms have been described in Chapter 2 and a description of their modelling is given in Chapter 3. The BM response and the pressure distribution in the cochlea are determined, in order to understand the cochlear response due to these mechanisms of excitation. The results are compared with experimental data and the results of other models.

The BM response results are presented normalised to the excitation velocity for each mechanism. This means, for acoustic simulation, that the BM velocity is normalised to the imposed oval window velocity, while for the inertia bone conduction simulation, the BM response is normalised to the external vibrations of the skull. The BM response due to the rocking motion of the stapes is normalised to the maximum velocity of the oval window, which is the velocity at the outer edge to the oval window. Calculating the relative BM response allows for a comparison of the different mechanisms of excitation.

In this model the peak BM response is assumed to be proportional to the hearing response. In order to determine the frequency response of the BM due to each excitation mechanism, the BM response was calculated at multiple individual frequencies and the peak response found. The results for all frequencies were collected together to determine the overall frequency response due to the excitation mechanism.

4.2 Comparison of Response along the Basilar Membrane due to Multiple Excitation Methods

The magnitude and phase of the BM response due to excitation via air conduction, the two inertial components of BC and the rocking motion of the stapes, at 1 kHz, were determined and are shown in Fig. 4.1. Although the magnitude of the BM response is greatly dependent on the excitation mechanisms, the position of the peak value is the same. It is assumed throughout these results that the peak BM response is proportional to the hearing response, so a greater BM response leads to a louder hearing perception. The responses at 1 kHz are shown here as an example, but the difference between the magnitude of the responses and the position of the peak response is dependent on frequency, which will be further examined later.

The phase variation along the BM has a similar shape for each mechanism, where the phase falls with an increasing rate as the wave travels along the BM. At locations past the peak response, the phase of all the responses are equal. However, there is a phase difference for the BM response between the different excitation mechanisms at locations close to the base, where the travelling wave is generated. This phase difference is due to the different excitation mechanisms and the excitation frequency. Hence, this comparison between the phase graphs is not representative of all frequencies, however, the shape of the phase response is similar for the audible frequency range.

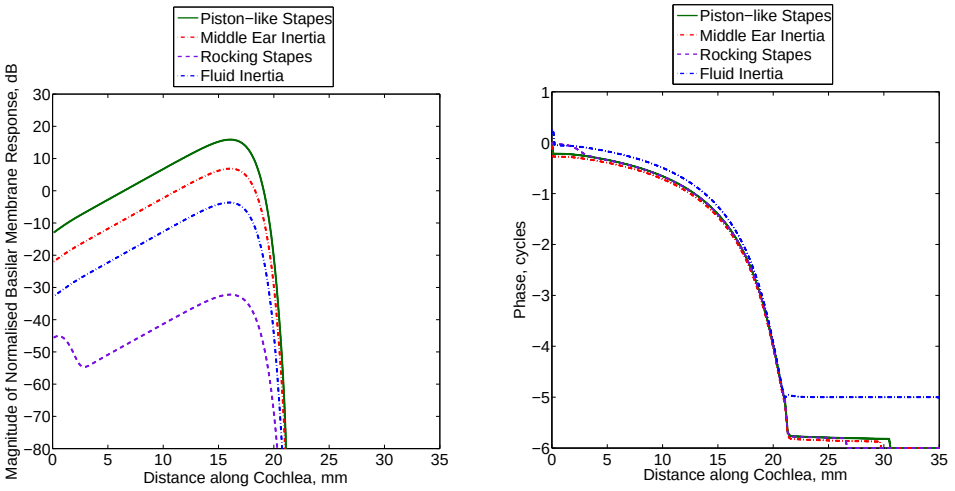

(a) (b)

Figure 4.1: Graph comparing the phase and magnitude of the BM response for a piston-like motion at the stapes (green), the two inertia BC components, middle ear inertia (red) and fluid inertia (blue), and the rocking motion of the stapes (purple) when excited at 1 kHz. All excitation mechanisms show a very similar shape of phase, however, the magnitude is excitation mechanism and frequency dependent.

The instantaneous BM displacement, at various frequencies was determined for the different excitation mechanisms, in order to compare the shape of the response at an instant in time. As shown above, the magnitude of the BM response and phase differs for each response and so for clarity in comparing the responses, the displacements were normalised to their peak value and the phase altered such that the responses were at the same point in their cycle. A snap-shot of the normalised BM displacements at a single instant in time is shown in Fig. 4.2 for excitation at 1 kHz, but the similarities in shape are the same for the range of audible frequencies considered. It can be clearly seen that this model predicts that no matter how the cochlea is excited, a travelling wave along the BM is produced. This is in agreement with the discovery last century that a travelling wave is produced that travels from the base to the apex no matter where along the length of the cochlear the excitation occurs Bekésy (1955). It is also in agreement with the majority consensus in the literature that the motion of the travelling wave is fundamental in the production of a hearing response. It is therefore not unexpected that a travelling wave is produced for every excitation mechanisms, but it is significant that for non-volumetric excitation such a wave is seen. It has only been reported by one other group that this similar wave will be produced by non-volumetric excitation of the cochlea (Edom et al., 2013). The shape of the wave is very similar at locations away from the base, however, close to the base of the cochlea, there is a deviation when excited by the rocking motion of the stapes. This deviation is similar to that found by Edom et al. (2013) for this kind of excitation, and will be further discussed in Section 4.4.

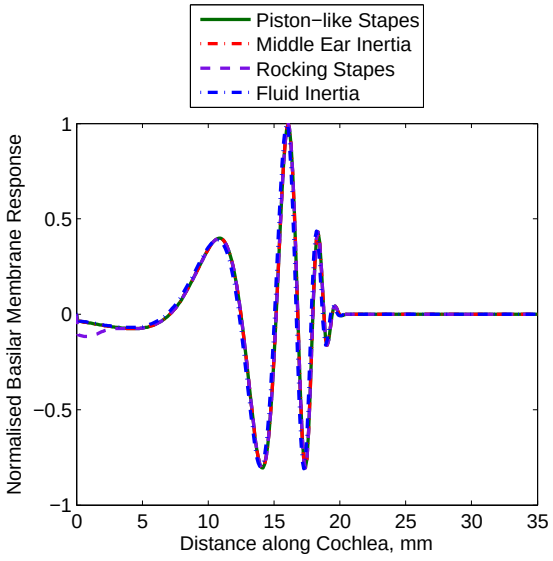

Figure 4.2: Graph comparing the normalised BM response for a piston-like motion at the stapes (green), the two inertia BC components, middle ear inertia (red) and fluid inertia (blue), and the rocking motion of the stapes (purple) when excited at 1 kHz. All excitation mechanisms have a very similar shaped travelling wave along the BM at locations greater than 5 mm from the base. Only the rocking motion of the stapes produces a small peak in the response close to the cochlear base.

4.3 The Response to Piston-like Motion of the Stapes

A uniform velocity was applied at the oval window to simulate a piston-like motion of the stapes, which is assumed to dominate when the cochlea is excited by AC. The magnitude of the relative BM velocity response and the phase, for a range of frequencies, is shown in Fig. 4.3a and 4.3b. The BM velocities are relative to the velocity of the oval window.

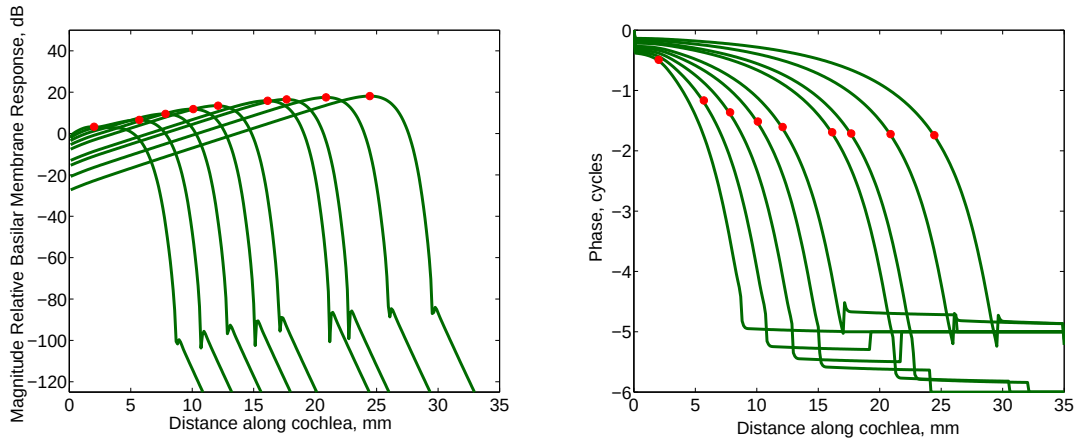

(a) (b)

Figure 4.3: The magnitude (a) and phase (b) of BM response, relative to the velocity of the stapes, due to excitation via a piston-like motion of the stapes at 6, 4.5, 3.3, 2.4, 1.8, 1, 0.8, 0.5, 0.3 kHz, where the highest frequency is the first plot on both graphs and the lowest the last plot. The red dots illustrate the position of the peak response.

Fig. 4.3a shows that the BM response increases until it peaks, and then sharply declines. This is due to the variation of the admittance along the BM, and is consistent with the measured BM response in the real cochlea when it is passive. The cochlea has a passive response when either it is excited by high level of stimulus, or when it is lifeless. The peak response is frequency dependent, and increases along the length. The red markers in Fig. 4.3a denote the peak response at any one excitation frequency. When calculating the frequency response of the BM, it is these values that are calculated and then plotted, as shown in Fig. 4.4. The phase of the response decreases along the length, with increasing magnitude, with an overall phase shift of about 2 cycles at the position of the peak response, as seen in Robles and Ruggero (2001). The ripples in the BM response seen at low amplitudes are similar to those found in Elliott et al. (2011); de Boer and Viergever (1982); Watts (2000), which are due to multiple wave propagation (Elliott et al., 2013).

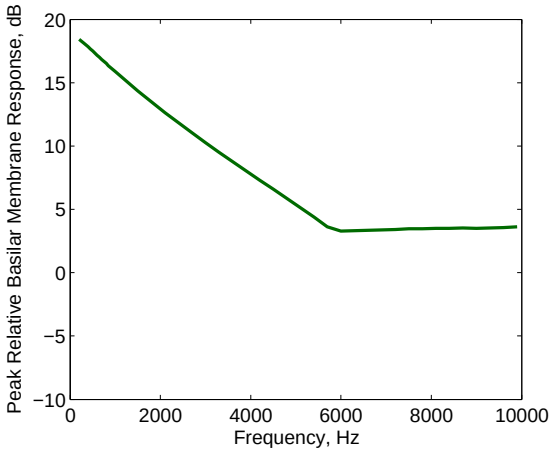

Figure 4.4: Frequency response of the peak BM velocity, relative to the stapes velocity, due to excitation via a piston-like motion of the stapes.

The relative peak BM response was predicted to decrease with frequency, until about 6 kHz, where it levels off, as shown in Fig. 4.4. A decrease in the BM response, relative to the excitation velocity of the stapes has also been found by Edom et al. (2013).

4.3.1 Comparison of the Models Results with Experimental Data

Stenfelt et al. (2003a) measured the BM velocity per stapes velocity, at one location along the cochlear length, in human cadavers, over a range of frequencies. The BM response is passive in cadavers and so the BM response predicted by this passive model can be directly compared to these experimental results. The location of the measurements made by Stenfelt et al. (2003a) was 12 ± 0.5 mm from the round window. It was assumed that the distance between the round window and the base of the cochlea was in the region of $2 - 3$ mm and so the location along the cochlear model chosen as a comparison was about 15 mm from the base of the cochlea. The geometry of the cochlea in the hook region is very complex and so given the simplified geometry of the cochlear model only an estimate of comparable locations can be used.

The BM response at this location was calculated for a range of frequencies and compared against the Stenfelt et al. (2003a) results.

The magnitude and phase of the BM response at 15 mm from the base is shown in Fig. 4.5a and 4.5b and Stenfelt et al. (2003a) results are shown in Fig. 4.6, labelled as BM_{AC}. Also shown in the Fig. 4.6 are the results of a similar measurement carried out by Gundersen et al. (1978) for comparison. The other plots shown in this figure (labelled OSL2 and OSL1) are not relevant to this discussion and so should be ignored. When comparing the magnitude of the two responses, experimental and calculated, it can be seen that the overall shape of the relative BM frequency response at one location are

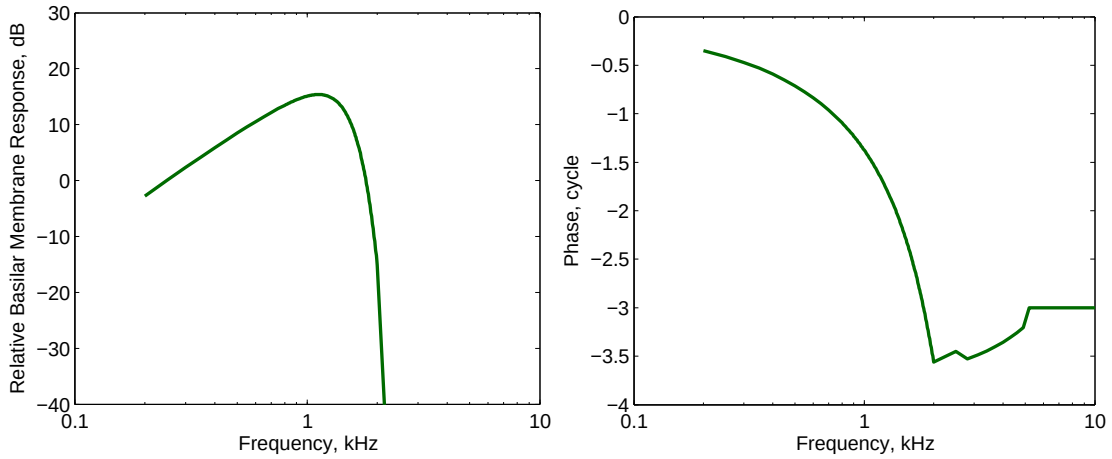

(a) (b)

Figure 4.5: Basilar membrane frequency response, relative to the input stapes velocity, at 15 mm along the cochlea from the base. The magnitude is shown in (a) and the phase in (b).

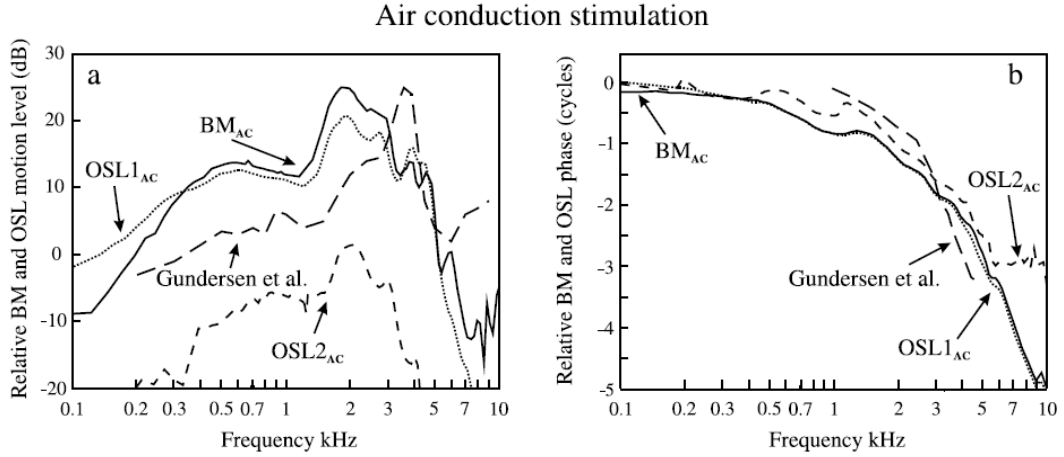

Figure 4.6: Results taken from Stenfelt et al. (2003a) of the measurements BM response, relatively to the stapes motion, at 12 ± 0.5 mm from the round window. The relative magnitude is shown in (a) and the phase in (b). Other plots shown on this graph (labelled OSL2 and OSL1) are not relevant to this discussion and so should be ignored.

similar. There is a peak in the response between 1 and 2 kHz which then falls off sharply. The location of the peak is dependent on the location along the cochlea chosen to take the measurements or in this case calculate the response. When experimental measurements are taken there is always some discrepancy between the chosen locations of measurements between specimen, however, this is not the case when calculating the relative response in a model. Hence, the small discrepancy between the peak BM responses are probably due to the exact location chosen to calculate the BM response. The magnitude of the peak relative BM response is predicted as about 20 dB by this model, which is slightly lower than that measured by Stenfelt et al. (2003a) and Gundersen et al. (1978) at about

25 dB. This could be due to the size of the oval window chosen. The larger the window the greater the excitation volume velocity and hence the greater the stimulus, so that, if a larger window was chosen then the response would be greater. The shape of the calculated phase of the relative BM response is similar to that measured by Stenfelt et al. (2003a) and Gundersen et al. (1978), with a lag of about 2 cycles at the frequency of peak response.

4.3.2 Cochlear Pressure Distribution

The piston-like motion of the stapes into the cochlea causes a displacement of fluid in the scala vestibuli which is compensated at the round window by a fluid displacement out of the scala tympani. This is called a volumetric excitation mechanism, as there is net fluid flow in and out of the cochlea due to the motion of the cochlea windows. The pressure distribution created in the cochlea, at one instant in time, due to this type of excitation is shown in Fig. 4.7b, with an exaggerated BM displacement laid over the top. This pressure distribution is a result of both the motion of the oval window and of the BM. The oval window in this case is moving into the cochlea, which creates the positive pressure that is seen at the base of the scala vestibule. The round window moves outwards, acting as a pressure release and so the pressure at the round window is zero, as seen in Fig. 4.7b.

There is a mean-pressure created in the cochlea, which is due to the fast wave propagation. The mean-pressure does not contribute to the slow cochlear wave propagation along the cochlea and so it is subtracted from the cochlea fluid pressure, with the resulting pressure distribution shown in Fig. 4.7c. This pressure distribution was further separated into its plane wave, Fig. 4.7d, and near field Fig. 4.7e components. The plane wave component is defined to be the pressure distribution along the walls parallel to the BM in each scala, and is constant in the transverse direction of each scala. The cochlear windows are located within these walls and so for locations in close proximity to the windows, the plane wave pressure distribution was taken at a distance further away from the window where the effect of near-field pressures due to the oval window and BM were minimised. The pressures for each axial location in each scala were then duplicated in the transverse direction over the whole cochlea so that the plane wave pressure distribution was produced. The near field pressure distribution was calculated by subtracting the plane wave component from the total pressure distribution.

The plane wave component was found to be the dominant pressure distribution in this case, as the maximum value of the near field component is about a quarter of the value of the maximum plane wave pressure. The near field pressure in this case is largest close to the BM, at the locations where the BM excitation is highest and so the local acceleration of the fluid is greatest. A small near field pressure is also visible in the locations close to the cochlear windows, which is due to the motion of the windows.

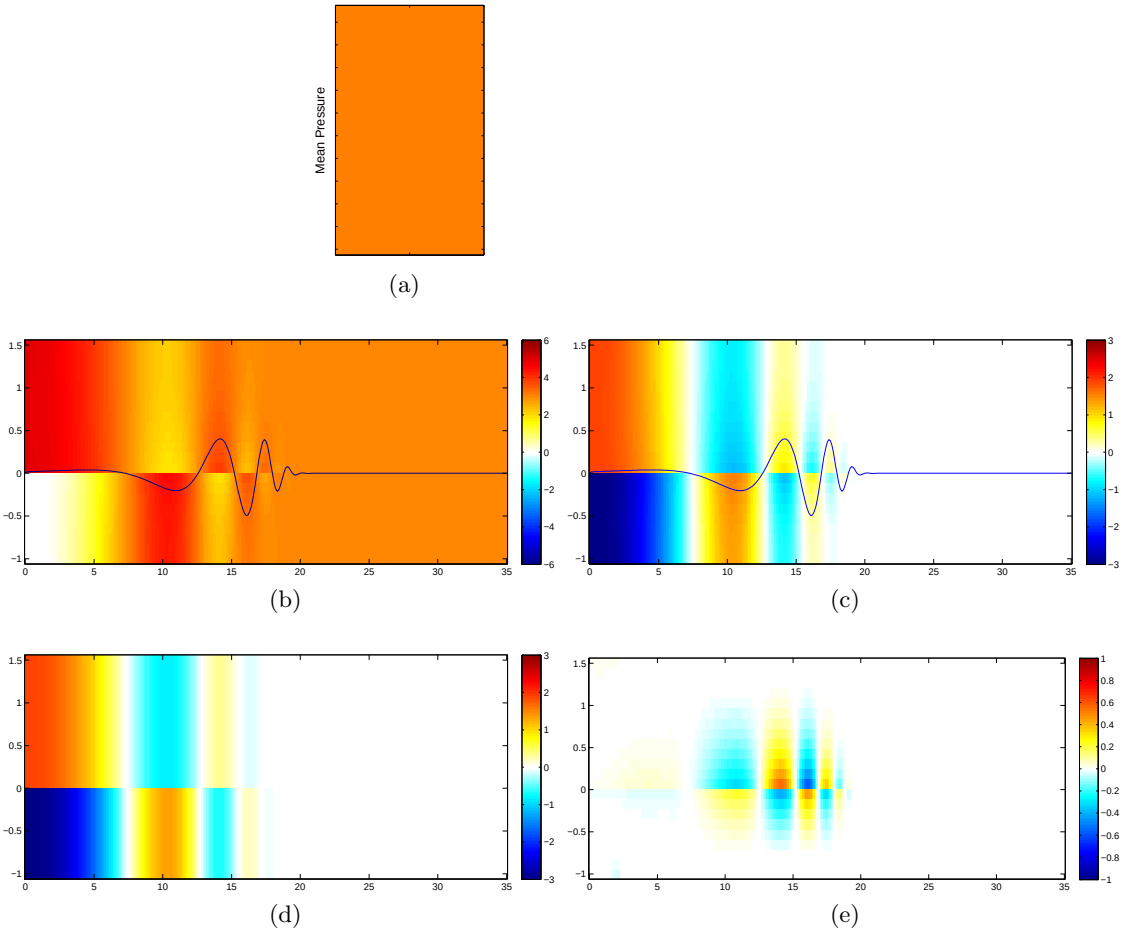

Figure 4.7: Illustration of the pressure distributions in the cochlea due to excitation via a piston-like motion of the stapes. The total pressure distribution is shown in (b). The resultant pressure distribution after the mean pressure causing the fast wave propagation, (a), is subtracted is shown in (c). The plane wave and near-field components of the pressure distribution are shown in (d) and (e) respectively.

4.4 Rocking Motion of the Stapes

The results of the investigation into the rocking component of the complex motion of the stapes, due to AC stimulus, are presented and discussed in this section. The BM response, due to a modified model, are compared to those of Edom et al. (2013), where a 2D box model of the cochlea was also used to investigate this cochlear excitation mechanism. Although a considerably more complicated model of the fluid, including viscosity, was used by Edom et al. (2013), they did not include any damping in the modelling of their BM.

4.4.1 The Response of the Cochlea due to the Rocking Motion of the Stapes

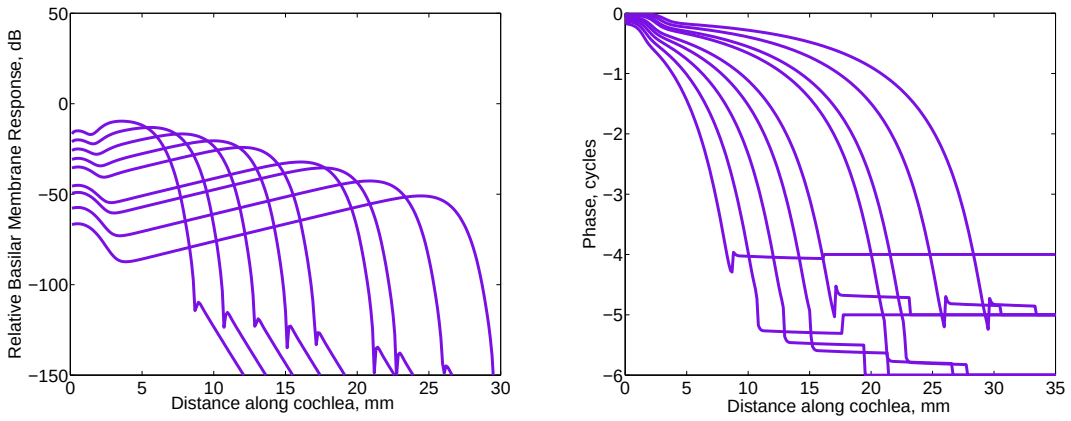

(a) (b)

Figure 4.8: The magnitude (a) and phase (b) of the BM response, relative to the maximum velocity, due to the rocking motion of the stapes at 6, 4.5, 3.3, 2.4, 1.8, 1, 0.8, 0.5, 0.3kHz, where the response at 0.3 kHz peaks near the apex and 6 kHz at the base.

The magnitude and phase of the BM response, for a range of frequencies is shown in Fig. 4.8a and 4.8b. It can be seen that the shape of the magnitude and phase of the BM response is similar to that of the other excitation mechanisms at distances more than about 5 mm from the base of the cochlea, which is due to the similar shape of travelling wave along the BM. A small peak in the magnitude and phase can be seen close to the apex of the cochlea. This peak in response close to the apex is due to the method of excitation, as will be discussed when the pressure distribution in the cochlea is examined.

The magnitude of the relative peak BM response due to the rocking of the stapes is shown in Fig. 4.9, and for comparison, the magnitude of the relative peak due to the piston-like motion of the stapes is also included. The BM response is normalised to the peak stapes velocity in both cases. The peak response due to the rocking motion of the stapes is very low below 1 kHz, but increases with excitation frequency. The response to the rocking component rises approximately proportional to the frequency, indicating that it is the acceleration of the fluid that causes the near field excitation. It can be seen that the rocking of the stapes generates a much lower BM response than that of a piston-like motion of the stapes. The difference between the BM response of these two mechanisms decreases as the frequency increases, from about 80 dB at 200 Hz to about 10 dB at 8 kHz. In order to understand the difference between the two mechanisms of excitation the pressure distribution in the cochlea is examined, and is shown in Fig. 4.10a.

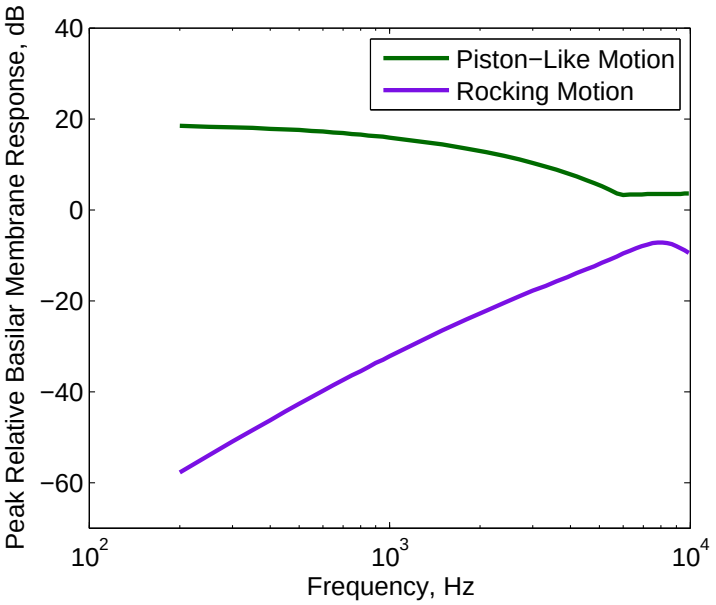

Figure 4.9: Frequency response of the peak BM velocity, relative to the maximum stapes velocity, due to excitation via the rocking motion of the stapes (purple).

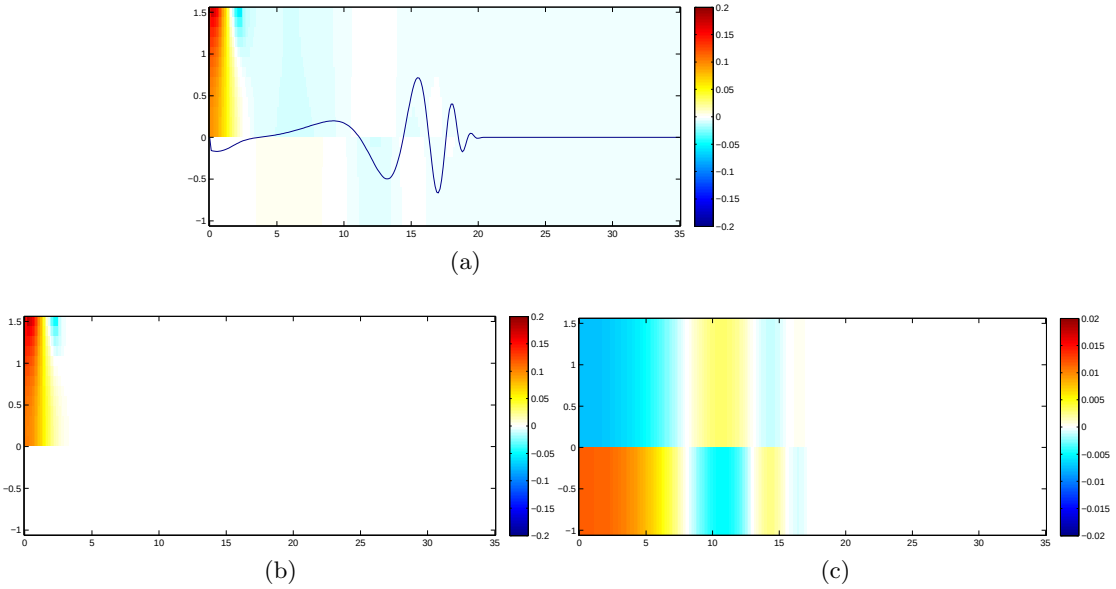

Figure 4.10: Pressure distribution sin the cochlea due to the rocking motion of the stapes. The total pressure distribution is shown in (a) and the plane wave and near-field components are shown in (b) and (c) respectively.

It can be seen that the pressure distribution differs greatly from those produced by the piston-like motion at the stapes or vibration of the cochlea walls, which were shown in the previous sections. When the stimulus is a rocking motion of the stapes the pressure in the cochlea is dominated by the near-field pressure, at the base of the cochlea, close to the oval window. This is in contrast to the volumetric excitation where the plane wave component dominates the pressure distribution. The pressure close to the oval

window is divided into a positive and negative near-field pressure that extends as far as the BM. The pressure adjacent to the oval window is positive when the stapes velocity is downwards and negative when the velocity is upwards, although it then becomes distorted by the effect of the end wall of the cochlea at positions further away from the oval window. It is this near field pressure established at the oval window that drives the BM into motion and is the origin of the small peak in the BM response at the base of the cochlea. As can be seen from the BM travelling wave overlaid in Fig. 4.10a, the shape of the BM deflection near the base of the cochlea follows the shapes of the near-field pressure distribution. It should be noted that a mean pressure still occurs when the cochlea is excited by this non-volumetric excitation. The pressure distribution from the rocking excitation mechainsm is similar to that found by Edom et al. (2013).

The overall pressure distribution, once the mean field pressure was subtracted, was again further separated into the plane wave and near field components, which are shown in Fig. 4.10b and 4.10c. The near field pressure distribution is now dominated by the pressure at the oval window due to the rocking motion of the oval window. The near field pressure close to the BM at the locations of its maximum response is again present. This is due to the travelling wave, but is in this case it is about two orders of magnitude less than the near field pressure extending from the oval window. The plane wave component is now a factor of 20 times smaller than the near field pressure component but has a similar form to that due to volumetric excitation since it is associated with the slow wave propagation causing the peak BM motion.

4.4.2 Comparison with Edom et al. 2D Model

The cochlear response, due to the rocking of the stapes, is compared with those found by Edom et al. (2013). It is important to compare results with other models as it is a method of indicating the robustness of the results. If a problem is approached from two different angles, and the results are reasonable comparable, then this increases the likelihood that they represent reality. If the results of two models are found to be considerably different, then there is a possibility that one or more assumptions in one or both models are unsuitable. This is, however, not to say if two models agree that they must be predicting realistic results, they may just happen to predict the same unrealistic result.

Edom et al. (2013) built a 2D box model of the cochlea and solved it using the Navier Stokes equations, for excitation via a piston motion at the stapes and rocking of the stapes. The results found by the Edom et al. (2013) investigation can be compared to those found by the present cochlear model. The Edom et al. (2013) model differs in geometry as well as the method of modelling the BM, as discussed in Chapter 4. The 2D finite element model presented here was altered to reflect the geometry and admittance variation along the BM of the Edom et al. (2013) model, for a better comparison between

models. The cochlear chambers were altered so they were symmetrical and had a height of 0.72 mm and a length of 36 mm. The oval window was positioned parallel to the BM with the centre of the stapes 2.1 mm from the base and its length extended to 3 mm. The location of the round window was moved so it was on the end wall, perpendicular to the BM.

In the Edom et al. (2013) model, the physical mass of the BM is assumed to be zero and the structural damping is neglected, assuming that the majority of the damping can be described by the fluid viscosity. Hence, the values and the variation along the cochlea of the effective damping and mass are inherent in the model and were not separately reported. Instead of trying to match the parameter values, the tonotopic map of the Edom et al. (2013) model was matched by the peak BM displacement position frequency map of this 2D finite difference model, shown in Fig.4.11. The parameters that are used to describe the variation in the stiffness of the BM in the model, ω_B, l, m_{add}, as well as the damping, c_{BM}, were modified so that the best place frequency map matched that in Edom et al. (2013). ω_B was set to equal 23 kHz to match that of the base frequency and then l was arbitrary altered so that the gradient of the tonotopic map of the cochlea was similar to that of the Edom et al. (2013) model, to give $l = 4.6 \times 10^{-3}$. The variation in c_{BM} was decreased by multiplying it by a factor, so that the peak BM response for the rocking motion of was similar to that in Edom et al. (2013). The added mass in this model needed to correlate the tonotopic maps was 0.3 kgm^{-2} and the damping was altered by a factor of 0.37. The BM response predicted by this altered model is shown in Fig. 4.12a. The results are shown in dimensionless units for ease of comparison with Edom et al. (2013), with $L^* = 3 \times 10^{-3}$m.

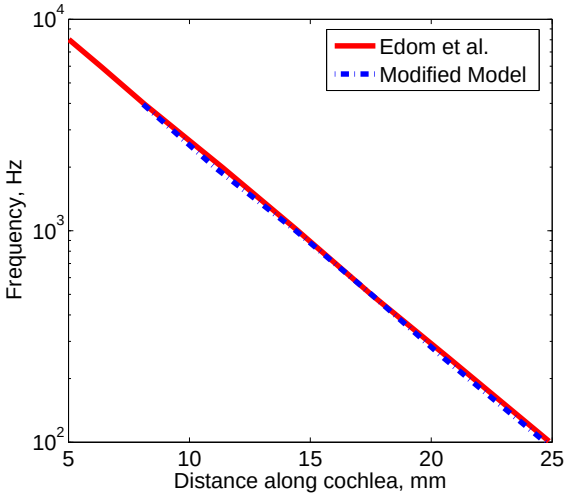

Figure 4.11: Comparison of Edom et al. (2013) tonotopic map and that from the altered 2D finite difference model.

The BM displacement results, found by the modified model described above, are shown in Fig. 4.12a in a form that allows them to be compared with that of Edom et al. (2013) which are shown in Fig. 4.12b.

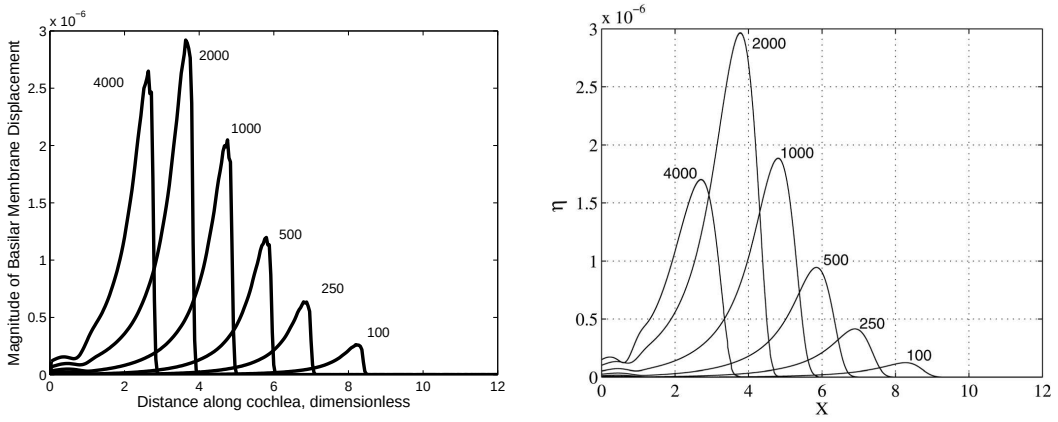

(a) (b)

Figure 4.12: Magnitude of BM displacement, relative to the maximum stapes displacement, when the stimulus is rocking of the stapes and with the modified geometry and BM admittance (a). Results from Edom et al. (2013) of the magnitude of BM displacement, relative to the maximum stapes displacement, when the stapes was rocked (b). The frequencies of excitation are labelled adjacent to each plot.

As can be seen from Fig. 4.12a and 4.12b, when the Edom et al. (2013) geometry is used and the BM parameters altered, there is a reasonable correlation between the Edom et al. model results and those produced here. Edom et al. (2013) predicted there to be an increase in BM response with frequency up to 2 kHz and then a reduction at 4 kHz. The magnitude of the BM response is similar between the two sets of results between 100 and 2 kHz. The reduction in the BM response at 4 kHz is reproduced, although not to the same extent as that found by Edom et al. (2013). Another difference between the results is the width of the envelopes. The results from Edom et al. (2013) decay over a greater length and are more symmetrical about the peak than those found here. This is due to the difference in the travelling wave along the BM. Edom et al. (2013) model predicts that the travelling waves decays in roughly 7 cycles, rather than 4 cycles predicted by this model. As discussed in Chapter 3, the damping in Edom et al. (2013) is incorporated into the cochlear fluid however, in this model it is defined in the BM. The comparison of the models results show that similar results can be obtained through either method of defining damping into the system. A alteration of the magnitude of this damping will change the number of cycles in which the travelling wave decays.

There is a decrease in response, predicted by both the Edom et al. (2013) model and the modified 2D finite difference model, at 4 kHz. The unmodified model present in this thesis does not predict such a decrease, which can be seen in the peak BM response, Fig. 4.9. This shows that the model parameters can have significant effect on the predicted

results. However, all variations of this model and that of Edom et al. (2013), predict an increasing response with frequency below 2 kHz.

4.5 The Cochlear Response due to the Inertial Components of Bone Conduction Hearing

The cochlear response due to the two inertial BC components, the middle ear inertia and fluid inertia, are presented in this section. As previously described, the middle ear inertia is simulated by applying a uniform velocity to the oval window generating a piston-like motion, where the input velocity is calculated from a lumped parameter model of the middle ear ossicles. The fluid inertia is simulated by applying a velocity to the upper and lower cochlear walls in order to simulate vibration in the vertical plane. When simulating the BC pathways, the BM response is calculated relative to the assumed external vibration of the temporal bone.

4.5.1 Cochlear Response due to the Inertial Bone Conduction Pathways

The relative magnitude and phase of the BM response due to the two inertia components of BC, for a number of frequencies, are shown in Fig.4.13. The shape of the BM response is similar for each response, however, the amplitude is excitation and frequency dependent. The variation in the initial phase of the BM response due to the middle ear inertia is due to the complex input, calculated from the middle ear response to vibrations.

Fig. 4.14 shows the peak relative BM response due to the two inertial components of BC. This model predicts that above 500 Hz frequency the middle ear inertia is the dominant mechanism of BC, and that below 500 Hz both components have similar magnitude. The fluid inertia response gradually increases with increasing frequency, while the middle ear inertia response rises to a peak, at around 1.7 kHz, and then decreases with frequency. The peak in response to the middle ear inertia is due to the resonance of the middle ear when the temporal bone is vibrated. The results of the BC components over 1 kHz must be taken with caution since a rigid body excitation is assumed in this model, whereas, above about 1 kHz the vibration of the skull becomes more complex as the skull is deformed by structural wave propagation.

The form of the pressure distribution due to the middle ear inertia is exactly the same as those shown in Fig. 4.7 as the cochlea is excited by a piston-like motion of the oval window. The only difference is the magnitude of the response and hence the magnitude of the pressure in the cochlea. The pressure distribution in the cochlear due to excitation via the fluid inertia components of BC, at 1 kHz, is shown in Fig. 4.15b.

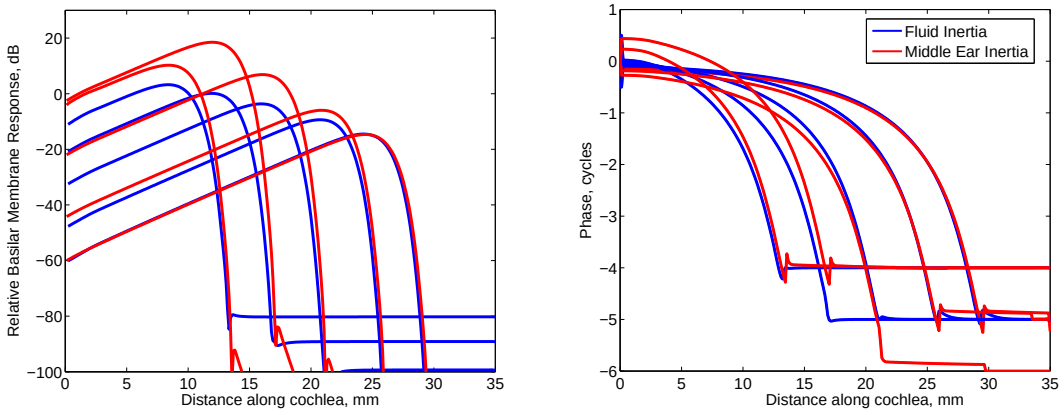

(a) (b)

Figure 4.13: Basilar membrane response, relative to vibration of the temporal bone, due to the fluid inertia (blue) and middle ear inertia (red) components of bone conduction hearing. (a) shows the magnitude and (b) the phase of the response at 3000, 1800, 1000, 500, 300 Hz, where the response at 3000 Hz is the closet to the base, and at 300 Hz is closet to the apex of the cochlear.

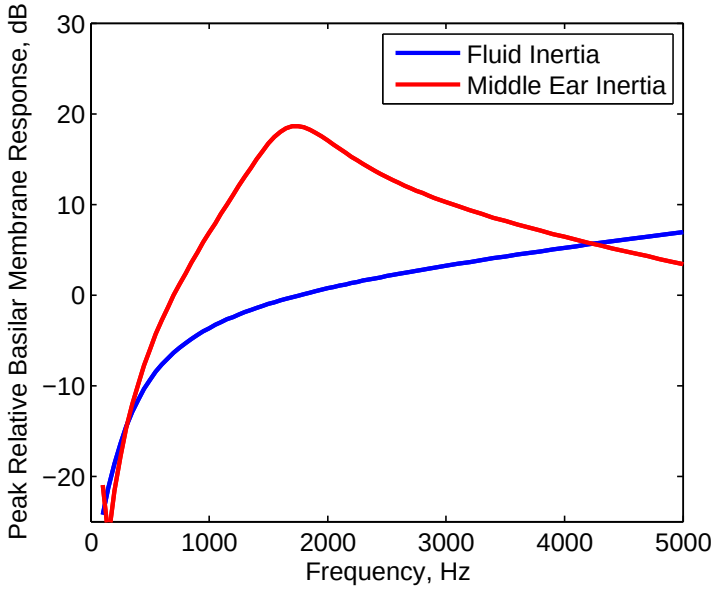

Figure 4.14: Peak BM frequency response, relative to vibration of the temporal bone, due to the fluid inertia (blue) and middle ear inertia (red) components of bone conduction hearing.

The fluid pressure distribution produced in the cochlea, due to the vibration of the cochlear walls, at first looks complicated and very different from that produced by applying a velocity at the oval window. At locations near the apex of the cochlea the pressure distribution consists of a constant decline in pressure from the top to the bottom wall. This pressure distribution is due to the motion of the cochlear walls. An upwards velocity on the upper cochlear wall will produce a negative pressure there but

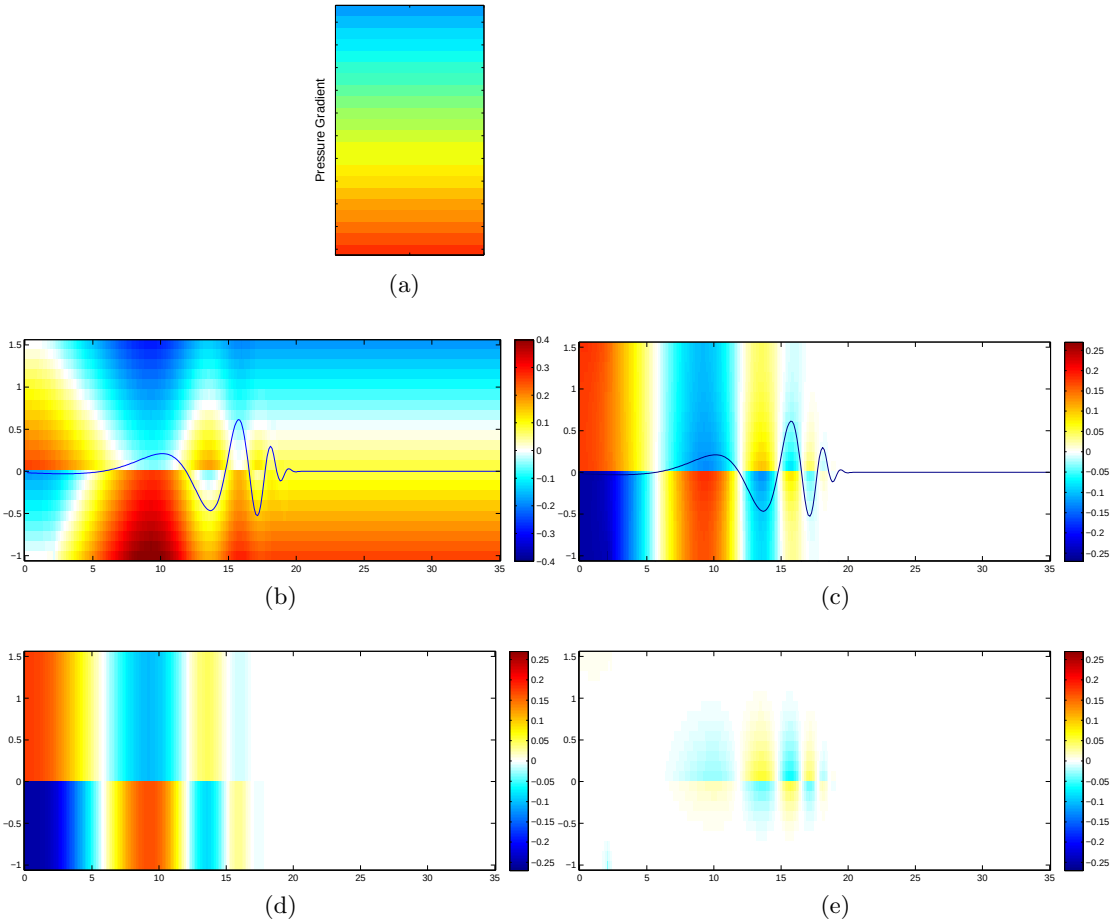

Figure 4.15: Illustrations of the pressure distributions in the cochlea due to excitation via the fluid inertia component of bone conduction hearing. The total pressure distribution is shown in (b), and the resultant pressure distribution after the pressure gradient due to the vibration of the cochlear walls, (a), is subtracted (c). The plane wave component (d) and near field component (e) of the pressure distribution are also shown.

a positive pressure at the lower cochlear wall, generating a uniform pressure gradient down the height of the cochlea as described in Appendix A. This pressure gradient is illustrated in Fig. 4.15a and exists all the way along the length of the cochlea. Once this pressure gradient is subtracted from the overall pressure distribution, the remaining distribution of pressure in the cochlea looks very similar to that of excitation via the piston-like motion at the oval window, shown in Fig 4.15c. This similarly is maintained when the pressure distribution was then further separated into the plane and near field components, as shown Fig. 4.15d and 4.15e respectively. Although these results do not fully represent the pressure excitation of the coiled 3D cochlea, they do provide a reasonable first approximation to visualising the pressure distribution, for this method of excitation.

The similarity in the pressure field between the direct stapes excitation and the fluid inertia of BC suggests that both mechanisms excited the cochlea via the same mechanism. This was confirmed by measuring the stapes excitation that resulted from imposing a

velocity on the horizontal walls of the model. This was found to be the same, per unit peak BM displacement, as when the stapes was directly excited. This result agrees with the results found by Kim et al. (2011) who used a 3D finite element box model of the cochlea and middle ear to investigate the fluid inertia component of BC. In this study it was found that the fluid inertia excitation is driven by the volume velocity through the oval window, hence a volumetric excitation. This 2D model and the 3D box model of Kim et al. (2011) thus both predict that the underlying mechanisms of the fluid inertia component of BC hearing are due to volumetric excitation.

4.6 Discussion and Conclusions

The 2D cochlear model described in the Chapter 3, was used to investigate multiple excitation mechanisms of the cochlea. It was shown that no matter how the cochlea was excited, a similar travelling wave was produced along the BM. If this wave was normalised to the peak response it is was shown that it takes the same shape for all excitation mechanisms. Air conduction hearing was simulated by assuming a piston-like motion of the stapes. It was shown that the BM response was comparable to experimental data and that the shape of the BM response and phase was similar to previous measurements.

The two inertial components of BC hearing were then simulated. It was predicted from these results, that the response due to the middle ear inertia was dominant over the fluid inertia component for most frequencies. At low frequencies, below 500 Hz, however, the contribution from both components were similar. The pressure distributions in the cochlea were similar for both inertial excitation mechanisms, and it was shown that both mechanisms stimulate the cochlea via a volumetric excitation. The pressure distribution due to volumetric excitation was separated into a plane wave and a near field components. The plane wave component was dominant over the near field component for these volumetric types of excitation, showing that the BM motion couples mainly into the plane pressure wave. The near field component was greatest at positions where it was driven by the acceleration of the BM.

A non-volumetric excitation mechanism, of the rocking of the stapes, was also examined, and it was shown that the response due to this component was less efficient at exciting the cochlea than a volumetric excitation mechanism, particularly at low frequencies. The pressure distribution in the cochlea due to this mechanism differed significantly from that of the volumetric excitation. A large near field component extended from the oval window to the BM at the base of the cochlea. It was this pressure component which drove the BM travelling wave. The near field component in this case was dominant over the plane wave component of the pressure distribution.

The results of this model, due to the rocking of the stapes, were compared to that of Edom et al. (2013) and show similar trends. The BM response due to the rocking motion of the stapes was predicted to increase with frequency by both models. The 2D finite difference model was adapted to reflect the modelling parameters and geometry used by Edom et al. (2013) and the BM response found to be comparable, even though the detailed implantation of the two models, particularly the form of the damping, was significantly different in the two cases.

Chapter 5

Effects of the 'Third Window' and an Immobile Oval Window on the Cochlear Response

This chapter mainly focuses on the effects of the 'third window' on the cochlear response to various cochlear excitation mechanisms. In the literature it has been suggested that, apart from the oval and round windows, a number of other fluid outlets in the cochlea, termed the 'third window', may have an effect on the hearing response of the cochlea, under certain conditions. In this chapter, two of these fluid outlets, the vestibular aqueduct and cochlear aqueduct, have been incorporated into the 2D cochlear model and their effect on the cochlear response investigated.

Firstly, the effect of these aqueducts on the response of a healthy cochlear is examined, where the peak BM response was used as a measure of its effect. The cochlear response is then examined when the cochlea is diseased with otosclerosis. Otosclerosis is a hearing condition which causes the oval window to become immobile, and so limits the excitation mechanisms that can stimulate the cochlea. It is thought that the 'third window' effects are particularly important under these conditions. Two cochlear excitation mechanisms, fluid inertia and local excitation of the round window, are investigated under a condition of an immobile oval window, simulating otosclerosis. The model was also used to predict the change in BC threshold due to the otosclerosis disease. This results was then compared with the clinical results of patients exhibiting a Carhart notch.

It has been shown in the literature that patients with a large vestibular aqueduct, LVA, have abnormal hearing thresholds. The change in AC and BC hearing thresholds, due to an LVA, is also investigated in this chapter using the 2D finite difference model. The results from the model are compared against clinical results and the changes in

thresholds described. The effect of a LVA on the cochlear response to local excitation at the round window is also discussed.

5.1 Description of Aqueduct Model

The cochlear aqueduct and vestibular aqueduct were included in the 2D cochlear model as shown in the diagram in Fig. 5.1. The vestibular aqueduct is located on the upper cochlear wall near to the oval window, only 4 elements away, which is roughly 0.5 mm, and extends over two elements, each of 0.12 mm in length. The cochlear aqueduct is positioned on the lower wall in close proximity to the round window, with only one element separating the two structures, which is about 0.12 mm, and extends only a single element.

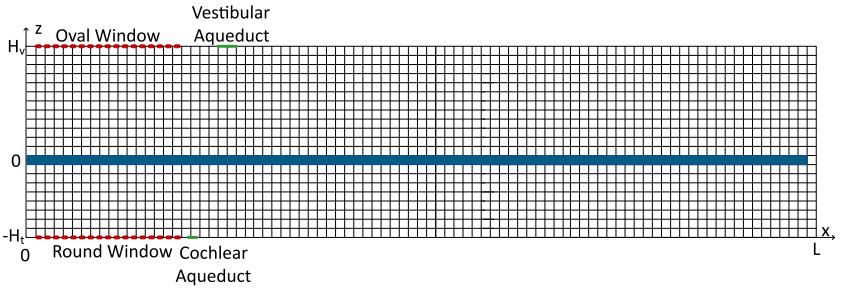

Figure 5.1: Diagram of the 2D finite difference box model of the cochlea with the inclusion of the aqueducts. The BM is shown in blue, the cochlear windows in red and the aqueducts in green.

The aqueducts are modelled in the same manner as the cochlear windows, where the fluid velocity at the surface of the model at the aqueduct position is related via its admittance to the pressure at the aqueduct location,

$$v_{CA}(x, H_t) = -Y_{CA} p(x, H_t), \tag{5.1}$$

$$v_{VA}(x, Hv) = Y_{VA} p(x, H_v). \tag{5.2}$$

The velocities are incorporated into the model through the relationship between the velocities and the pressure gradients at the aqueducts,

$$\left.\frac{\partial p(x,z)}{\partial z}\right|_{z=H_t} = -i\omega\rho v_{CA}(x, H_t), \tag{5.3}$$

$$\left.\frac{\partial p(x,z)}{\partial z}\right|_{z=H_v} = -i\omega\rho v_{VA}(x, H_v), \tag{5.4}$$

The admittances of the aqueducts in this model were calculated from the model given in Stenfelt (2014). In Stenfelt (2014) it was assumed that the aqueducts were fluid filled cylindrical ducts that terminate in the cranial space, which was modelled as a larger fluid-filled space. The cochlear aqueduct was assumed to have a radius of 0.075 mm and a length of 10 mm, while the vestibular aqueduct was modelled as two connecting cylinders, the first having a radius of 0.15 mm and length 1.5 mm and the second a 0.6 mm radius and 8.5 mm length. They both terminated in the cranial space of volume, V, which was calculated by assuming a sphere of radius 50 mm. The wave admittances of the aqueducts, Y_{jA}, equal to linear velocity over pressure, were calculated here using the area of the aqueducts, A_{jA}, and the inverse of the acoustic impedance equation in Stenfelt (2014),

$$Y_{jA} = \frac{1}{A_{jA}(i\omega L_{jA} + R_{jA} - i\frac{1}{i\omega C_{jA}})}, \tag{5.5}$$

where,

$$L_{jA} = i\omega\frac{4\rho l_{jA}}{3\pi r_{jA}^2}, \quad R_{jA} = \frac{8\eta l_{jA}}{\pi r_A^4}, \quad C_{jA} = \frac{\rho c^2}{V}, \tag{5.6}$$

where, j may either denote the cochlear or vestibular aqueduct, l_{jA} and r_{jA} are the length and radius of the aqueducts respectively, η and ρ are the viscosity and density of the cochlear fluid and, c, the speed of sound in the cochlear fluid.

The variation with frequency of the acoustic admittances (volume velocity per unit pressure) of the cochlear windows and the aqueducts resisting the fluid flow out of the scala vestibuli and scala tympani, are shown in the Fig. 5.2a and 5.2b, respectively. These graphs show that the admittances of the aqueducts are greater than the windows at low frequencies, meaning that the fluid can flow more easily through the aqueducts than the cochlear windows at these frequencies. The vestibular aqueduct resists the fluid flow less than the oval window below 1 kHz, as shown in Fig. 5.2a, although the oval window is also externally driven for many forms of excitation. The cochlear aqueduct is less resistant than the round window to the fluid flow below 200 Hz, as show in Fig. 5.2b.

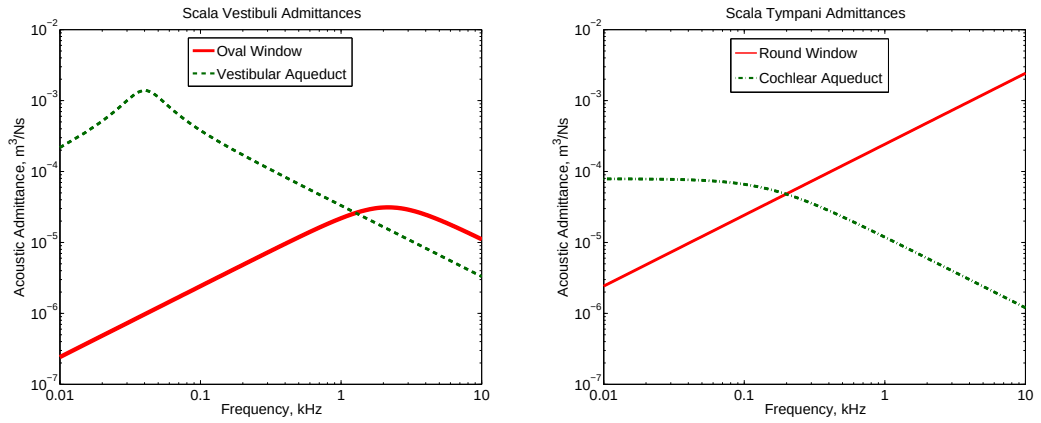

(a) (b)

Figure 5.2: Graphs illustrating the variation of the acoustic admittances with frequency of the compliant structures in the cochlear model. (a) shows the admittances of the oval window (thick red) and the vestibular aqueduct (green dashed) which are located in the scala vestibuli while (b) shows the admittances of the round window (thin red) and the cochlear aqueduct (dashed dotted green) which are located in the scala tympani.

5.2 Effect of Aqueducts on the Healthy Cochlear Response

The effects of adding the two 'third window' structures, the cochlear and vestibuli aqueduct, into the box model on the cochlear response were investigated on the cochlear excitation mechanisms report in Chapter 4. This included, the two stapes motion components of AC hearing; piston-like and rocking, and the two inertial components of BC hearing; middle ear inertia and fluid inertia.

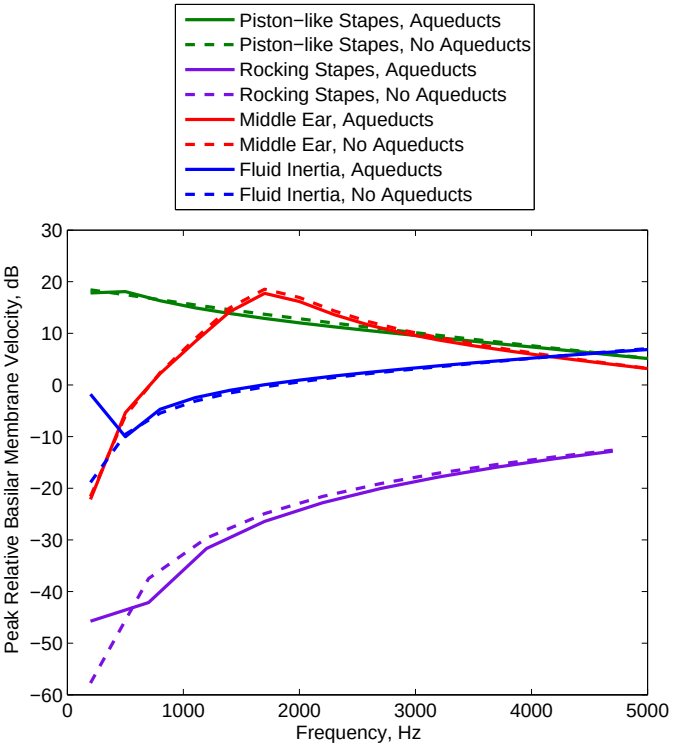

Figure 5.3: Peak relative BM response due to the excitation of a piston-like motion at the stapes, (red), fluid inertia (blue) and rocking of the stapes (purple) with and without the inclusion of the 'aqueduct' in the model.

Fig. 5.3 shows the frequency response of the peak BM response, relative to the excitation velocity, with and without the inclusion of the aqueducts in the model for the different excitation mechanisms. It can be seen that at frequencies above about 500 Hz the presence of the aqueducts had little effect on the overall BM response for all the mechanisms. They also did not affect the BM response below this frequency for excitation via a piston-like stapes motion, but the aqueducts did increase the BM response by a maximum of about 15 dB when the cochlea was excited by the rocking of the stapes and at about 20 dB at 100 Hz when excited by the fluid inertia component.

The increase in response due to the fluid inertia, at low frequencies, is due to the aqueducts increasing the overall admittance experienced by the fluid flow out of the scalae. This produced a greater volume velocity in and out of the cochlea, increasing the BM response to this excitation mechanism. At higher frequencies the admittances of the cochlear windows dominate and so the BM response is unchanged by the inclusion of the aqueducts. The aqueducts a have significant effect on increasing the response to the due fluid inertia pathway at low frequencies, but have no effect on the middle ear

pathway. Hence, the aqueducts change the relative significance of the pathways to the overall BM response. At very low frequencies the fluid inertia component dominates, whereas with no aqueducts included in the model both components are similar.

The increase in the BM response due to the rocking of the stapes has been found to be due to fluid flowing out through the vestibular aqueduct and hence producing a small volumetric component to the excitation mechanism, although, since there is little rocking motion of the stapes at low frequencies (Heiland et al., 1999; Sim et al., 2010; Hato N, 2003), this is not likely to be an important effect.

5.3 Otosclerosis and Local Excitation at the Round Window

Otosclerosis is a disease which can cause a bony growth over the oval window, eventually resulting in its immobilisation. Patients who present with this disease have shown to be still able to hear through BC, and hence have a large air-bone gap in their audiograms. It is clear that in this case the cochlea cannot be excited through the motion of the middle ear, but a hearing sensation can still potentially be produced through direct excitation of the cochlea, for instances through the fluid inertia component. Otosclerosis was simulated in the model by increasing the stiffness from 830 Nm^{-1} to 8.3×10^{28} Nm^{-1}, which effectively makes the oval window immobile. The mechanisms by which a hearing sensation could be produced under such conditions as well as the role of the aqueducts is examined in this section.

Excitation at the round window has been investigated as a potential method of treating otosclerosis (Colletti et al., 2006; Beltrame et al., 2009; Schraven et al., 2011). Weddell et al. (2014) investigated the idea that the round window could act simultaneously as a location of stimulus and of pressure release. This is possible due to the size of the floating mass transducer used to stimulate the round window, where the area in contact with the round window, typically 1.8 mm^2 (Colletti et al., 2006), is smaller than the round window itself, roughly 3.2 mm^2. Hence, the there is a section of the round window not in contact with the transducer, that has the potential to act as a pressure release. This type of excitation is simulated in the cochlear model by using a combination of a flexible section of the round window, where the velocity is an output of the model, and excitation over another section of the round window, where the velocity is an input to the model. The middle 1.1 mm of the 2.2 mm length of the round window is driven, and so its velocity is assigned, while the 0.6 mm either side is compliant, as shown in Fig. 5.4. This mechanism of excitation allows for the round window to simultaneously act as an excitation location and as a pressure release.

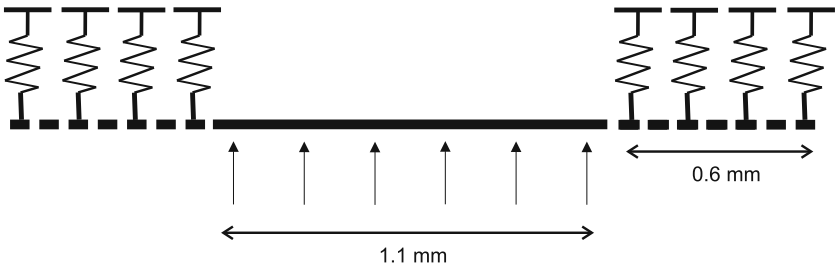

Figure 5.4: Diagram showing the excitation of the cochlea via local excitation of the round window. The arrows represent an applied velocity and the springs represent the flexible sections of the round window. When exciting by this method, a velocity is applied to the middle section of the round window and the pressure can be released by the flexible outer quarters.

This method of excitation was investigated when it was assumed that the cochlea was diseased with otosclerosis, thus the oval window was assumed to be immobile. The effect of the inclusion of the aqueducts, under these conditions, are also investigated in this chapter.

5.3.1 Pressure Distribution in the Cochlea due to Local Excitation of the Round Window with No Aqueducts

Fig. 5.5b shows the pressure distribution in the cochlea, due to stimulation by the local excitation at the round window, at 1 kHz, when the oval window was assumed to be immobile and no aqueducts were modelled. This condition only allows for non-volumetric excitation to occur, as there is only a fluid outlet on one side of the BM.

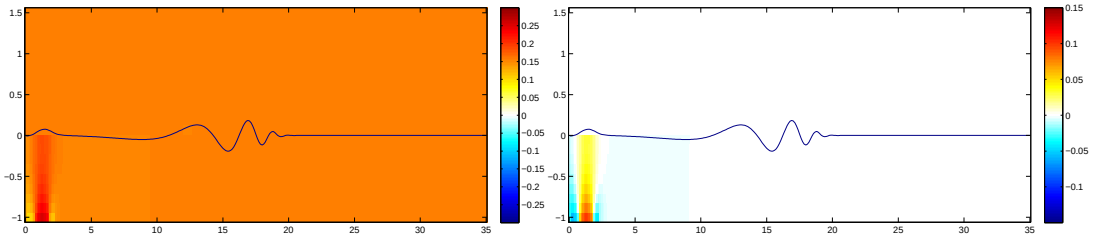

(a) (b)

Figure 5.5: Pressure distribution in the cochlea due to local excitation at the round window. (a) illustrates the distribution before the average alternating pressure was subtracted and (b) the near field component, after the subtraction of the average alternating pressure.

The theory in Weddell et al. (2014) describes how two pressure components are created with this excitation mechanism, which are, the average alternating pressure and near field pressure. The average alternating pressure is constant over the whole of the cochlea,

and can be clearly seen at locations away from the cochlea base in Fig. 5.5a. This average pressure was subtracted from the distribution and the resulting near field pressure distribution shown in Fig. 5.5b. There is a clear near field component extending from the round window to the BM at the base of the cochlea. It is this near field pressure which forces the BM into motion and generates the cochlear travelling wave. This is a similar form of excitation to the near field pressure produced at the oval window when the stapes is rocked, generating a BM travelling wave motion. However, the shape of the near field pressure is different in the two cases due to the variation in the shape of the cochlear window motion. At the time instant shown in Fig. 5.5b, the middle section of the round window is moving inwards and so a positive pressure is created, represent in red. This motion forces the ends of the round window to move outwards, and so a negative pressure is created, represented in blue.

Weddell et al. (2014) predicted that the average alternating pressure would be controlled by the linear stiffness of the freely moving section of the round window, S, and would be given by to $\frac{Sq}{i\omega A^2}$, where q the volume velocity through this section of the round window, and A the area. If this is true then the average alternating pressure should decrease with frequency as $\frac{1}{\omega}$. The near field pressure however, which generates the BM motion, was expected to scale with the acceleration of fluid close to the moving part of the round window and thus be proportional to $i\omega\rho q$.

The average pressure and near field pressure, predicted by the model with no aqueducts included, were calculated for a range of frequencies and are shown in Figs. 5.6a and 5.6b. The near field pressure was calculated as the pressure, opposite the round window, at the location of the BM, once the average pressure was subtracted from the pressure distribution. The average pressure is the pressure that is constant throughout the cochlea. It was taken from a location far from the base near the apex of the cochlea, where all other pressure components were not present as they had decayed away. The predicted mean pressure follows the inverse of the angular frequency well up to about 1 kHz, while at greater frequencies it starts to increase. This contradicts the prediction of Weddell et al. (2014), where it was assumed the pressure was dominated by the stiffness of the window. The deviation from this model, could perhaps be due to the inertia of the fluid affecting the average pressure at higher frequencies, and so the pressure would be controlled by a stiffness and a mass. This is supported by the evidence that the round window is mass and resistance dominated at higher frequencies (Nakajima et al., 2009). Fig. 5.6b, shows that the predicted near field pressure is quite closely proportional to the excitation frequency, as predicted by Weddell et al. (2014), and it is this component that excites the BM response.

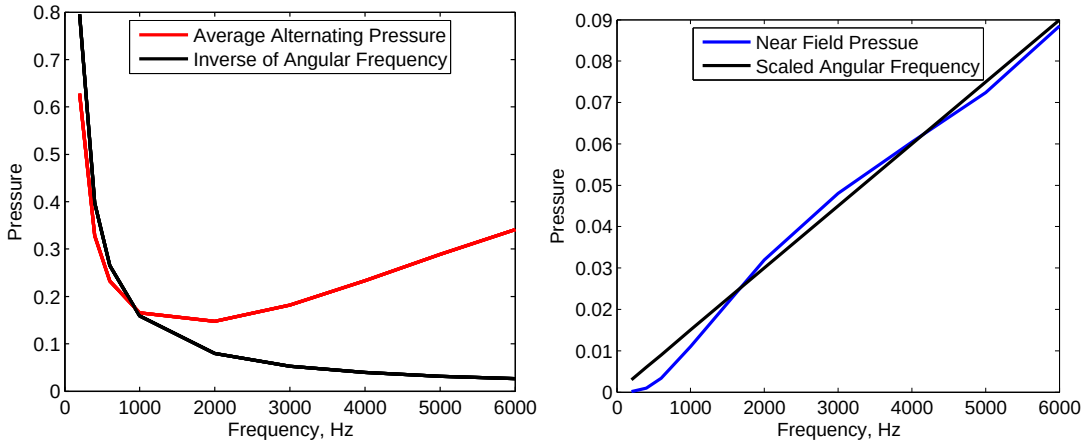

(a) (b)

Figure 5.6: Frequency variation of the calculated average alternating pressure (a) and the near-field pressure (b) due to local excitation at the round window with an immobile oval window. The inverse of the angular frequency is shown in (a) and a scaled angular frequency in (b) (black) are also shown for comparison.

5.3.2 Effect of the Aqueducts on the Cochlea Response due to Local Excitation at the Round Window with an Immobile Oval Window

The effect of the aqueducts on the cochlear response, when excited by local excitation at the round window with an immobile oval window, was investigated using the model described above. Fig. 5.7 shows the peak relative BM response due to local excitation at the round window with [i] both aqueducts, [ii] each aqueduct separately included and [iii] no aqueducts included in the model. The presence of the vestibular aqueduct, close to the oval window, has a significant effect on the BM response at low frequencies, while the presence of the cochlear aqueduct, close to the round window, has very little effect. When the oval window is immobile, and no aqueducts are modelled, the only possible excitation mechanism is non-volumetric, i.e. via the near-field pressure as shown in Fig. 5.5b, as there is only a compliant structure on one side of the BM. Including the cochlear aqueduct in the model does not restrict this near-field excitation from occurring, but including the vestibular aqueduct introduces a compliant structure on the upper wall of the cochlea, meaning that volumetric excitation can now also be generated. The BM response due to local excitation at the round window is predicted to be increased by more than 50 dB at low frequencies by the inclusion of the vestibular aqueduct, although, at around 2 kHz, the BM response is reduced by up to 10 dB and then at higher frequencies the response becomes comparable to a model with no aqueducts present.

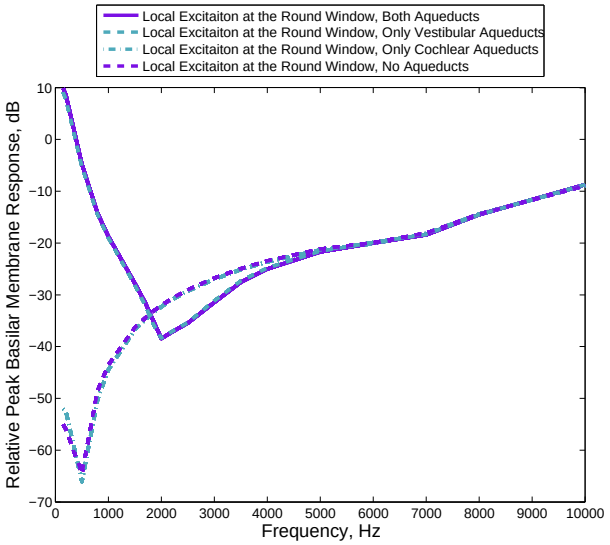

Figure 5.7: Graph comparing the BM response to local excitation at the round window with an immobile oval window when both aqueducts were modelled (purple solid line), with only the vestibular aqueduct modelled (light blue dashed line), only the cochlear aqueduct modelled (light blue dashed dotted line) and when no aqueducts were modelled (purple dashed line).

These results suggest that when the vestibular aqueduct is included, the overall BM response is due to a combination of both non-volumetric and volumetric excitation. This was investigated by calculating the non-volumetric and volumetric response and then summing them together. The sum was compared to the total response to insure that they had been separated correctly. An incompressible fluid was modelled here, so it was easy to separate the two excitation components, since the total volume velocity through the upper and lower cochlear wall must be exactly the same. This had no significant effect on the BM response. The volumetric excitation component was predicted by calculating the volume velocity through the vestibular aqueduct when the model was excited by local round window excitation with both aqueducts included, and then using this velocity value as an input into the model. The model was then excited with a piston-like motion at the round window, such that the volume velocity through the round window was the same as that calculated through the vestibular aqueduct, to simulate the volumetric component of excitation. The magnitude of the non-volumetric excitation is assumed to be the response when local excitation is simulated, when no aqueducts were modelled and the oval window was immobile. The frequency response of the magnitude of the peak BM velocity for the predicted non-volumetric and volumetric excitations, and for the sum of these responses and total excitation are shown in Fig. 5.8.

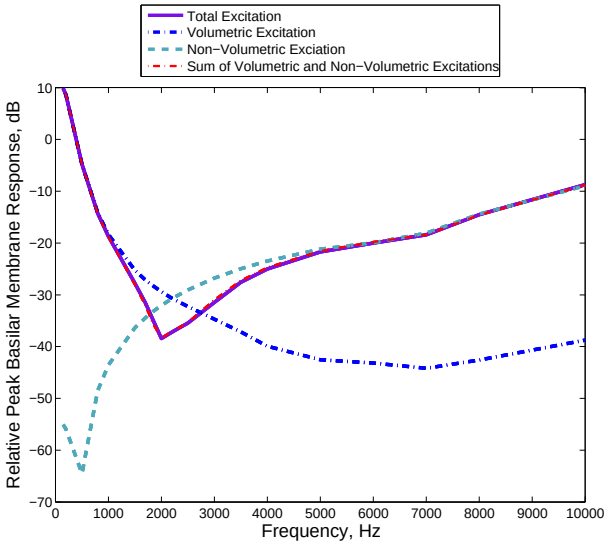

Figure 5.8: The total BM response (purple solid line) separated into its volumetric (blue dashed-dotted line) and non-volumetric (light blue dashed line) components. The sum of the two components (red dashed dotted line) is shown for comparison with the total excitation, to show that they are the same.

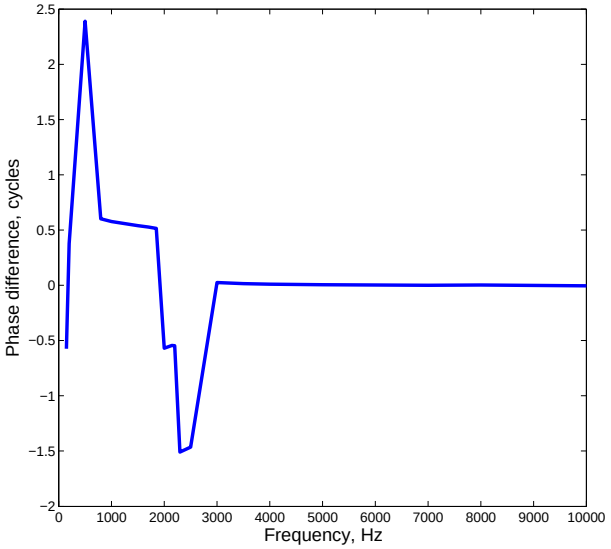

Figure 5.9: The phase difference, in cycles, between the volumetric and non-volumetric components of excitation at 2000 Hz

It can be seen in Fig. 5.8 that the vector sum of the non-volumetric and volumetric responses is very similar to the total response which suggests that the two components have been successfully separated. At low frequencies the volumetric component dominates, while at high frequencies this switches and the non-volumetric dominates. Between about 1 kHz and 3 kHz the magnitude of the components are similar, however, the total response is lower. The reason for this is made clear in Fig. 5.9, where the difference in phases between the volumetric and non-volumetric components at the peak BM response

is plotted. The phases are shown in cycles and therefore at any point where the phase difference ends in 0.5 the travelling waves of the two components are out of phase. The jagged nature of this plot is due to the spacing between the frequency measurements, however, it does illustrated where the components are in and out of phase clearly. At frequencies below 3000 Hz the two components are out of phase and therefore the resultant wave is smaller than either original wave. This difference in phase between the volumetric and non-volumetric components, and that they are of similar magnitudes, is thus the reason for the reduction in the BM response between 1 kHz and 3 kHz. This is further represented in Fig. 5.10 where the total BM response and its two components are shown at three key frequencies.

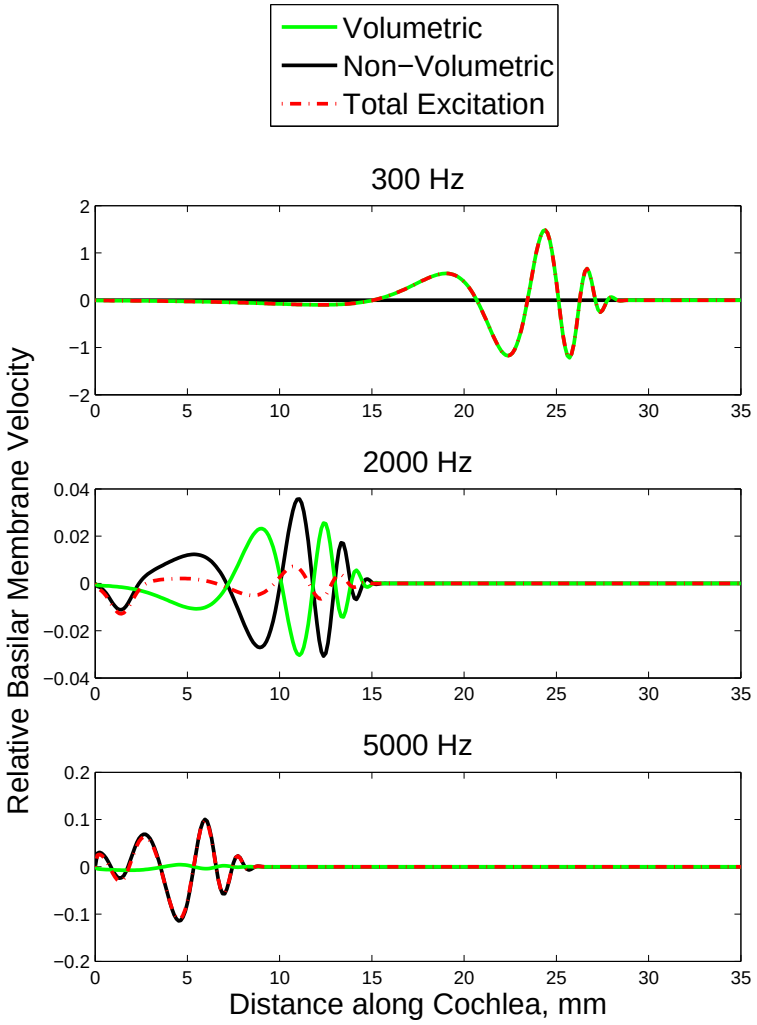

Figure 5.10: Graphs of the relative BM velocity at three frequencies, 300, 2000 and 5000 Hz. The total response (red dashed dotted line) and the two components, the volumetric (green solid line) and non-volumetric (black solid line) are shown in all three graphs.

The domination of the volumetric component at 300 Hz and the non-volumetric at 5000 Hz can clearly be seen in Fig. 5.10. However, at 2000 Hz, the volumetric and non-volumetric components have a similar magnitude, but they are opposite in phase, as shown in Fig 5.9. When combined, the resultant response is of smaller magnitude than the two components. The geometry of the cochlea could have a potentially large effect on the phases of the two components. Since a realistic geometry is not modelled here, it cannot be definitely concluded that phase cancellation between the two components

will occur in the real cochlea at the frequency predicted by the model. However, the model does suggest that both the components need to be considered when examining this method of excitation, as their relative phases can make significant difference to the total response. It also predicts that at low frequencies the volumetric component dominates, while at high frequencies the non-volumetric component dominates.

Weddell et al. (2014) found little difference in the cochlear response to local excitation at the round window in guinea pigs whether the stapes were mobile or fixed with glue, as shown in their Figure 9. The measurements were only taken at frequencies above 5 kHz however, so the notch effect predicted here may still have occurred at a lower frequency than measured. The geometry of the guinea pig cochlea and the human cochlea are also rather different, as are the sizes of the windows and aqueducts, so it is not clear where such a notch would occur in the guinea pig cochlea.

Round window excitation experiments were also carried out by Lupo et al. (2009), but in this case on chinchillas. It was found that the cochlear microphone, compound action potential and auditory brainstem thresholds due to excitation at the round window all increased with the fixation of oval window. In this mammal it was found that the difference in responses was greater at high frequencies than at low. This is in contrast to the predictions of the model presented here, however, this is a comparison between different mammalian cochlea, of difference sizes and frequency detection range, and so it is not unsurprising that there are differences. The results in Lupo et al. (2009) do however do show that when the stapes is fixed there is still a mechanisms that excites the BM in a mammalian cochlear. This mechanism could either be due to non-volumetric excitation of volumetric excitation through the 'third window', or a mixture of both. It is not clear to what extend the transducer covered the round window and so non-volumetric excitation could be a possibility. The difference in results from Weddell et al. (2014) and Lupo et al. (2009) suggests that the effects of the 'third window' varying from species to species which could be due to the details the size and impedance of the aqueducts.

In Stieger et al. (2012) experiments were carried out on temporal bones to investigate reverse direction excitation of the cochlea, ie through the round window. In order to investigate the reverse direction excitation, intra-cochlear pressure, stapes velocity and round window velocity measurements were taken. It was found that, unlike for excitation at the stapes, the motion of the stapes was not a good estimation for the BM excitation when the cochlea was excited via the round window. This suggests that the excitation is not solely driven by the net volume displaced at the cochlear windows, as with conventional excitation at the oval window. It was proposed that this result is due to the 'third window' in the scala vestibuli having a functional role in the cochlear response. The model presented here supports this theory at low frequencies, where the excitation was found to be predominantly volumetric due to the flow the

through vestibular aqueduct. In this model the oval window was assumed to be immobile, however, in Stieger et al. (2012) the oval window was flexible, so the total volumetric excitation would be a combination of the flow through the oval window and the vestibular aqueduct. A further explanation to the results in Stieger et al. (2012) is that at high frequencies the non-volumetric component will dominate the excitation and so the net motion of the oval window is zero, and hence not proportional to the BM response. The results from the Stieger et al. (2012) study, along with the results from the model presented here strongly suggests that the 'third window', in particular the vestibular aqueduct, has a significant effect at lower frequencies when the cochlea is excited at the round window. This model further predicts that non-volumetric excitation may also be a significant method of excitation when the excitation is at the round window, and it is only partially occluded.

5.4 Effect of the Aqueducts on the Cochlear Response due to Fluid Inertia Excitation with an Immobile Oval Window

The effect of the aqueducts on the cochlear response when excited by the fluid inertia component of BC hearing, and with the oval window assumed to be immobile, was investigated and the results are presented in this section. This is the only method of excitation for BC hearing when the oval window is immobile, since it is not possible to excite the cochlear via the middle ear.

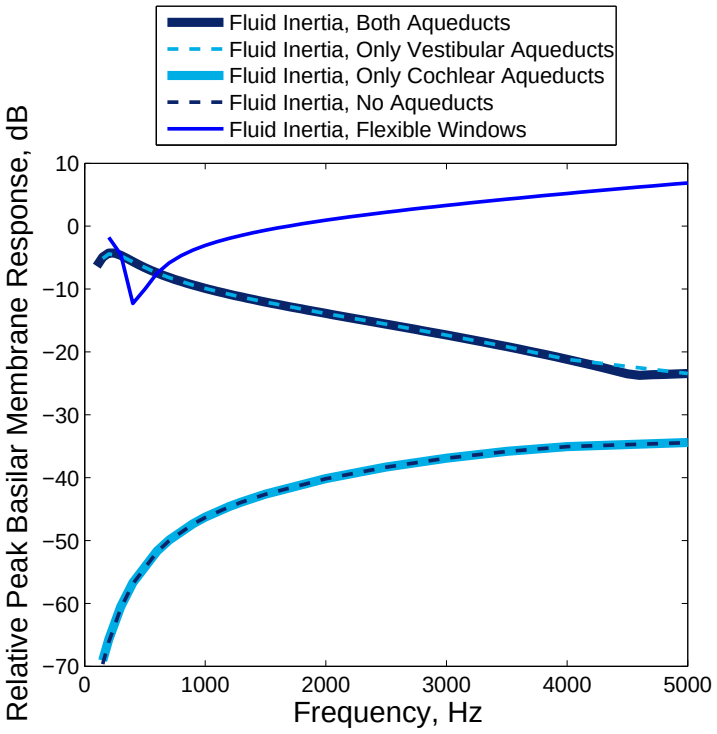

Figure 5.11: Peak BM response, with an immobile oval window, when excited by the fluid inertia component, when both aqueducts were modelled (solid blue line), with only the vestibular aqueduct modelled (light blue dashed line), only the cochlear aqueduct modelled (light blue solid line) and when no aqueducts were modelled (blue dashed line). The response with a mobile oval window (solid dark blue line) is shown for comparison.

Fig. 5.11 shows the peak relative BM frequency response due to the fluid inertia excitation, with the oval window immobile, with no aqueducts, with only one aqueduct and when both aqueducts are included in the model. For comparison, the BM frequency response when the oval window was flexible and with both aqueducts included is also shown in Fig. 5.11, which was first presented in Fig. 5.3. It can be seen that when the oval window is immobile, and when no aqueducts are included in the model, the BM response due to fluid inertia is very much lower at all frequencies than when the oval window is flexible. This is because there is only a fluid outlet on the scala tympani side of the cochlea and no outlet on the scala vestibuli side. This means volumetric excitation is not possible and only non-volumetric excitation can occur. When the cochlear aqueduct is included, there is still no fluid outlet on the scala vestibuli side, so again, only non-volumetric excitation can occur. This produces the low BM response seen in Fig. 5.11 for this condition.

Inclusion of the vestibular aqueduct into the model, with the immobile oval window, considerable increases the BM response over the whole frequency range shown. The increase is more pronounced at low frequencies, while as the frequency increases the

difference between BM responses, with and without the vestibular aqueduct, decreases. This increase in response is due to there being a compliant structure on either side of the BM for this condition, and so volumetric excitation can take place. It has been shown in Chapter 4 that volumetric excitation is more efficient at exciting the BM than non-volumetric and so an increase in response is seen. At low frequencies, below about 1 kHz, the BM responses with a flexible oval window and an immobile oval window are similar when the vestibular aqueduct is modelled. However, at higher frequencies the BM response with a flexible window is much greater. This is due to the relative admittances of the oval window and vestibular aqueduct. At high frequencies, the oval window admittance is greater than the vestibular aqueduct and so dominates the volumetric response, as seen in Fig. 5.2a.

The BM response due to the fluid inertia excitation, when both aqueducts are incorporated into the model, was separated into the volumetric and non-volumetric components in order to examine the types of excitation occurring. This was done in a similar way to that described in section 5.3.2. Fig. 5.12 shows these components, along with the total response and the sum of the two components for comparison.

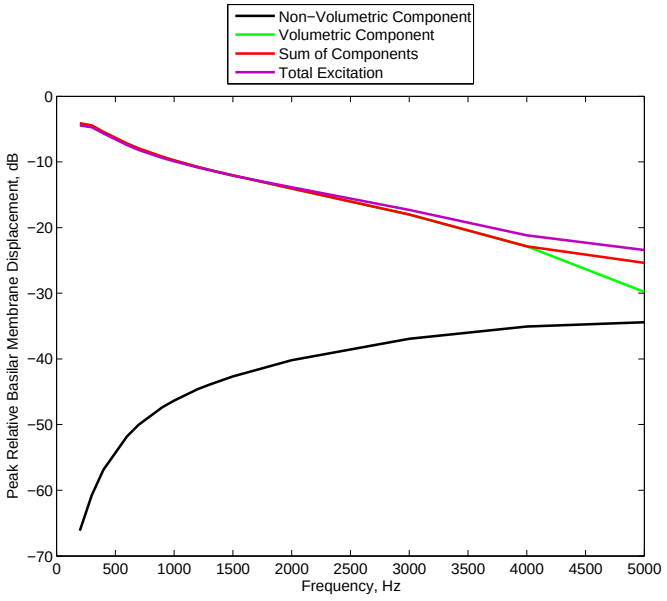

Figure 5.12: Peak relative BM response to the fluid inertia component, where the total response (solid purple line) is separated into the volumetric (solid green line) and non volumetric (solid black line) components. The sum of the two components (solid red line) is also included to show that it is the same as the total response.

It can be seen that BM response is dominated by the volumetric excitation, but as the frequency increases, the non-volumetric excitation component becomes more significant. This explains why the introduction of the vestibular aqueduct increases the BM response, by over 50 dB, at low frequencies. The inclusion of the vestibular aqueduct changes the

dominant excitation mechanism from non-volumetric to volumetric and the difference between these two types of excitation is largest at low frequencies.

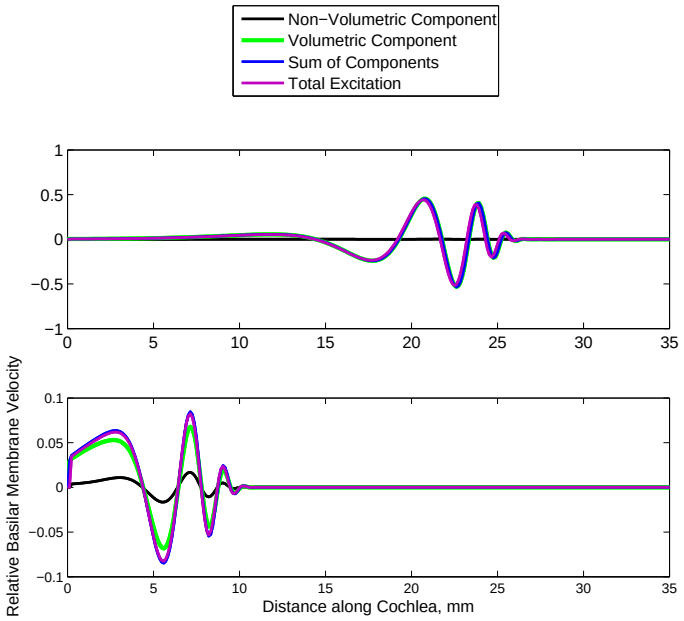

Figure 5.13: Individual total BM velocity (solid purple line) at 400 Hz and 4 kHz, separated into the volumetric (solid green line) and non-volumetric (solid black line) components. The sum of the two components (solid blue line) is also included to show that it is the same as the total response.

To further investigate the types of excitation occurring, the individual BM responses were determined at 400 and 4 kHz. The response due to both types of excitation and the total response were calculated and are shown in Fig. 5.13. At 400 Hz, the volumetric and total BM response are equal, showing that the volumetric component is dominant and the non-volumetric component has little effect on the total BM response. At 4 kHz the volumetric and non-volumetric components add together and so the total response is greater than both individual responses. This model therefore predicts at this frequency that the non-volumetric component significantly contributes to the total response.

The model thus predicts that the vestibular aqueduct has a significant effect on the BM response, when a cochlea with an immobile oval window is excited by the fluid inertia component of BC hearing. The inclusion of the vestibular aqueduct allows for volumetric excitation to occur, even when the main compliant structure in the scala vestibule, the oval window, is immobile. Without the vestibular aqueduct the BM response to the fluid inertia pathway is very low, particularly at low frequencies. However, the inclusion of

the vestibular aqueduct increases the response which, to some extent, can explain why BC hearing is still possible when the cochlea is diseased with otosclerosis. This will be examined further in the next section.

5.4.1 Carhart's Notch

It is well documented that the stiffening of the oval window due to otosclerosis mostly affects BC hearing threshold at around the 2 kHz region, where there is a dip in response, which is termed Carharts notch. The change in BC hearing thresholds due to the stiffening of the oval window has been predicted using the model in the previous section. The difference between the combined peak BM response due to the inertial BC components in a healthy cochlea and one with a stiff oval window was assumed to be a measure of the change in BC thresholds due to otosclerosis.

The combined BM response due to the inertial components of BC was determined by summing together the individual BM responses for each component, at each frequency, along the length of the cochlea. The peak of this combined BM response was then calculated to predict the hearing frequency response due to BC hearing in a healthy cochlea. The BC hearing response, in a cochlea diseased with otosclerosis, was assumed to be the peak response of the model, with a stiff oval window and including the aqueducts, when being excited by fluid inertia. The difference between these peaks responses were then determined in order to predict the change in BC hearing thresholds and this is shown in Fig. 5.14.

In reality, the magnitude of the hearing reduction due to otosclerosis is variable between individual people and so two sets of clinical data are also shown for comparison; the values calculated in Ginsberg et al. (1978), after the analysis of 2405 cases and those from Carhart (1962), which were extracted from a graph in Stenfelt (2014).

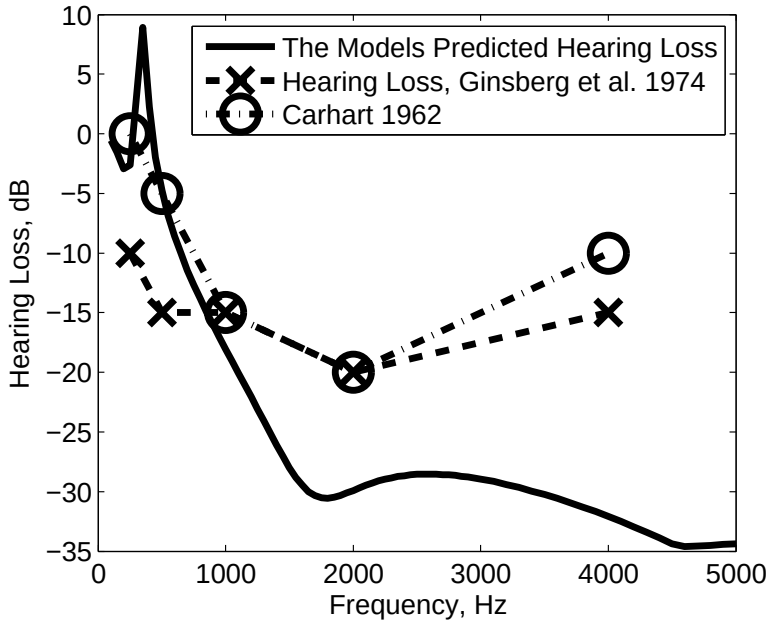

Figure 5.14: Comparison of predicted bone conduction hearing loss, due to stiffening of the oval window, from the present model (solid black line) and from two sets of clinical data for patients with otosclerosis; Ginsberg et al. (1978) (dotted line with X) and Carhart (1962) (dashed dotted with O).

The present model predicts the greatest hearing loss at around 2 kHz, which is similar to that in the data used in Ginsberg et al. (1978) and Carhart (1962), but the model predicts the magnitude of the hearing loss is greater than found by both studies. This may be due to other BC pathways, most likely the compression and expansion component, significantly contributing to the total response, which are not included in this model. Another reason could be due to the phase difference between the two inertial components. The simplified geometry used in this model may mean that the phase difference between the two components, and hence their sum, do not reflect reality. This means, at for instance, at 2 kHz, the combination of the two inertial components could be less, and hence the hearing loss reduced.

At low frequencies the model predicts a small hearing gain, while Ginsberg et al. (1978) predicts a small hearing loss. The predicted hearing response is more similar to those from Carhart (1962), however with a large spike in hearing level between the 100 and 500 Hz measurements. At low frequencies a small hearing loss, or over a narrow frequency range, hearing gain, is predicted by the model. This results is due to the effect of the vestibular aqueduct on the cochlea response when excited by the fluid inertia component and the oval window is immobile. Without the vestibular aqueduct the BM response due to the fluid inertia would be considerably lower at low frequencies, as shown in Fig. 5.11. However, the vestibular aqueduct allows for volumetric excitation and so the BM response is of a similar magnitude to that of the combined BC inertial response in the healthy cochlea. This model therefore suggests that the 'third window' and in

particular the vestibular aqueduct, is part of the explanation of why the BC threshold is not considerably changed at low frequencies by the stiffening of the oval window.

5.5 The Effect of a Large Vestibule Aqueduct

It has been reported that some patients have a vestibular aqueduct that is larger than the normal range, which has an effect on their hearing abilities, as discussed in Chapter 2. The effect of a large vestibular aqueduct, LVA, on the hearing response from multiple hearing mechanisms is investigated using this model. A LVA is modelled here by an increase in the radius of the vestibular aqueduct and then calculating the admittance with a larger radius using Eq. 5.5. Instead of calculating the admittance based on two connected cylinders, a single cylindrical tube of length 10 mm and radius 0.75 mm was assumed. There is great variation in the sizes of large vestibular aqueducts, but 0.75 mm is a conservative estimate, based on findings reported in Gopen et al. (2011). Fig. 5.15 shows the frequency response of the acoustic admittance of the modelled LVA, together with the normal vestibular aqueduct and oval window admittances included for comparison. It can be seen that the LVA admittance is greater than the oval window admittance for a wide range of frequencies. The LVA admittance and the admittance of the normal vestibular aqueduct are similar at low frequencies, but at frequencies above about 700 Hz the LVA admittance is larger, with a large peak around 1.5 kHz, and dominates the acoustic admittance of the oval window at high frequencies.

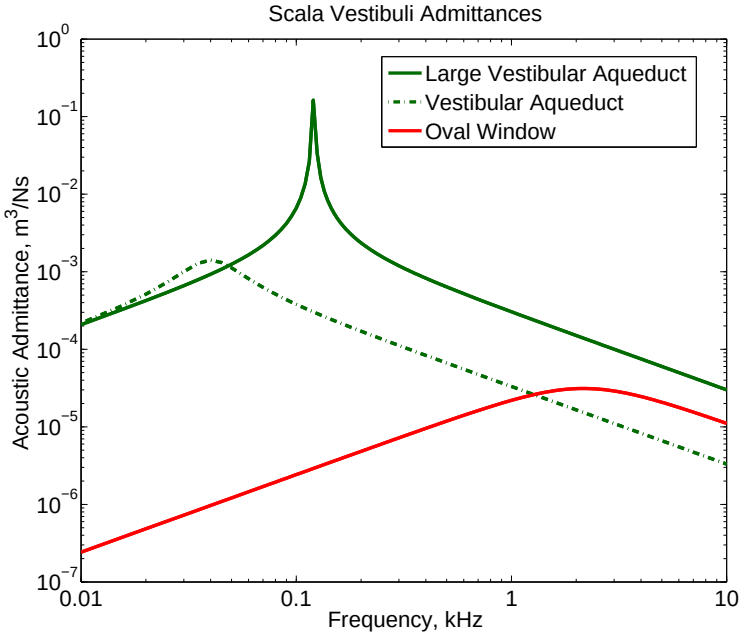

Figure 5.15: A comparison of the variation with frequency of the large vestibular aqueduct (solid green line) acoustic admittance, with a normal size vestibular aqueduct (green dashed dotted line) and the oval window (solid red line).

5.5.1 Effect of a Large Vestibular Aqueduct on Excitation via a Stapes Piston-Like Motion

Fig. 5.16 shows the peak BM response due to the piston-like motion of the stapes, when a LVA was modelled and for comparison, when a normal vestibular was modelled. The model predicts that a LVA has a significant effect on reducing the BM response below about 4 kHz. The peak BM response with the LVA modelled is 40 dB lower at around 200 Hz, and over 10 dB lower at 2 kHz. The effect of the LVA on the BM response decreases with frequency, and has little effect at excitation frequencies greater than 5 kHz.

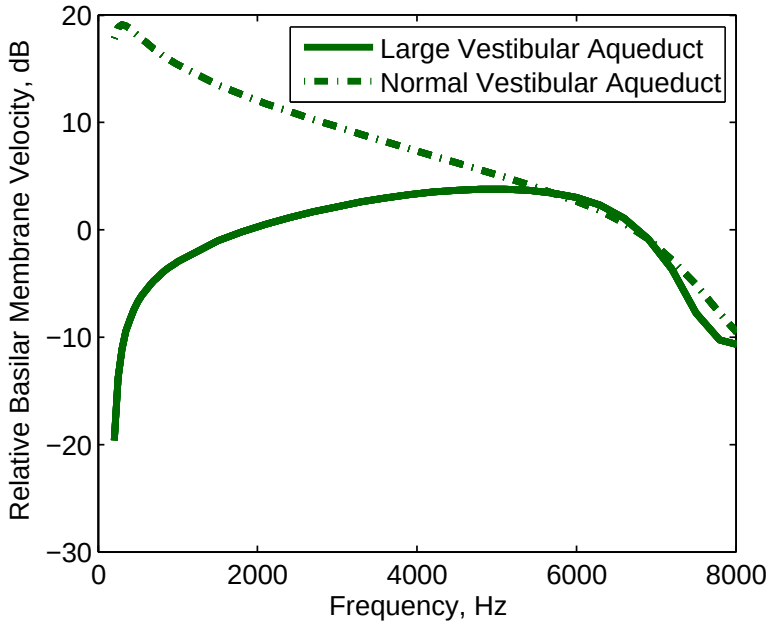

Figure 5.16: A comparison of the peak BM response with a large vestibular aqueduct (solid green line) and a normal vestibular aqueduct (dashed green line) when excited by a piston-like motion of the stapes.

The reduction in the BM response is a result of the cochlea fluid being forced out of the LVA by the pressure in the scala vestibuli. This decreases the overall volume velocity which is driving the excitation via the stapes. This mechanism is illustrated well by the pressure distribution shown in Fig. 5.17, where there is an opposite pressure at the oval window and the LVA, indicating the fluid acceleration at these structures are in opposite directions. The admittance of the LVA decreases with frequencies, increasing the resistance to the fluid flow out of the LVA, and hence at higher frequencies the LVA has a lesser effect.

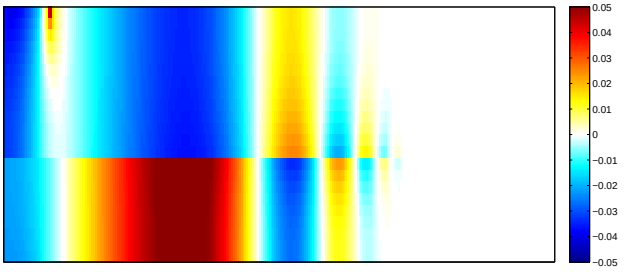

Figure 5.17: Pressure distribution, at 400 Hz, due to a piston-like motion at the stapes, when a large vestibuli aqueduct is assumed.

5.5.2 Large Vestibular Aqueduct Effect on Excitation via Fluid Inertia

The effect of a LVA on the fluid inertia component of BC was examined in healthy cochlea, i.e. with a flexible oval window. Fig. 5.18 shows the peak relative BM response due to the fluid inertia component of BC, with a normal vestibular aqueduct and a LVA. The enlargement of the vestibular aqueduct can be seen to significantly increase the BM response due to the fluid inertia component at frequencies above 500 Hz. This finding suggests that a LVA would decrease the BC threshold and so a person with a LVA would be more sensitive to hearing via the fluid inertia component of BC. This is in agreement with the findings in Merchant SN (2008); Govaerts et al. (1999); Gopen et al. (2011); Mimura et al. (2005), where an air-bone gap at low frequency in patients with a LVA was found. The results for this inertial BC components need to be treated with some caution above 1 kHz, due to the assumption of a rigid head model, as discussed earlier.

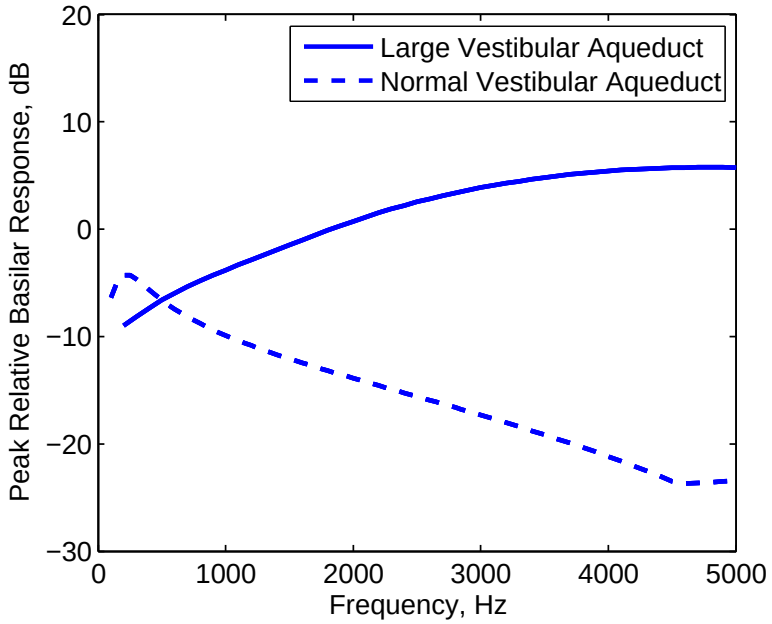

Figure 5.18: A comparison of the peak BM response, relative to the assumed vibration of the temporal bone, with a large vestibular aqueduct (solid line) and a normal vestibular aqueduct (dashed line) when excited via the fluid inertia component of BC.

5.5.3 Air-Bone Gap due to Large Vestibular Aqueduct

The difference between the AC and BC hearing thresholds is called an air-bone gap. As discussed in Chapter 2, it has been reported that patients who have a LVA often have an air-bone gap at low frequencies (Govaerts et al., 1999; Mimura et al., 2005; Merchant et al., 2007a; Merchant SN, 2008; Gopen et al., 2011). The present model has been used to predict the AC and BC hearing thresholds with a LVA modelled and the difference between them was calculated to determine the air-bone gap. The peak BM response when a normal vestibular aqueduct is modelled, is taken as the healthy hearing level for each excitation mechanism. The difference between these peak responses and the peak response when a LVA is modelled is the hearing thresholds predicted by the model due to the presence of a LVA. Hence, for AC hearing, the change in hearing threshold with a LVA is calculated as the difference between the two lines plotted in Fig. 5.16.

For BC hearing, the peak response is defined as the peak response due to the combination of both the fluid inertia and middle ear inertia responses, as discussed in Section 5.4.1. This peak response was found when both a normal and a LVA were modelled, which is shown in Fig. 5.19. The effect of the LVA on the fluid inertia component has already been shown in Fig. 5.18. The middle ear inertia ultimately excites the cochlea via a piston-like motion of the stapes and so the BM response due to this BC component is decreased due to the LVA by the same level at each frequency as is shown in Fig. 5.16. The two inertial components of BC hearing, above about 500 Hz, are affected in opposite

ways by an LVA, giving the combined inertial BC peak response which is shown in Fig. 5.19. Both the BC peak response with a LVA and with a normal aqueduct are shown, and the difference between them is the predicted change in BC hearing threshold caused by a LVA.

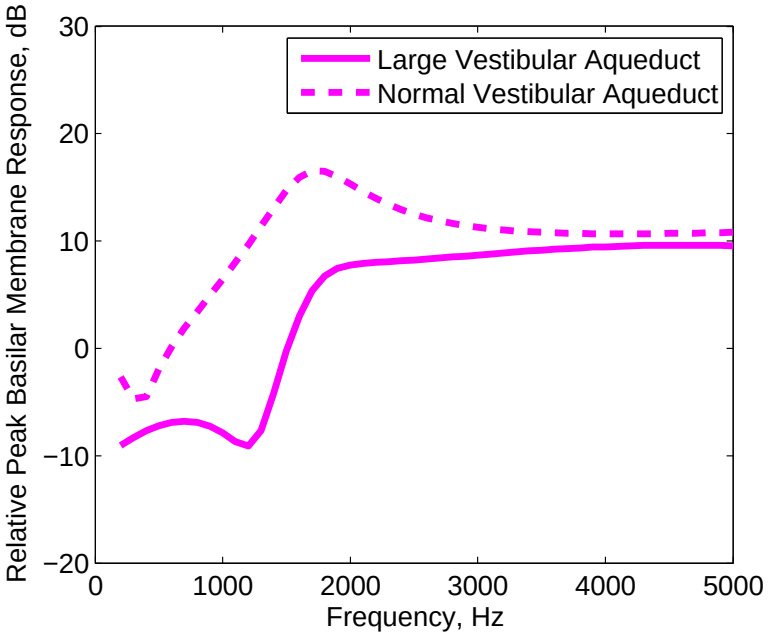

Figure 5.19: Comparison of the peak BM response due to the combination of the two inertial bone conduction pathways, with a normal and large vestibular aqueduct.

The air-bone gap due to a LVA is defined as the difference between the AC and BC threshold with a LVA modelled. Fig. 5.20 shows the calculated AC and BC thresholds with a LVA, as well as the air-bone gap. It can been seen that there is predicted to be a significant air-bone gap at low frequencies, which is around 25 dB at 500 Hz, and decreases with frequency, until it is only a few dB at 5 kHz. At frequencies below about 500 Hz the air-bone gap is dominated by the increase in the AC threshold due to the LVA, as the BC threshold is fairly constant due to the balance between the increases of the fluid inertia response and decreasing of the middle ear inertia response. As the frequency increases the air-bone gap then falls as the AC and BC thresholds become more comparable. From about 1 kHz the thresholds are within 5 dB of each other.

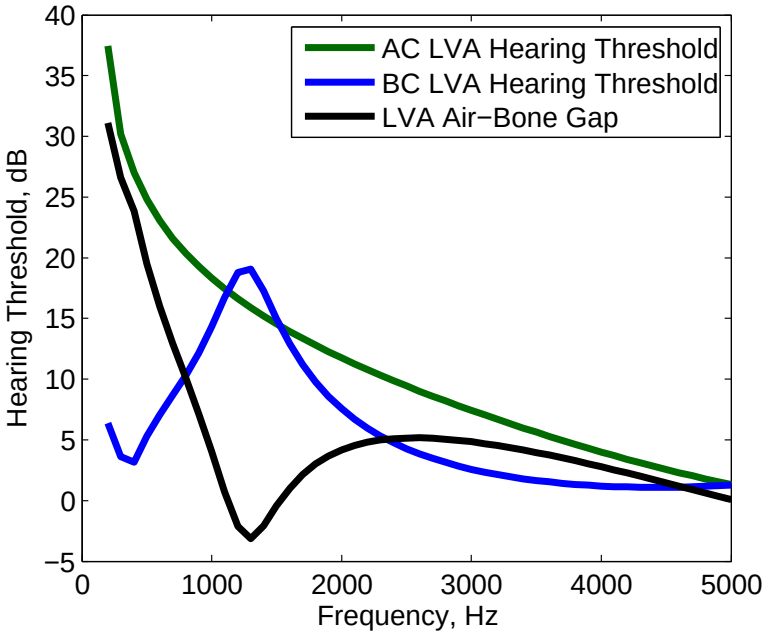

Figure 5.20: Predicted air conduction (solid green line) and bone conduction (solid blue line) hearing level when a large vestibular aqueduct is modelled. The air-bone gap, which is the difference between the two thresholds, is shown (solid black line).

This model predicts that the air-bone gap seen in patients with a LVA is mainly due to the increase in the AC threshold, which is caused by the pressure in the scala vestibuli forcing flow out through the vestibular aqueduct, reducing the overall volumetric excitation into that scala. There is a smaller change in BC thresholds due to a LVA, but the air-bone gap seen is dominated by the effect of the LVA on the AC threshold.

In reality the audiograms of patients with LVA are often complicated due to other hearing problems, and have been shown to change over time. There is a great variation between different patient's audiograms and it can therefore be difficult to determine what component is due to the effect of a LVA. The AC and BC thresholds predicted by the model have been compared against the audiograms of patients who have a LVA, and are shown in Fig. 5.21. It can be seen that the results from the model correlate well with the particular audiograms chosen from the Merchant et al. (2007a) study. The comparison must be taken with some caution, however, as there is great variations between patients. The change in BC thresholds, at low frequencies, is predicted by the model with only the two inertial components of BC, without taking into account the other pathways, which may lead to errors, particularly at higher frequencies.

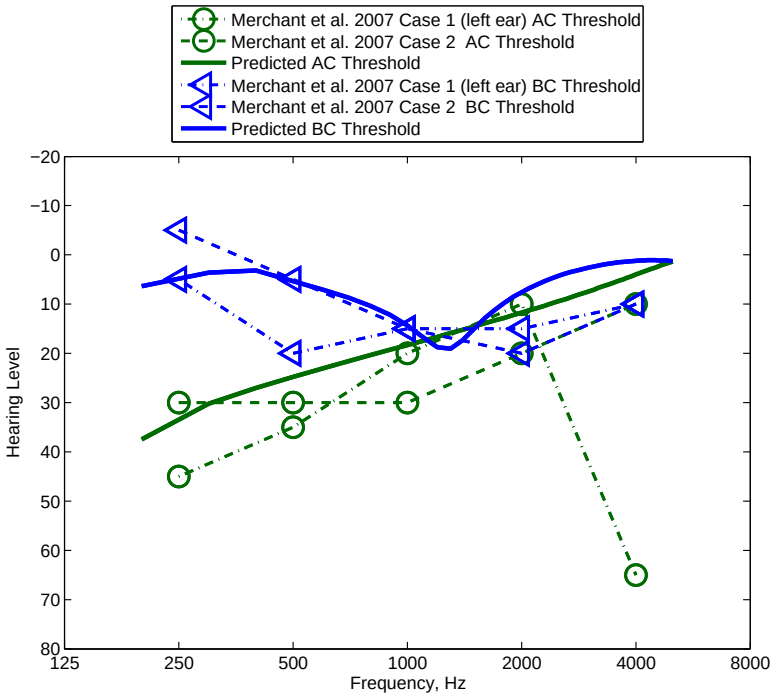

Figure 5.21: Comparison of the predicted AC and BC thresholds with those taken from patients who exhibit a large vestibular aqueduct.

The air-bone gap, due to a LVA, was determined from AC and BC thresholds of two cases report in Merchant et al. (2007a). The air-bone gap predicted by the model is shown in Fig. 5.22, along with the average air-bone gap determine from all the cases reported in Merchant et al. (2007a). For the two cases chosen, the model prediction the low frequency air-bone gap well, which supports the conclusions drawn of how this gap occurs.

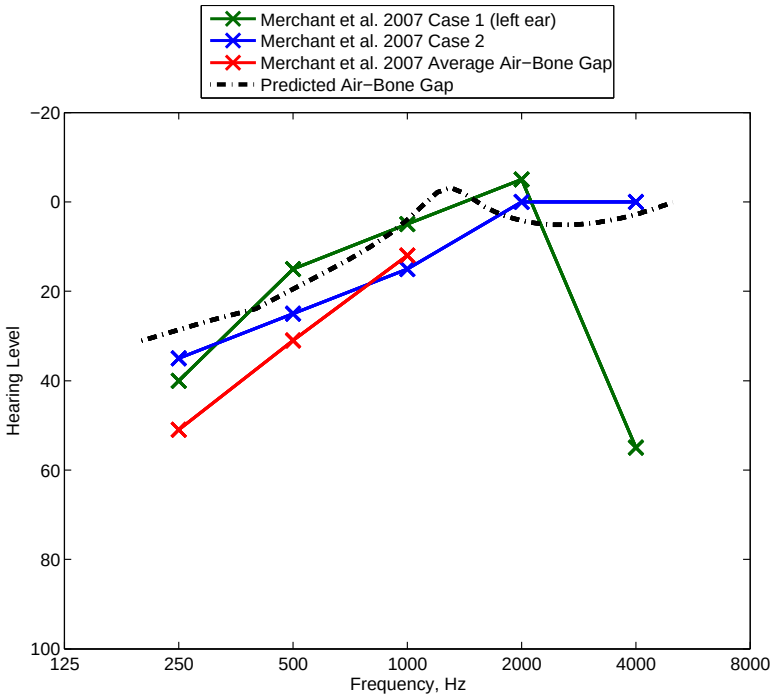

Figure 5.22: Comparison of the air-bone gap predicted by the model and those found in patients report in Merchant et al. (2007a).

5.5.4 Large Vestibular Aqueduct Effect on Excitation via Local Excitation at the Round Window

The inclusion of the vestibular aqueduct into the model was shown to have profound effect on the BM response when stimulated by local excitation at the round window, with a stiff oval window, see section 5.3.2. In this section, the effect of a LVA on the BM response is examined, under these conditions.

Fig. 5.23 shows the peak BM response due to local round window excitation, when a LVA was modelled, and also with a normal size aqueduct for comparison. It can be seen that the overall BM response, at most frequencies, is increased by the enlargement of the vestibular aqueduct. This is primarily due to the large increase in the volumetric component of excitation compared with the normal sized vestibular aqueduct in Fig. 5.8, as expected.

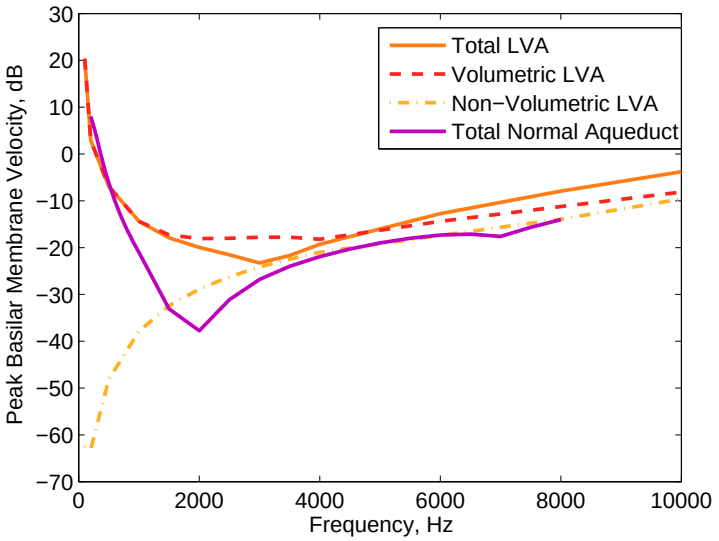

Figure 5.23: The total peak BM response, due to local excitation at the round window, when a large vestibular aqueduct was modelled (orange solid line) and the oval window immobile. The volumetric (red dashed line) and non-volumetric components (light orange dot dashed line) components of the total response are shown. The total response when a normal vestibular aqueduct was modelled is shown for comparison (purple solid line).

It was found that the total response is dominated by the volumetric component over a greater frequency range when a LVA is modelled. This is because of the increased admittance of the LVA above about 500 Hz, and hence a greater fluid flow through the aqueduct at higher frequencies, which increases the volumetric component. The notch due to the cancellation of the volumetric and non-volumetric components thus moves up in frequency, but is now less pronounced. The vestibular aqueduct is thus likely to have a significant role to play in the processes of hearing via local excitation of the round window, when the oval window is assumed to be immobile, especially at low frequencies.

5.6 Discussion and Conclusions

This chapter has examined the effect of the 'third window' on the cochlear response due to multiple hearing mechanisms. The 'third window' was included in the model by incorporation of the cochlear and vestibular aqueducts. It was found that in the healthy cochlea, the inclusion of the aqueducts had little effect on the BM response at most frequencies due to the excitation mechanisms investigated: piston-like motion of the stapes, rocking of the stapes and fluid inertia component of BC hearing. Only at low frequencies was there an effect when the stapes was rocked or when excited by the fluid inertia component of BC. The increase at low frequencies on the fluid inertia component

was significant because it then caused this component to dominate over the middle ear inertia component at low frequencies.

Two other cochlear excitation mechanisms were then investigated, the fluid inertia and local excitation at the round window, when the oval window was assumed to be immobile, simulating otosclerosis. Without the aqueducts included, for both cochlear excitation pathways, only non-volumetric excitation can occur. In this case, when excited at the round window, it was shown that the near-field pressure drove the BM motion, in much the same way as when the stapes was rocked. It was shown that the inclusion of the aqueducts, and most importantly the vestibular aqueduct had a significant effect on the BM response, especially at low frequencies. The inclusion of the vestibular aqueduct allowed for volumetric excitation to occur, and hence increased the BM response due to the more efficient way of exciting the cochlea. It was found that under the condition of an immobile oval window, the vestibular aqueduct has a significant effect on the underlying mechanisms of exciting the cochlea.

The model also predicted that when the cochlea with a immobile oval window was excited at the round window, such that not all of it was occluded, then both the non-volumetric and volumetric excitations occur, with the dominance of each type changing with frequency. The volumetric component was shown to dominate at low frequencies and the non-volumetric at high. It was found that the phase difference between the two types of excitation was important, especially at mid frequencies, as it was predicted to cause a dip in the response. In the model, the cochlea geometry is greatly simplified, but the shape of the cochlea may have a significance effect on the phase response of the two types of excitation. The next step in the investigation would be to use a 3D finite element cochlear model, with a realistic geometry to examine this hearing mechanism, as then the realistic phase difference could be determined. When a LVA was modelled, an increase of the overall BM response was found. The frequency range at which the two types of excitation were out of phase shifted upwards. This illustrates how that the details of the vestibular aqueduct have an effect on the BM response. The differences between the vestibular aqueduct between people could lead to its effect on the hearing response being unique to each person. This may have interesting effects when modelling this hearing mechanism on a $3D$ finite element model, as difference in the geometry of the model may have varying effects on the total response.

The change in BC hearing threshold due to the stiffening of the oval window was predicted using the model and compared against clinical measurements of Carharts notch. It was shown they had a similar trend, with a notch around 2 kHz. Although there is large variation in the individual audiograms of patients with an immobile oval window, at low frequencies the model was shown to predict the BC threshold hearing threshold reasonably well. The 'notch' in the BC hearing threshold was found at a realistic frequency, though the magnitude of it was somewhat larger than that seen in some clinical

measurements. This could be due to a number of reasons, such as other BC pathways having a significant effect on the overall response, the geometry of the cochlea influencing the response or the skull not vibrating as a rigid body, as assumed. However, the model does suggest that Carharts notch could be explained by just the two inertial components of BC hearing, where the notch is due to the loss of the middle ear inertia component.

An investigation was also carried out on the effect of a large vestibular aqueduct, LVA, on the BM response when excited by both AC and BC. It was found that the response to the fluid inertia component mostly increased with a LVA, though there was a small decrease in response predicted below 500 Hz. In contrast, when the cochlea was excited via a piston-like motion at the stapes, either through AC or the middle ear inertia, the BM response was found to be greatly decreased by a LVA. This was found to be due to the pressure in the scala vestibuli forcing fluid out of the vestibular aqueduct, decreasing the overall net volume of fluid into the scala vestibuli. The AC and BC hearing thresholds were predicted using the model and found to be similar to audiograms of patients with a LVA shown in Merchant et al. (2007a). The change in BC thresholds with a LVA is due to a combination of effects on the fluid inertia and middle ear inertia response, which for most frequencies oppose each other. The realistic prediction of the change in BC thresholds due to an LVA is further evidence that at low frequencies the inertial components of BC dominate the total BC response.

The air-bone gap at low frequencies predicted by the model was shown to be comparable to two sets of clinical results. Often, a LVA does not exist on its own, but other malformations occur in ears with a LVA and thus the audiograms can be very variable between patients. However, the predicted hearing thresholds of the model is within range of realistic audiograms. The cause of such a gap at low frequencies was shown to be mostly due to the decrease in hearing response due to AC hearing, not an increase in BC hearing. The gap predicted was however somewhat smaller than the average found in Merchant et al. (2007a). The effect on the hearing response due to a LVA is dependant on many factors. It would be possible to change the assumed size of the large vestibular aqueduct to produce a different air-bone gap that would correlate better with the average result found in Merchant et al. (2007a). This, however, does not seem worthwhile since the cochlea and vestibular aqueduct have been simplified in the modelling to such as extent it would not provide any more insight. What the model does show is the underlying mechanisms which cause an air-bone gap when a LVA is present and that it is mostly caused by the increase in the AC thresholds.

A LVA has similar clinical affect as a semi circular canal dehiscence. It has been suggested by the simple model in Rosowski et al. (2004) that the compressional component of BC hearing is reduced by a semi circular canal dehiscence. There are similarities between this condition and a LVA, in that they both produce a decrease in admittance

in the scala vestibuli side of the cochlea. It has been shown that the size and shape of a dehiscence has a large effect on the cochlear response (Kim et al., 2013) as is the case with a LVA. The AC hearing thresholds predicted by Rosowski et al. (2004) due to a semi circular canal dehiscence are similar to those predicted here due to a LVA, however, the corner frequency discussed in Rosowski et al. (2004) was not found to be as pronounced as the model. The similarity between the two results is reasonable as both models greatly simplify the geometry of the cochlea. A more geometrically realistic cochlear model would be a potentially effective tool to investigate in more detail the effect of these conditions.

Chapter 6

Conclusions and Future Work

6.1 The Model

The human cochlea is a very small, complex organ that is intrinsic in the process of us perceiving the sound environment around us: it is to hearing, what the eye is to sight. We, as humans, rely heavily on our ability to hear in order to communicate, perceive danger as well as to experience the more enjoyable things in life. It is therefore important to understand the workings of the cochlea in order to improve medical treatments for hearing impairments. Also, there is a drive to study the cochlea from a purely scientific interest, in order to gain a great understanding of how humans function and perceive the world around us.

Due to the location and the delicacy of the cochlea, as well as ethical considerations, experimental studies have limitations, particularly in humans. Mathematical models, however, do not have these same limitations and so can provide a useful tool for understanding of the physics of the cochlear function. There have been many approaches to modelling the cochlea, all with varying simplification and assumptions, from 1D models, to 2D box models, to 3D geometrically realistic finite element models. Different forms of models have been found to be necessary to explain different hearing phenomenon. A long-term aim would be to have a consensus between the predictions of the cochlea response, from a set of models of varying complexity and dimension to fully understand the cochlea mechanisms. For robustness and reliability, a variety of predictions from the models would need to be comparable to experimental and clinical results on real cochleae.

This thesis has been concerned with using a 2D mathematical model of the cochlea to further understand its workings. A 2D model is the simplest model to be able to represent the effects of near field pressures close to the vibrating parts of the cochlea. The geometry of the cochlea was simplified to a rectangular box shape and the structures

modelled included the basilar membrane and oval and round window. The models ability to be easily manipulated was utilised by further extending it to incorporate the cochlear and vestibular aqueducts, which are two of many structures collectively known as the 'third window'. The model was solved using a finite difference method, which has been outlined in Chapter 3. A benefit of this model is that it can be readily replicated, since it does not rely on a specific commercial solver. The model is also versatile, such that multiple excitation mechanisms were able to be investigated using this same model allowing for a comparison to be made within one framework.

It is important to compare the output of a model against relevant experimental data in order to ensure realistic predictions, and to understand the limitation of the model. Throughout this thesis the predictions of the cochlear model, as well as the lumped parameter model of the middle ear ossicles, were compared against experimental and clinical data, where possible. The confidence in the predictions of the model increases as more comparisons are made with varying experimental data. It is not always possible to compare predicted results, either due to the lack of real data or because it is impossible to carry out such experiments. In Chapter 4 the BM response due to a piston-like motion of the stapes was compared against data from temporal bones experiments and found to be similar. In Chapter 3, the predicted motion of the lumped parameter model of the middle ear, due to vibration of the temporal bone, was compared against measurements from real middle ears ossicles and found to be similar. The change in hearing thresholds, due to the stiffening of the oval window and a LVA, predicted by the model were compared against clinical data of the hearing thresholds of patients with conditions that cause these malformations in Chapter 5.

A comparison of results from the model were also made with a geometrically similar model, from Edom et al. (2013), which was solved using a different method and assuming different parameters. The parameters of the model were altered somewhat in order for a better comparison and it was found that both models predicted a similar trend for excitation via the rocking of the stapes. However, the results were not identical, which highlights the need for many different approaches in order to reach a full understanding of the cochlea. It is also important to understand that the choice of parameters used influences the output of the model. The comparisons with experimental and clinical data, as well as those from other models, suggests that this model is fairly robust. Perhaps the greatest limitation of the model is its simplification of the cochlear geometry, particularity in the hook region, although some care was taken with the placement of the windows for this to be somewhat representative.

6.2 The Model Predictions

This model was solved for the 2D pressure distribution in the cochlea. The total pressure field was separated into its components and the way that they differ with the type of excitation was investigated. In all cases there is a mean-pressure created by the fast wave propagation. As there is no interaction between this wave and the BM it was subtracted from the total pressure for the purpose of this study. The resultant pressure distribution is made up of the plane wave and near-field pressure distributions. The plane wave pressure distribution is vertically uniform within each scala at any one point and couples to the BM along the length of the cochlea. The near-field pressure is generated close to the vibrating structures in the cochlea, either the BM or cochlear windows in this study. It decays at a greater rate than that of the plane-wave pressure components, and so is only present locally. The relative dominance between these two pressure components was shown to differ, based on whether the cochlea is excited due to a volumetric or non-volumetric excitation mechanism. Volumetric excitation mainly couples into the plane wave pressure distribution. However, for non-volumetric excitation, it is the near field pressure distribution at the stimulated cochlear windows that drives the BM into motion. This study also showed that however the cochlea was excited a travelling wave of similar profile is produced further along the BM. The model used in this thesis predicted that non-volumetric excitation mechanisms, such as the rocking of the stapes, were less efficient at inducing a travelling wave along the BM than the volumetric excitation mechanisms, for a given input velocity. Hence, the plane wave pressure distribution is a superior driver of the BM motion than the near-field pressure field at the cochlear window due to the non-volumetric excitation. In the healthy cochlea it was shown that the non-volumetric excitation was unlikely to have an effect on the total BM response (though this would have to be further investigated at high frequencies). However, under certain conditions, where there were malformations to the cochlea, it was shown that this excitation mechanism could become significant at high frequencies.

The model was also used to investigate the effect that the 'third window', in this case the vestibular and cochlear aqueducts, has on the BM response due to different excitation mechanisms, and also with a immobile oval window. This was the first time such an investigation has been carried out with the 2D cochlea model. The model predicted that the vestibular aqueduct acted as a fluid outlet when the oval window was immobile. This allowed volumetric excitation to occur, and due to the greater efficiency of driving the BM, an increase in BM response was seen. This BM increase was seen to be frequency dependant, with a greater effect predicted at lower frequencies. Under this conditions the volumetric excitation component was shown to dominate at low frequencies, but, at high frequencies the non-volumetric excitation component became significant. In particular, when excited locally at the round window, there was predicted to be clear transition between volumetric and non-volumetric excitation dominance.

Patients with a large vestibular aqueduct are found to have a large air-bone gap in their audiograms. The cause of this gap is under debate, and there are multiple theories in the literature. The effect of a LVA on the hearing threshold was investigated using this model, and is discussed in Chapter 5. It was predicted that the dominate factor was the increase of the AC hearing threshold due to the fluid being pushed out of the vestibular aqueduct. This reduces the volumetric excitation, and hence causes a reduction in the BM response.

The 2D model has shown to be sufficient to show the physics behind a number of excitation mechanisms, yet simple enough for the results to be efficiently processed and visualised.

6.3 Comparison with 3D Finite Element Model

An attempt was made to carry out similar investigations as that on the 2D model on a 3D finite element model, with a realistic geometry, in order to compare results. Access was arranged to the 3D coiled model developed by Kim et al. (2014) but, due to software problems it was difficult for this to proceed. This model was built and run on two separate commercial finite element software packages. Access to the software in which the model was built was arranged, but unfortunately, the commercial software in which the model was originally solved did not run under the universities licences. It was also found that the model was not able to run on a different, but similar, software package available on the university licences due to the differences in the definitions of material properties between the two software packages.

It became clear that although there are multiple similar 3D finite element packages, they are not all compatible with each other. They vary in their definitions of parameters which cannot be altered and sometimes it is difficult to determine how they are defined and what calculations are being carried out. This highlights the value of simpler models that can be easily interpreted and the need for a collection of models, of varying complexity and dimensions, which are in agreement with each other and the clinical data.

6.4 Future work

This model could easily be further developed to include an active BM, such as that in Neely and Kim (1986). This would not change the underlying processes behind the excitation of the BM, but could be used, for example, to examine the amplification of low level excitation via non-volumetric pathways.

It would also be interesting to modify the geometry of the 2D model to represent that assumed in the lumped parameter representation of Stenfelt (2014), which would allow a

direct comparison of the results of these two cochlear models. The 2D box model could also be adapted to allow the two outer walls to move out of phase, to represent compression, instead of in phase, to represent the effect of the fluid inertia, as in section 3.5.4. The lumped parameter model is not able to reproduce near-field pressure excitation of the BM, but a comparison of the predictions of the two models for different types of BC excitation may help illustrate the strengths and weaknesses of the two approaches.

The greatest simplification in this model is that of the geometry of the cochlea. It is clear that the effect of the complex cochlea geometry on the BM response would be a valuable extension to this work. The area near to the cochlear windows, the hook region, is particularly complex, as there is a bulge and the termination of the BM. The effect of the geometry in this region this area on BC hearing has already been investigated in Kim et al. (2014) using a 3D finite element model, where the excitation is mostly volumetric. It is clear from the 2D model reported in this thesis that the near-field pressure created at the windows can drive the BM into motion, and so the distribution of the pressure in this area is important. The 2D model predicts a very similar response when the oval window rocked or the round window excited locally. The detailed geometry of the hook region may have a significant effect on the near-field pressure distribution and therefore it would be interesting to investigate it effects on a more geometrical realistic cochlear model.

This model has predicted a clear transition between the dominance of a volumetric and non-volumetric excitation, when locally excited at the round window with an immobile oval window. It was shown that the characteristic of this transition changed with the enlargement of the vestibular aqueduct. This indicates that this phenomena is sensitive to the modelling of the of the aqueduct, and so again an investigation on a geometrically realistic cochlear model, which includes a vestibular aqueduct, could be of value. It is conceivable that not only is the cochlear response sensitive to the admittance of the aqueduct but also its location. There are great variations between individual aqueducts and so it could be of interest to explore if these differences have a significant effect on the total cochlear response.

Experiments have been carried out on guinea pigs to investigate the local excitation at the round window (Weddell et al., 2014). The guinea pig cochlea has a different geometry and frequency range to that of the human and so the effects of the 'third window' are likely to be different from that in the human. It would be possible to modify the model presented in this thesis to represent the guinea pig cochlea, in order to get a better comparison with this experimental data, although this was not attempted here due to the constraints of time.

Appendix A

A.1 Finite Difference Models for Simplified Geometries

Finite different models of simplified geometries, of increasing complexity, were built to validate the 2D finite difference cochlear model. The simplest of these was simply a box of fluid vibrated in the z-direction. A mass was then placed in the centre of the box and the its density varied. The model was further developed by attaching a spring and damper to the mass creating a BM element in the centre of a fluid filled box. A compressible fluid is not necessary to be modelled in the cochlear model since it has complaint windows and hence the volume of the fluid can remain constant, although modelling it makes little difference to the results. However, in these simple models there are no complainant windows and hence the fluid has to be modelled as compressible. The Laplace equation is,

$$\frac{\partial^2}{\partial x^2}p(x,z) + \frac{\partial^2}{\partial z^2}p(x,z) + \left(\frac{\omega}{c_o}\right)^2 p(x,z) = 0, \tag{A.1}$$

for an incompressible fluid, which has been already presented in Chapter 3, Eq. 3.6.

A.1.1 Simple Fluid Filled Box

A fluid filled box was vibrated in the z-direction by applying an acceleration at the horizontal walls, Fig.A.1a. The fluid pressure was solved for using a finite difference method. There are no complaint structures in this fluid filled box and so there can be no relative fluid flow. This means that all the fluid will move with the same velocity, which is the velocity of the horizontal walls. This constant velocity throughout translates into a vertical fluid pressure gradient with the greatest magnitude at the horizontal walls, however with opposite signs, and zero pressure in the middle. This is what was found when solving this simple model, Fig.A.1b.

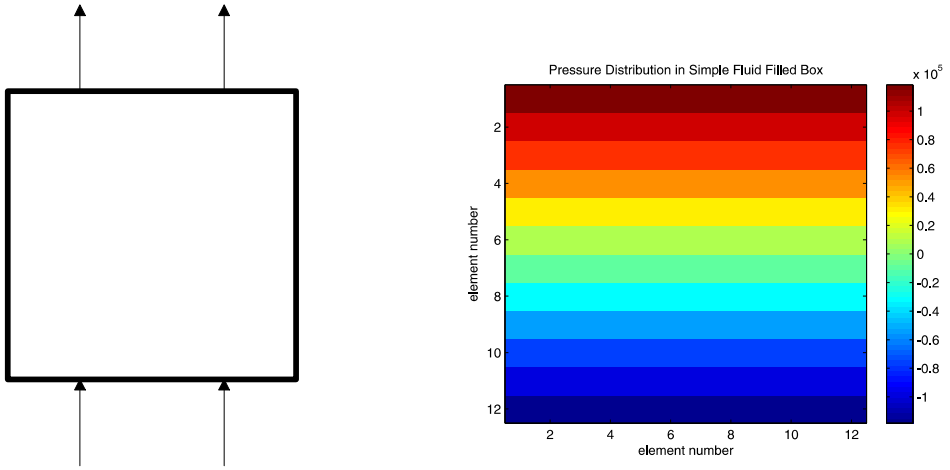

(a) (b)

Figure A.1: Diagram of simple fluid filled box showing the vibration direction (a) and the pressure distribution formed when vibrated vertically (b)

Using a finite difference method to solve for the pressure distribution in this simplest model gives a realistic result. This gives confidence to continue with more complicated models in order to validate this method for solving the cochlear model.

A.1.2 Fluid Filled Box with Mass

The next step was to place a mass in the centre of the box and, again, apply an acceleration to the horizontal walls, Fig.A.2a. The density of the mass was then changed to be, greater, equal and less than the density of the surrounding fluid. The relative motion of the mass was determined for all of these cases. This is a hypothetical model, since, if a mass was placed in the centre of the box it would either sink or float depending on its density.

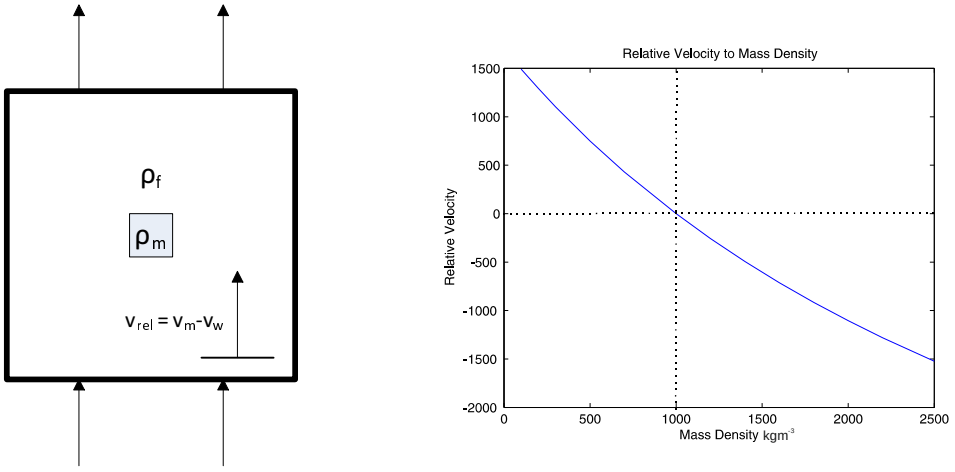

(a) (b)

Figure A.2: Diagram of simple hypothetical fluid filled box with mass placed inside (a) and graph showing the relatioship between the relative velocity of the mass and the density of the mass (b).

The relative velocity of the mass, v_m, to the velocity of the horizontal walls, v_w, $v_{rel} = v_m - v_w$, was plotted against the density of the mass, Fig.A.2b. The density of the surrounding fluid was kept the same, 1000 kgm^{-3}. It can be seen that when the density of the mass is the same as the fluid the relative velocity is zero, and hence the mass moves with the surrounding fluid. This is as expected, because from an inertial point of view there is no difference between the mass and fluid. As the mass density increased the mass becomes heavier and more force is needed to move it. Hence, it is expected that as the mass increases its absolute velocity will decrease. This model predicts this will happen. As the density of the mass becomes greater than the fluid density, the velocity of the mass becomes less than the wall velocity and so the relative velocity becomes negative. Similarly, as the mass decreases due to the decrease in density the motion of the mass is of greater amplitude than the fluid and therefore relative velocity increases.

A.1.3 Fluid Filled Box with Mass on a Spring

The complexity of the model was increased by adding a spring and damper to the mass, creating a BM element, that is used in the cochlear model, in the centre of a fluid filled box, Fig.A.3.

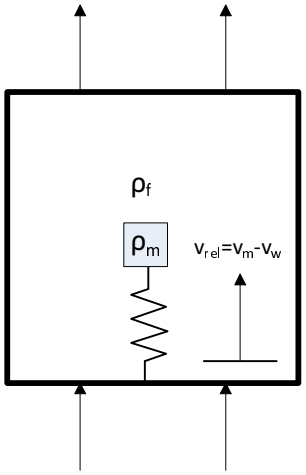

Figure A.3: Diagram of simple fluid filled box with a mass a spring within.

In the real cochlea the density of the BM and the fluid are very similar. This means that the interaction between the fluid pressure and the BM motion is expected to be strong. To determine if the BM element behaves as expected to vibrations of the walls, without the effect of the fluid, a model was built that assumed that the fluid was air and density of the BM mass as steel. It would be expected that the results from this model would represent that of a mass on a spring with no interaction between the fluid and the system. The results of this model were compared to the response of a simple mass, spring, damper system with the same values, excited at the base. The stiffness per unit area of the spring was equal to $3 \times 10^9\ Nm^{-3}$, the resistance $2.5 \times 10^4\ Nm^{-3}s$, and the mass per unit area equal to $\rho_{steel}\Delta z$. This gives a natural frequency of 1446 Hz.

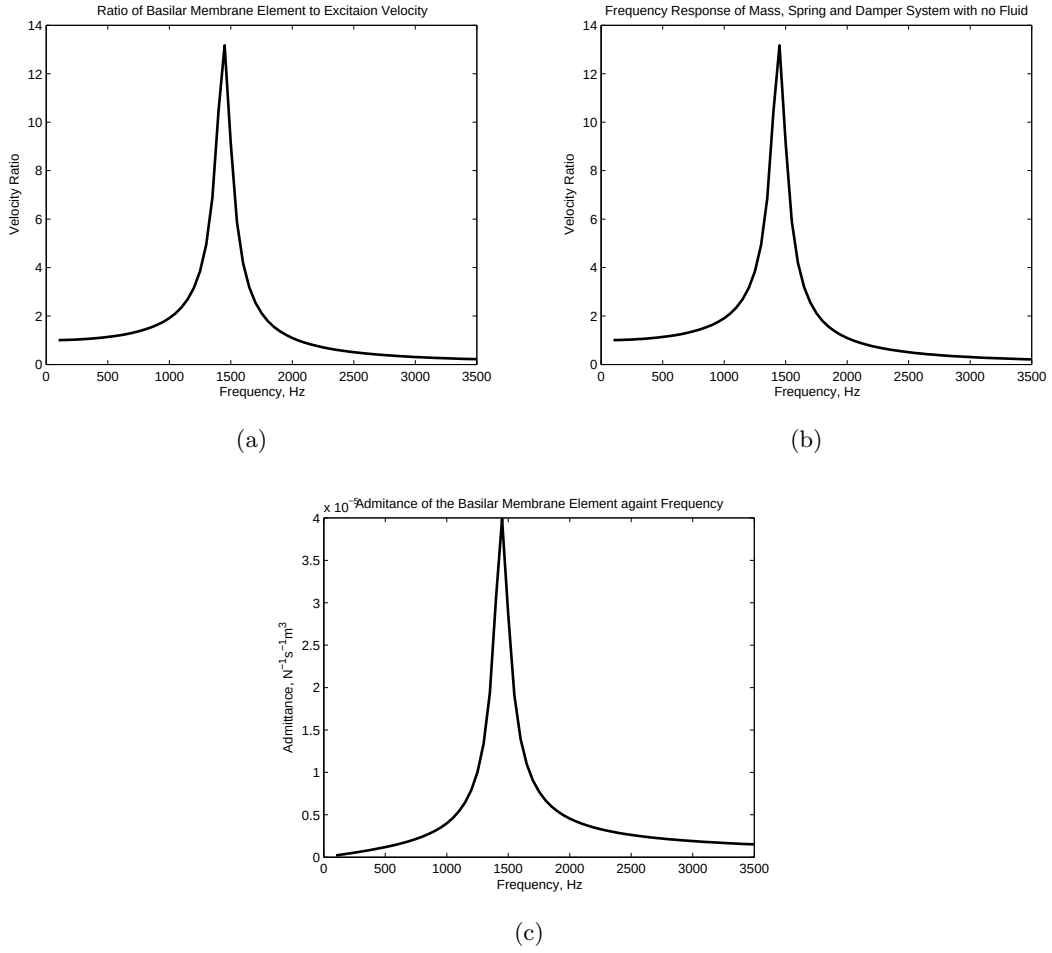

Figure A.4: Response of mass in fluid filled box when the density of the mass was that of steel and the fluid of air (a). Frequency response of a similar mass, spring and damper not surrounded by fluid but excited at the base, (b). Variation of admittance of mass, spring, damper system with frequency, (c).

Comparing the Fig.A.4a and Fig.A.4b it can be seen that the response of the BM element and that of a similar mass, spring damper system, excited at the base, are the same. The peak of the response is at the same frequency as peak of the admittance, Fig.A.4c. So, when the density of the fluid is small compared to the density of the BM element the fluid does not affect the motion of the BM.

The next step was to investigate what the effect was of a fluid with a similar density as the mass has on the BM element motion. A simple model was built, with a mass of BM equal to 0.3 kgm^{-2}, the stiffness 3×10^9 Nm^{-3} and resistance 2.5×10^2 $Nm^{-3}s$. The density of the fluid was then altered and the frequency response of the BM element found. It was found that increasing the density, decreased magnitude of the maximum response and the frequency of the peak response, Fig.A.5

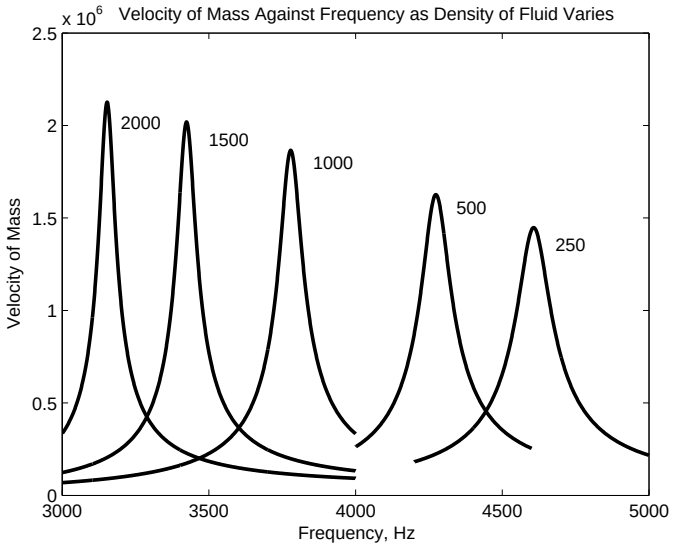

Figure A.5: Velocity of constant mass against frequency as fluid density is varied. Each peak is labelled with corresponding fluid density.

If the fluid was not interacting with the BM element the density of the fluid would have no effect of the frequency of the peak response. It is clear, Fig.A.5, that this is not the case and hence there is an interaction between the fluid and the mass. It is expected that this interaction causes the effective mass of the BM element to increase and hence there being an 'added' mass, m_{fluid}. This would mean that the resonant frequency of the BM element would equal,

$$\omega_n = \sqrt{\frac{k_{BM}}{m_o + m_{fluid}}}. \tag{A.2}$$

This can be rearrange to give,

$$\frac{1}{{\omega_n}^2} = \frac{m_o + m_{fluid}}{k_{BM}}. \tag{A.3}$$

The magnitude of this added mass for different fluid densities and size of elements was investigated. The mass inside the box was kept constant and the density of the fluid changed. The inverse of the squared angular frequency of the peak response of the BM element was found and plotted against the fluid density, Fig.A.6. This was repeated for a finer and a coarser element grid with the same size of fluid box and hence a smaller and larger element size.

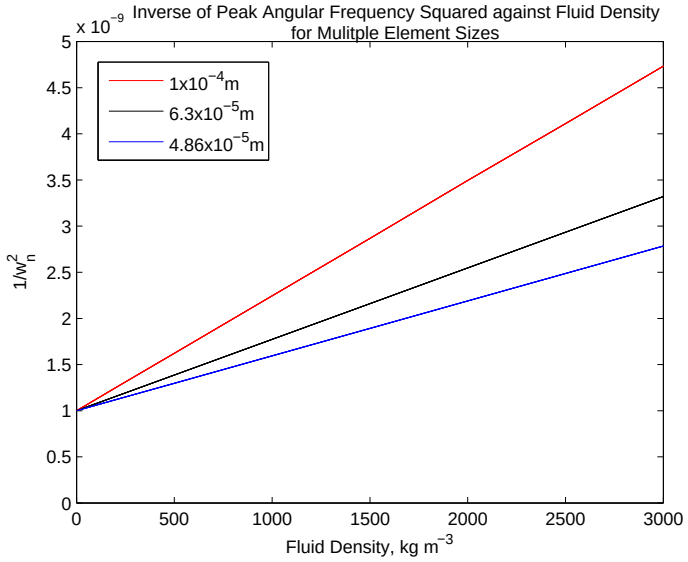

Figure A.6: Inverse of the squared angular frequency at which the peak response occurs against fluid density for various elements size when the box size is constant.

The intercept in Fig.A.6 is at 1×10^{-9} which is equal to $\frac{m_o}{k_{BM}}$. This is showing that when the fluid density is zero and the added mass must also be zero, which agrees with reason. The values of m_o and k_{BM} are kept constant and hence as the fluid density increases the value of the added mass increases too. The gradient of the plots in Fig.A.6 are proportional to $\frac{m_{fluid}}{\rho_f}$ and hence the volume of acting as a load on the BM element. As the size of elements the model is separated into increases, so does the gradient of the plot. This is showing that the element size affects the volume of fluid loading the BM element. The detail of this is not necessary to understand here, however, the important conclusion when related this to the cochlear model is that size of the model elements does alter the added mass term. This means the added mass term has to be calculated for a given cochlear model.

References

Bárány, E. (1938). *A Contribution to the Physiology of Bone Conduction.* Acta oto-laryngologica: Supplementum. Appelbergs boktryckeriaktiebolag.

Bekésy, G. v. (1955). Paradoxical direction of wave travel along the cochlear partition. *The Journal of the Acoustical Society of America*, 27(1):137–145.

Bekésy, G. v. and Wever, E. G. (1960). *Experiments in hearing.* McGraw-Hill, New York.

Beltrame, A. M., Martini, A., Prosser, S., Giarbini, N., and Streitberger, C. (2009). Coupling the vibrant soundbridge to cochlea round window: auditory results in patients with mixed hearing loss. *Otology & Neurotology*, 30(2):194–201.

Böhnke, F. and Arnold, W. (1999). 3d-finite element model of the human cochlea including fluid-structure couplings. *ORL*, 61(5):305–310.

Braun, K., Bhnke, F., and Stark, T. (2012). Three-dimensional representation of the human cochlea using micro-computed tomography data: Presenting an anatomical model for further numerical calculations. *Acta Oto-laryngologica*, 132(6):603–613.

Brockmannderivativ, C. L. and Komorniczak, M. (2009). Anatomy of the human ear blank. Licensed under CC BY 2.5 via Wikimedia Commons.

Carhart, R. (1950). Clinical application of bone conduction audiometry. *Archives of Otolaryngology Head and Neck Surgery*, 51(6):798.

Carhart, R. (1962). Effect of stapes fixation on bone conduction response. *Otosclerosis. Boston: Little, Brown and Company*, pages 175–97.

Carhart, R. (1971). Effects of stapes fixation on bone-conduction response. *Hearing measurement: a book of readings. Ventry, I.M. and Chaiklin, J.B. and Dixon, R.F. (Eds).*

Colletti, V., Carner, M., and Colletti, L. (2009). Torp vs round window implant for hearing restoration of patients with extensive ossicular chain defect. *Acta oto-laryngologica*, 129(4):449–452.

Colletti, V., Soli, S. D., Carner, M., and Colletti, L. (2006). Treatment of mixed hearing losses via implantation of a vibratory transducer on the round window. *International Journal of Audiology*, 45(10):600–608.

Cuda, D., Murri, A., and Tinelli, N. (2009). Piezoelectric round window osteoplasty for vibrant soundbridge implant. *Otology & Neurotology*, 30(6):782–786.

Dallos, P., Popper, A. N., and Fay, R. (1996). *Springer Handbook of Auditory Research - The Cochlea*. Springer.

de Boer, E. and Viergever, M. (1982). Validity of the liouville-green (or wkb) method for cochlear mechanics. *Hearing research*, 8(2):131–155.

de La Rochefoucauld, O., Decraemer, W., Khanna, S., and Olson, E. (2008). Simultaneous measurements of ossicular velocity and intracochlear pressure leading to the cochlear input impedance in gerbil. *Journal of the Association for Research in Otolaryngology*, 9(2):161–177.

Decraemer, W. F., de La Rochefoucauld, O., Dong, W., Khanna, S. M., Dirckx, J. J. J., and Olson, E. S. (2007). Scala vestibuli pressure and three-dimensional stapes velocity measured in direct succession in gerbila). *The Journal of the Acoustical Society of America*, 121(5).

Droual (2007). Middle ear. `http://droualb.faculty.mjc.edu/Lecture%20Notes/Unit%205/special_senses%20Spring%202007%20with%20figures.htm`. Date accessed 01/11/16. This file was modified.

Edom, E., Obrist, D., Henniger, R., Kleiser, L., Sim, J. H., and Huber, A. M. (2013). The effect of rocking stapes motions on the cochlear fluid flow and on the basilar membrane motion. *J Acoust Soc Am*, 134(5):3749–3758.

Elliott, S. J., Lineton, B., and Ni, G. (2011). Fluid coupling in a discrete model of cochlear mechanics. *The Journal of the Acoustical Society of America*, 130(3):1441–1451.

Elliott, S. J., Ni, G., Mace, B. R., and Lineton, B. (2013). A wave finite element analysis of the passive cochlea. *The Journal of the Acoustical Society of America*, 133(3):1535–1545.

Elliott, S. J. and Shera, C. A. (2012). The cochlea as a smart structure. *Smart Materials and Structures*, 21(6):064001.

Freeman, S., Sichel, J. Y., and Sohmer, H. (2000). Bone conduction experiments in animals - evidence for a non-osseous mechanism. *Hearing research*, 146(1-2):72–80.

Ginsberg, I. A., Hoffman, S. R., Stinziano, G. D., and White, T. P. (1978). Stapedectomy ??? in depth analysis of 2405 cases. *The Laryngoscope*, 88(12):1999???2016–1999???2016.

Gopen, Q., Rosowski, J. J., and Merchant, S. N. (1997). Anatomy of the normal human cochlear aqueduct with functional implications. *Hearing Research*, 107(12):9 – 22.

Gopen, Q., Zhou, G., Whittemore, K., and Kenna, M. (2011). Enlarged vestibular aqueduct: Review of controversial aspects. *The Laryngoscope*, 121(9):1971–1978.

Govaerts, P., Casselman, J., Daemers, K., Ceulaer, G. D., Somers, T., and Offeciers, F. (1999). Audiological findings in large vestibular aqueduct syndrome. *International Journal of Pediatric Otorhinolaryngology*, 51(3):157 – 164.

Gray, H. (1918). *Anatomy of the Human Body*. Lea and Febiger. Illustrator Henry Vandyke Carter.

Gundersen, T., Skarstein, ø., and Sikkeland, T. (1978). A study of the vibration of the basilar membrane in human temporal bone preparations by the use of the mossbauer effect. *Acta oto-laryngologica*, 86(1-6):225–232.

Hakansson, B., Brandt, A., Carlsson, P., and Tjellstrom, A. (1994). Resonance frequencies of the human skull in vivo. *The Journal of the Acoustical Society of America*, 95(3):1474–1481.

Hato N, Stenfelt S, G. R. L. (2003). Three-dimensional stapes footplate motion in human temporal bones. *Audiol Neurotol*, 8:140–152.

Heiland, K. E., Goode, R. L., Asai, M., and Huber, A. M. (1999). A human temporal bone study of stapes footplate movement. *American Journal of Otology*, 20:81–86.

Henry, P. and Letowski, T. R. (2007). Bone conduction: Anatomy, physiology, and communication. *Army Research Laboratory*, 2ARL-TR-4138.

Homma, K., Du, Y., Shimizu, Y., and Puria, S. (2009). Ossicular resonance modes of the human middle ear for bone and air conduction. *The Journal of the Acoustical Society of America*, 125(2):968–979.

Huber, A. M., Sequeira, D., Breuninger, C., and Eiber, A. (2008). The effects of complex stapes motion on the response of the cochlea. *Otology & Neurotology*, 29(8):1187–1192.

Kiefer, J., Arnold, W., and Staudenmaier, R. (2006). Round window stimulation with an implantable hearing aid (soundbridge®) combined with autogenous reconstruction of the auricle–a new approach. *ORL*, 68(6):378–385.

Kim, N., Homma, K., and Puria, S. (2011). Inertial bone conduction: Symmetric and anti-symmetric components. *Journal of the Association for Research in Otolaryngology*, 12(3):261–279.

Kim, N., Steele, C. R., and Puria, S. (2013). Superior-semicircular-canal dehiscence: Effects of location, shape, and size on sound conduction. *Hearing Research*, 301(0):72 – 84.

Kim, N., Steele, C. R., and Puria, S. (2014). The importance of the hook region of the cochlea for bone-conduction hearing. *Biophysical journal*, 107(1):233–241.

Koike, T., Wada, H., and Kobayashi, T. (2002). Modeling of the human middle ear using the finite-element method. *The Journal of the Acoustical Society of America*, 111(3):1306–1317.

Liberman, C., Merchant, S., Wang, H., and Northrop, C. (2009). 3D model of the human temporal bone.

Linder, T. E., Ma, F., and Huber, A. (2003). Round window atresia and its effect on sound transmission. *Otology and Neurotology*, 24(2):259–263.

Lupo, J. E., Koka, K., Holland, N. J., Jenkins, H. A., and Tollin, D. J. (2009). Prospective electrophysiologic findings of round window stimulation in a model of experimentally induced stapes fixation. *Otology & Neurotology*, 30(8):1215–1224.

Marchbanks, R. J. and Reid, A. (1990). Cochlear and cerebrospinal fluid pressure: Their inter-relationship and control mechanisms. *British Journal of Audiology*, 24(3):179–187.

Marquardt, T. and Hensel, J. (2013). A simple electrical lumped-element model simulates intra-cochlear sound pressures and cochlear impedance below 2 khz. *The Journal of the Acoustical Society of America*, 134(5):3730–3738.

Mason, M. J. (2003). Bone conduction and seismic sensitivity in golden moles (chrysochloridae). *Journal of Zoology*, 260:405–413.

Merchant, S. N., Nakajima, H. H., Halpin, C., Nadol, J. B., Lee, D. J., Innis, W. P., Curtin, H., and Rosowski, J. J. (2007a). Clinical investigation and mechanism of air-bone gaps in large vestibular aqueduct syndrome. *Annals of Otology, Rhinology and Laryngology*, 116(7):532–541.

Merchant, S. N., Ravicz, M. E., and Rosowski, J. J. (1996). Acoustic input impedance of the stapes and cochlea in human temporal bones. *Hearing Research*, 97(12):30 – 45.

Merchant, S. N., Rosowski, J. J., and McKenna, M. J. (2007b). Superior semicircular canal dehiscence mimicking otosclerotic hearing loss. *Advances in oto-rhino-laryngology*, 65:137–145.

Merchant SN, R. J. (2008). Conductive hearing loss caused by third-window lesions of the inner ear. *Otology and neurotology: official publication of the American Otological Society, American Neurotology Society [and] European Academy of Otology and Neurotology*.

Mimura, T., Sato, E., Sugiura, M., Yoshino, T., Naganawa, S., and Nakashima, T. (2005). Hearing loss in patients with enlarged vestibular aqueduct: Air-bone gap and audiological bing test. *International Journal of Audiology*, 44(8):466–469.

Minor, L. B., Carey, J. P., Cremer, P. D., Lustig, L. R., and Streubel, S.-O. (2003). Dehiscence of bone overlying the superior canal as a cause of apparent conductive hearing loss. *Otology and neurotology*, 24(2):270–278.

Mojallal, H., Schwab, B., Hinze, A.-L., Giere, T., and Lenarz, T. (2015). Retrospective audiological analysis of bone conduction versus round window vibratory stimulation in patients with mixed hearing loss. *International journal of audiology*, (0):1–10.

Mudry, A. and Tjellstrom, A. (2011). Implantable bone conduction hearing aids. *Advances in Oto-Rhino-Laryngology*, 71:74.

Nageris, B. I., Attias, J., Shemesh, R., Hod, R., and Preis, M. (2012). Effect of cochlear window fixation on air and bone conduction thresholds. *Otology and Neurotology*, 33(9):1679–1684.

Nakajima, H., Dong, W., Olson, E., Merchant, S., Ravicz, M., and Rosowski, J. (2009). Differential intracochlear sound pressure measurements in normal human temporal bones. *Journal of the Association for Research in Otolaryngology*, 10:23–36.

Neely, S. T. (1981). Finite difference solution of a two-dimensional mathematical model of the cochlea. *The Journal of the Acoustical Society of America*, 69(5):1386–1393.

Neely, S. T. and Kim, D. (1986). A model for active elements in cochlear biomechanics. *The journal of the acoustical society of America*, 79(5):1472–1480.

Oarih (2009). Cochlea-crosssection, made in inkscape by Oarih. `https://en.wikipedia.org/wiki/Organ_of_Corti#/media/File:Cochlea-crosssection.svg`. This file is licensed under the Creative Commons Attribution-Share Alike 3.0 Unported license, Subject to disclaimers. Date accessed 01/11/16.

Perez, R., de Almeida, J., Nedzelski, J. M., and Chen, J. M. (2009). Variations in the" carhart notch" and overclosure after laser-assisted stapedotomy in otosclerosis. *Otology and Neurotology*, 30(8):1033–1036.

Pórschmann, C. (2000). Influences of bone conduction and air conduction on the sound of one's own voice. *Acta Acustica united with Acustica*, 86(6):1038–1045.

Puria, S. (2003). Measurements of human middle ear forward and reverse acoustics: Implications for otoacoustic emissions. *The Journal of the Acoustical Society of America*, 113(5):2773–2789.

Quaranta, N., Besozzi, G., Fallacara, R. A., and Quaranta, A. (2005). Air and bone conduction change after stapedotomy and partial stapedectomy for otosclerosis. *Otolaryngology - Head and Neck Surgery*, 133(1):116 120.

Reinfeldt, S., Ostli, P., Hkansson, B., and Stenfelt, S. (2010). Hearing ones own voice during phoneme vocalizationtransmission by air and bone conduction. *The Journal of the Acoustical Society of America*, 128(2):751–762.

Robles, L. and Ruggero, M. A. (2001). Mechanics of the mammalian cochlea. *Physiological reviews*, 81(3):1305–1352.

Rosowski, J. J., Songer, J. E., Nakajima, H. H., Brinsko, K. M., and Merchant, S. N. (2004). Clinical, experimental, and theoretical investigations of the effect of superior semicircular canal dehiscence on hearing mechanisms. *Otology and Neurotology*, 25(3):323–332.

Schraven, S. P., Hirt, B., Gummer, A. W., Zenner, H.-P., and Dalhoff, E. (2011). Controlled round-window stimulation in human temporal bones yielding reproducible and functionally relevant stapedial responses. *Hearing research*, 282(1):272–282.

Sim, J., Chatzimichalis, M., Lauxmann, M., Roosli, C., Eiber, A., and Huber, A. M. (2010). Complex stapes motions in human ears. *Journal of the Association for Research in Otolaryngology*, 11(3):329–341.

Sohmer, H. and Freeman, S. (2004). Further evidence for a fluid pathway during bone conduction auditory stimulation. *Hearing research*, 193(1-2):105–10.

Sohmer, H., Freeman, S., Geal-Dor, M., Adelman, C., and Savion, I. (2000). Bone conduction experiments in humans - a fluid pathway from bone to ear. *Hearing research*, 146(1-2):81–8.

Steele, C. R. and Zais, J. G. (1985). Effect of coiling in a cochlear model. *The Journal of the Acoustical Society of America*, 77(5):1849–1852.

Stenfelt, S. (2006). Middle ear ossicles motion at hearing thresholds with air conduction and bone conduction stimulation. *The Journal of the Acoustical Society of America*, 119(5):2848–2858.

Stenfelt, S. (2014). Inner ear contribution to bone conduction hearing in the human. *Hearing Research*.

Stenfelt, S. and Goode, R. L. (2005). Transmission properties of bone conducted sound: Measurements in cadaver heads. *The Journal of the Acoustical Society of America*, 118(4):2373–2373.

Stenfelt, S., Hato, N., and Goode, R. L. (2002). Factors contributing to bone conduction: The middle ear. *The Journal of the Acoustical Society of America*, 111(2):947–947.

Stenfelt, S., Hato, N., and Goode, R. L. (2004). Fluid volume displacement at the oval and round windows with air and bone conduction stimulation. *The Journal of the Acoustical Society of America*, 115(2):797–797.

Stenfelt, S., Puria, S., Hato, N., and Goode, R. L. (2003a). Basilar membrane and osseous spiral lamina motion in human cadavers with air and bone conduction stimuli. *Hearing Research*, 181(1-2):131–143.

Stenfelt, S., Wild, T., Hato, N., and Goode, R. L. (2003b). Factors contributing to bone conduction: The outer ear. *The Journal of the Acoustical Society of America*, 113(2):902–902.

Stieger, C., Rosowski, J. J., and Nakajima, H. H. (2012). Comparison of forward (ear-canal) and reverse (round-window) sound stimulation of the cochlea. *Hearing Research*, (0):–.

Tonndorf, J. (1962). Compressional bone conduction in cochlear models. *The Journal of the Acoustical Society of America*, 34(8):1127–1131.

Tonndorf, J. (1966). Bone conduction. studies in experimental animals. *Acta oto-laryngologica*, pages Suppl 213:1+. 5934763.

Traboulsi, R. and Avan, P. (2007). Transmission of infrasonic pressure waves from cerebrospinal to intralabyrinthine fluids through the human cochlear aqueduct: Non-invasive measurements with otoacoustic emissions. *Hearing Research*, 233:30 – 39.

Valvassori, G. and Clemis, J. (1978). The large vestibular aqueduct syndrome. *The Laryngoscope*, 88(5):723728.

Voss, S. E., Rosowski, J. J., and Peake, W. T. (1996). Is the pressure difference between the oval and round windows the effective acoustic stimulus for the cochlea? *The Journal of the Acoustical Society of America*, 100(3):1602–1616.

Watts, L. (2000). The mode-coupling liouvillegreen approximation for a two-dimensional cochlear model. *The Journal of the Acoustical Society of America*, 108(5):2266–2271.

Weddell, T. D., Yarin, Y. M., Drexl, M., Russell, I. J., Elliott, S. J., and Lukashkin, A. N. (2014). A novel mechanism of cochlear excitation during simultaneous stimulation and pressure relief through the round window. *Journal of The Royal Society Interface*, 11(93):20131120.

Wever, E. and Lawrence, M. (1954). *Physiological acoustics*. Princeton University Press.

Yoshida, M. and Uemura, T. (1991). Transmission of cerebrospinal fluid pressure changes to the inner ear and its effect on cochlear microphonics. *European Archives of Oto-Rhino-Laryngology*, 248(3):139–143.

Zhang, X. and Gan, R. Z. (2011). A comprehensive model of human ear for analysis of implantable hearing devices. *Biomedical Engineering, IEEE Transactions on*, 58(10):3024–3027.